JPRS-JST-91-005
31 JANUARY 1991

FOREIGN BROADCAST INFORMATION SERVICE

JPRS Report

Science & Technology

Japan

JPRS-JST-91-005
31 JANUARY 1991

SCIENCE & TECHNOLOGY

JAPAN

CONTENTS

Japanese Government's FY90 Nuclear Power Budget Proposal

90CF0359A Tokyo GENSHIRYOKU SANGYO SHIMBUN in Japanese 18 Jan 90 pp 4-5

[Text] Government Nuclear Power Budget Proposal in Tabular Form

Table 1. Science and Technology Agency [STA] General Account
(Unit: One million yen) *: National Treasury legal debt liability

Organization	FY89 budgeted amount	GY90 government budget proposal	Increase or decrease (-) over the previous year	Remarks
Japan Atomic Energy Research Institute	*32,912 94,845	*33,088 97,587 Percentage over last year (102.9%) New personnel 18 (-16 people)	* 176 2,742	Nuclear fusion *1,297 (*13,581) 22,435 (22,719) (1) Construction testing of JT-60 *1,297 (*13,581) 16,505 (16,507) Within this: Higher performance (*12,373) of JT-60 9,351 (4,884) Increasing deuterium *1,297 (* 1,207) content of JT-60 1,023 (393) (2)General research 5,930 (6,212) Within this: -International nuclear fusion test reactor (ITER) project member 1,281 (1,711) 2.Safety research *8,920 (* 8,175) 13,042 12,803) (1)Engineering safety research *8,920 (8,175) 11,908 (11,525) Within this: -Fuel cycle safety engineering research facility (NUCEF) construction *8,920 (* 8,175) 6,381 (5,581)

(2)Environmental
safety research
1,134 (1,278)

3. High temperature
engineering test
research *15,145 (* 3,873)
5,268 (4,171)
Within this:
Construction of heat
high engineering
15,145 (3,873)
test research
reactor 2,940 (1,284)

4. Research and
development of
nuclear-powered
vessel 3,689 (4,347)

(1) Trial voyage by
nuclear-powered
vessel Mutsu
3,394 (4,054)

(2) Research into
improving ship
reactors 295 (293)

5. General research, etc.
* 7,576 (* 7,283)
26,380 (25,755)

(1) Preparation of radiation
high technology research
facility* 617 (* 3,715)
4,384 (4,888)

(2) Preparation of large
radioactive light facility
* 994
1,167 (946)

(3) New superconductor
materials
research 143 (338)
1,452 (247)

Power Reactor and Nuclear Fuel Development Corporation	* 7,214 61,217	* 4,309 56,643 Percentage compared to last year (92.5%) New personnel 2 (-16 people)	* -2,906 -4,574	(4) Nuclear power base technology development 981 (803) 1. Fast breeder reactor development costs *2,757 (2,732) 13,694 (15,740) Within this: - Joyo operation *1,007 (* 157) 3,862 (4,363) - Research and development *1,680 (7,713 (10,224) 2. Power reactor common development costs (* 2,534) 11,492 (13,477) Within this: - Plutonium fuel (* 1,028) - Research and development 2,004 (4,086) 3. Recycling development costs 3,814 (4,651) Within this: - Fast breeder reactor recycling 2,375 (3,245) research and development Within this: Recycling equipment test facility 381 (1,322) 4. Environment technology development costs * 876 (* 882) 5,276 (4,692) Within this: - High level radioactive waste disposal technology development costs (882) 4,347 (4,080)
Other special companies	*37,311 83,461	*25,008 91,930 Percentage over last year (110.1%) New personnel 27 (-12 people)		
Total	*44,525 144,678	*29,316 148,573 Percentage over last year (102.7%) New personnel 29 (-28 people)		

				- Nuclide separation and destruction processing * 876 540 (290)
				5. Exploration development costs 3,172 (2,820)
				6. Fuel development costs 1,921 (1,706)
				7. Uranium enrichment development costs * 676 (* 1,067) 2,005 (2,446)
				Within this: - Laser technology enrichment development * 676 (* 1,067) 1,318 (875)
				- Nuclear power base technology comprehensive research 149 (99) (Redundant accounting)
Radiation Medical Laboratory	* 8,100 10,560	* 7,802 12,182 Percentage over last year (115.4%)	* -298 1,622	1. Safety analysis research expenses 50 (40) 2. Heavy particle medical uses research *7,802 (* 8,100) 6,524 (5,071)
				Within this: - Device development *4,711 (* 4,510) 2,843 (1,935)
				- Heavy particle ray room construction *3,091 (* 3,590) 2,774 (2,001)
				- Heavy particle ray cancer special research 166 (166)
				- Land purchase 740 (969)

				3. Preliminary research on the verification of the effect of a dose of radiation in a low radiation dose zone 30 (0)
4. Institute of Physical and Chemical Research	3,569	* 1,905 3,909 Percentage over last year (109.5%)	* 1,905 340	1. Heavy ion science research * 600 1,957 (2,298) Within this: - Accelerator room construction 32 (183) - Heavy ion science research * 600 1,925 (1,735) 2. Molecular laser method uranium enrichment technology development 364 (432) 3. Base technology development 252 (119) Within this: Nuclear power base technology comprehensive research 126 (54) 4. Preparation of large radioactive light facility *1,305 1,336 (719)
5. National test research organizations	2,043	2,060 Percentage over last year (100.8%)	17	1. Gross aggregate for 57 test research organizations belonging to 10 government ministries and agencies 2,060 (2,043)

6. Atomic Energy Commission	637	662 Percentage over last year (104.0%)	25	1. Atomic Energy Commission 183 (177) Within this: Special investigative costs 105 (101) 2. Atomic Energy Authority general administrative expenses 378 (361) 3. Increasing talents of scientists and technicians 101 (99)
7. Atomic Energy Safety Authority	1,991	* 200 2,034 Percentage over last year (102.2%)	8 200 43	1. Atomic Energy Safety Commission 307 (299) 2. Radiation Advisory Council 1 (1) 3. Atomic Energy Safety Authority general administrative expenses 917 (869) 4. Radioactive waste disposal measures 87 (114) 5. Radioactivity investigative research*200
Totals	*48,226 174,862	*47,304 175,078	-922 216	Percentage over last year 100.1%

Table 2. STA Comprehensive Atomic Energy-Related Budget
(Unit: One million yen) *: National Treasury legal debt liability

Item	FY89 budget amount	FY90 government budget proposal	Increase or decrease (-) over the previous year	Remarks
General account	* 48,226	* 47,304	* -922	100.1%
	174,862	175,078	216	
Electric power source development promotion policy special account	* 37,311	* 25,008	* 12,304	113.4%
	106,781	121,137	14,356	
Electric power source site account	18,642	24,177	5,535	129.7%
Electric power source diversified account	* 37,311	* 25,008	*-12,304	110.0%
	88,139	96,960	8,821	
Totals	* 85,537	* 72,312	*-13,226	105.2%
	281,643	296,214	14,572	

Table 3. STA Electric Power Source Special Diversified Account
(Unit: One million yen)

Item	FY89 budget amount	FY90 government budget proposal	Increase or decrease (-) over the previous year	Remarks
I.Electric power source site account				
I.1. Electric power source site policy cost	18,501	24,025	5,524	
I.1.(1)Atomic energy generation safety policy consignment costs	8,425	9,981	1,556	-Safety verification tests (Reprocessing facilities safety verification and 11 other tasks) 7,380 (6,519) -Nuclear fuel cycle related promotion and coordination consignment costs 2,108 (1,852) -Atomic energy related research enterprise consignment costs 117 (0)
(2)Atomic energy generation safety policy subsidy	198	0	- 198	
(3)Electric power source site promotion measures grants-in-aids	4,279	6,389	2,110	
(4)Electric power source site special grants-in-aid	2,142	2,263	121	-Atomic energy generator facilities vicinity grants-in-aid 1,711 (1,687) -Power ship-thru prefectures grants-in-aid 552 (455) -Radiation inspection grants-in-aid 2,403 (2,630)

(5) Atomic energy generator safety policy grants-in-aid	3,410	5,343	1,933	-Large reprocessing facilities radioactivity impact investigation grants-in-aid 1,200 (0) -Atomic energy generator facilities emergency safety policy grants-in-aid 924 (569) -International atomic energy organization contributions 37 (33)
(6)	47	50	3	-Economic cooperation development organization atomic energy organization contribution 13 (13)
I.2.Administrative business expenses	141	152	11	
II.Electric power source diversified account				
II.1.Power Reactor and Nuclear Fuel Development Corporation	*37,311 61,687	*25,008 91,930	*-12,304 8,469	
(1)New power reactor related expenses	*35,980 61,687	*25,008 63,772	*-10,972 2,085	-Construction of fast breeder reactor Monju *5,402 (*34,009)
(2)Spent nuclear fuel reprocessing related costs	10,945	15,365	4,420	-Reprocessing technology development 4,767 (3,869) -High level radioactive waste processing technology development 8,855 (1,594) -Nitric acid plutonium conversion facilities operation 1,134 (1,041)
(3)Uranium enrichment technology development related costs	*1,331 1,014	146	*-1,331 - 868	

II.2.General research	4,646	4,935	289	-Atomic reactor dismantling technology development consignment costs 2,241 (2,073) -Uranium enrichment enterprise investigation consignment costs 442 (827) -Reprocessing environmental security measures experimental research consignment costs 756 (598) -Large generator reactor development investigation consignment costs 186 (83) -Light water reactor nuclear fuel rod performance tests consignment costs 102 (88) -Radioactive waste disposal preliminary investigation consignment costs 474 (290) -Radioactive waste disposal technology development promotion costs subsidy 108 (103)
II.3.Administrative business expenses	32	95	63	-Electric power source diversified technology development evaluation costs 60 (0)
III.Sub-totals	* 37,311 88,139	* 25,008 96,960	*-12,304 8,821	Percentage over last year 110.0%
IV. Totals	* 37,311 106,781	* 25,008 121,137	*-12,304 14,346	Percentage over last year 113.4%

Table 4. Ministry of International Trade and Industry (MITI) Electric Power Source Special Diversified Account
(Unit: One million yen)

Item	FY89 budget amount	FY90 government budget proposal	Remarks
1.Uranium enrichment enterprise investigation consignment costs (MITI responsible portion)	496	532	-Investigative study of technology trends related to uranium enrichment new technology enterprises -Verification investigation of reconversion storage system technology of inferior uranium generated during uranium enrichment
2.Chemical uranium enrichment technology establishment costs subsidy	300	300	-Implementation of chemical uranium enrichment system development comprehensive investigation
3.Metal uranium production system development investigative costs subsidy	304	301	-Investigation of metal uranium production method applied to atomic laser uranium enrichment
4. Nuclear laser uranium enrichment technology system development investigation costs subsidy	2,599	2,705	-Technology development of laser systems and experimental equipment related to nuclear laser uranium enrichment technology
5. MOX [mixed oxide fuel] fuel technology for plutonium thermal use confirmation investigation consignment costs	900	875	-Confirmation tests of MOX fuel processing technology for plutonium thermal use readied for full-fledged use
6. Uranium enrichment centrifuge manufacturing technology establishment costs subsidy	352	593	-Establishment of technology to smoothly provide centrifuges used in state-run commercial uranium enrichment plants
7. Spent nuclear fuel reprocessing enterprise promotion costs subsidy	1,420	1,367	-Technology confirmation tests for reprocessing technology transferred from overseas

8. Reprocessing technology improvement investigation consignment costs	38	38	Investigation into the trends and economic value of technologies related to the improvement of the reprocessing process
9. Overseas reprocessing, return solid body acceptance system development investigation consignment costs	300	0	
10. Radioactive waste disposal criteria investigation consignment costs	710	1,230	-Confirmation tests of an improved still water system for the purpose of radioactive waste disposal -Investigation of the development of a system for the effective use of radioactive waste -Investigation of the development of a system for the disposal of uranium radioactive waste -Investigative study of disposal and storage of TRU [trans-uranium waste] radioactive waste
11. Radioactive waste disposal technology development promotion cost subsidy (MITI portion)	134	50	-Subsidy related to the development of nuclide measurement technology of low-level radioactive waste
12. Light water reactor improved technology confirmation tests consignment costs	9,424	9,545	-Confirmation tests of high combustible temperature high performance fuel, high-earthquake-resistant structure and site technology, and high performance steam generators; development of high inspection technology; development of maintenance inspection operational robots; development of human factors-related technology; and confirmation tests of spent fuel storage technology.
13. Consignment costs for the improvement of the safety analysis code for nuclear reactors used for commercial generation of electricity	2,042	1,391	-Drafting of a safety analysis code for cross-checking the safety analysis results done by applicants for the purpose of meeting completely the safety inspection when applying for the establishment of a nuclear power plant.

14. Earthquake-resistant safety analysis code improvement tests consignment costs	954	1,043	-Tests required for the establishment of a safety analysis code for cross-checking safety analysis related to earthquake resistance done by applicants for the purpose of meeting completely the safety inspection when applying for the establishment of a nuclear power plant.
15. Consignment costs for the investigation of the development of a new reactor for generating electricity (MITI portion)	615	625	-Comprehensive evaluation study for the commercialization of new reactors, like the fast breeder reactor, and the nuclear fuel cycle
16. New conversion reactor test reactor construction cost subsidy	1,987	2,279	-Subsidizing 30 percent of the ATR [advanced thermal converter] verification reactor construction costs required by the Electric Power Development Corporation
17. New generator reactor technology confirmation tests consignment costs	4,472	4,440	-Confirmation tests for technology related solely to a new reactor for the steady and appropriate realization of a fast breeder test reactor and a new conversion reactor test reactor
18. Consignment costs for the confirmation tests of equipment for abandoned nuclear reactors that were used for the commercial generation of electricity	676	713	-Confirmation tests for technologies for cutting up structures inside a reactor, a technology among reactor abandonment technologies
19. Nuclear power electricity generation support system development costs subsidy	643	692	-Development of a man/machine system to lighten the burden of the operators by handling quickly unusual phenomena in commercial light water reactors
20. Totals	28,370	28,720	

Table 5. MITI Treasury Financial Investments
(Unit: 100 million yen)

Item	FY89 projected amount	FY90 government draft budget proposal	Remarks
1.Overseas mining grants (Metal Mining Agency of Japan)	Internal figures of 8 [hundred million yen]	Internal figures of 9	-Grants to contribute to the positive mining and development of uranium overseas by Japanese corporations (grants and paid out investments), and development liability insurance
2.Japan Development Bank			
(1) Atomic energy	1,780	2,000	
(1)1. Nuclear power plant equipment	Internal figures	Internal figures	-Investment of low interest capital for equipment purchases for nuclear power plants being built by the nine electric power public utilities
(1)2. Nuclear power plant development	Internal figures	Internal figures	
(1)3. Nuclear fuel cycle	Internal figures	Internal figures	-Investment of low interest capital for construction work of the nuclear power plants being built by the Japan Nuclear Power Plant Corporation
2.(a)Nuclear fuel	Internal figures	Internal figures	-Investment of low interest capital for nuclear fuel processors and nuclear fuel parts manufacturers.
(b)Uranium enrichment	Internal figures	Internal figures	-Investment of low interest capital for uranium enrichment plant construction
(c)Spent nuclear fuel reprocessing	Internal figures	Internal figures	-Investment of low interest capital for reprocessing plant construction
(d)Low level radioactive waste disposal	Internal figures	Internal figures	-Investment of low interest capital for low level radioactive waste final storage facility construction
3. Electric Power Source Development Corporation	951	987	-ATR test reactor-related, etc.

Table 6. MITI General Account (Unit: 100 million yen)

Item	FY89 budgeted amount	FY90 government draft budget	Remarks
1. Nuclear power plant safety investigation supervision	175	191	-Placement of safety hearing, inspection, investigation, and operations management experts
2. Nuclear power plant administration	4	4	-Nuclear power plant administration
3. Nuclear power industry trends investigations	6	6	-Nuclear power industry internationalization direction (Investigation of advanced countries, investigation of developing countries, overall investigations)
4. Nuclear fuel industry establishment promotion measures	39	39	-Investigations and studies of every field of the nuclear fuel cycle
5. Radioactive waste disposal measures	22	20	-Establishment of a radioactive waste disposal system
6. Advancement of test research	883	869	-Implementation of nuclear power-related test research by test research institutes under the auspices of the Agency pf Industrial Science and Technology
7. General administrative costs	3	4	-Required expenses for the training of nuclear power-related employees
8. Totals	1,132	1,133	

Table 7. MITI Electric Power Source Special Company Site Account (Including STA Portion and Portion Other Than Nuclear Energy) (Unit: 100 million yen)

Item	FY89 budgeted amount	FY90 government draft budget proposal	Remarks
1. Electric power site advancement measures grants-in-aid	79,297	82,428	-Improvement of public facilities in vicinity surrounding power plant facilities
2. Electric power site special grants-in-aid	20,846	24,141	
(1) Nuclear power plant facilities vicinity grants-in-aid	14,021	14,916	-Grants of pay to residents and firms in the vicinity of nuclear power plant facilities, and measures for the introduction of firms and modernization of industry in regions where the residents of the region ordinarily commute to work
(2) Grant-in-aid to prefectures through which the power is shipped	6,825	9,225	-Measures for the introduction of firms and modernization of industry in regions where the residents of the vicinity of power plant facilities regularly commute to work
3. Hydroelectric power facilities vicinity grants-in-aid	3,994	6,029	-Expenses required for the easing of effects accompanying the establishment of hydroelectric power facilities
4. Nuclear power plant safety measures consignment costs	28,678	35,653	
(1) Nuclear power plant reliability verification tests consignment costs (MITI)	11,685	13,860	-Tests for verification of the safety of nuclear power plants (Nuclear power plant reliability verification tests consignment costs)

(2) Same as above (STA)	6,519	7,455	
(3) Electric power source site promotion investigation consignment costs	2,888	4,669	-Nationwide publicity concerning the necessity and safety nuclear power plants for electric power source site promotion
(4) Nuclear fuel cycle related promotion investigation consignment costs	2,253	2,530	-Publicity activity related to nuclear power plant-related facilities, such as reprocessing facilities
(5) Other	5,334	7,138	
5. Nuclear power plant safety measures subsidy	2,078	5,623	
(1) Electric power source region industry fostering assistance subsidy	1,151	3,260	-Subsidy for industry fostering enterprises cities and villages in the locale of the electric power source region carry out
(2) Electric power source region promotion costs subsidy	0	1,675	-Interest supply and various subsidies for advancing corporate sites in electric power source regions
(3) Other	927	668	
6. Nuclear power plant safety measurements grants-in-aid	5,113	7,022	
(1) Radioactivity inspection grants-in-aid (STA)	2,630	2,403	-Establishment and operation of radioactivity inspection facilities in the vicinity of nuclear power plant facilities
(2) Publicity and safety measures grants-in-aid	1,419	1,331	-Publicity and safety measures regarding nuclear power plants for the resident of the vicinity of nuclear power plant facilities run by local autonomous bodies
(3) Nuclear power plant facilities emergency safety measures grants-in-aid	796	1,163	-Improvement of the facilities required for the establishment of a disaster system in emergencies connected with nuclear power plant facilities

(4) Other	267	2,126	
7. International atomic energy organization contributions	80	87	-International Atomic Energy Agency (IAEA) (7.4 million yen) -Organization of Economic Cooperation and Development (OECD/NEA) (1.3 million yen)
8. Other	1,998	2,082	
9. Totals	142,085	163,066	

Gas Pressure-Sintered ($MoSi_2$-SiC)/TiAl FGM

91FE0069A Tokyo KEISHA KINO ZAIRYO KENKYUKAI in Japanese 22 May 90 pp 1-5

[A series of 19 slides used by Junzo Fujioka, Kawasaki Heavy Industries Ltd., for his presentation at the Ninth Workshop of the Functionally Gradient Material Research Association, 22 May 1990]

[Text]

No. 1

The Ninth Workshop, Functionally Gradient Material Research Association
(22 May 1990, Tokyo)

Development of ($MoSi_2$-SiC)/TiAl Functionally Gradient Material by Gas Pressure Sintering Method

Junzo Fujioka and Yuji Matsuzaki, Akashi Technical Research Institute, Kawasaki Heavy Industries Ltd.

No. 2

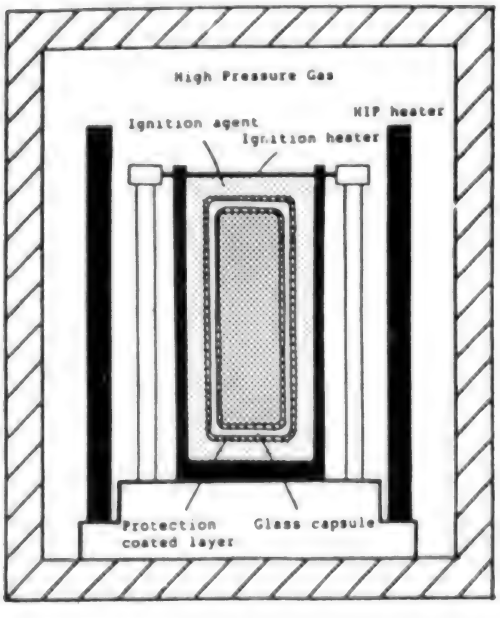

Schematic Diagram of Gas Pressure Sintering Method (as developed by the Industrial Research Institute, Osaka University)

No. 3

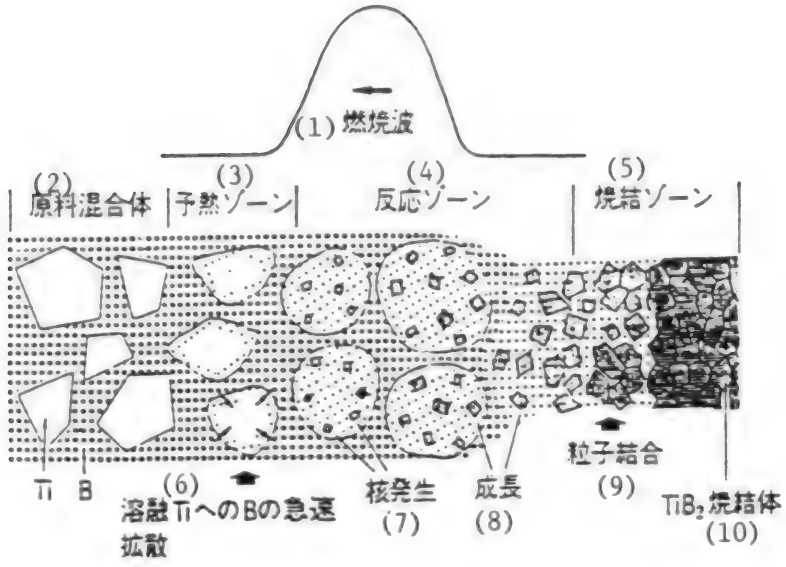

Illustration of Mechanisms of Gas Pressure Sintering Method

Key:

1. Combustion wave
2. Raw material mixture
3. Preliminary heating zone
4. Reaction zone
5. Sintering zone
6. Rapid dispersion of B into molten Ti
7. Nuclei creation
8. Growth
9. Grain bonding
10. TiB_2 ceramic material

No. 4

Characteristics of Gas Pressure Sintering Method

1. High-melting point materials (materials not to be readily sintered), such as carbides, borides, silicides and nitrides, can be sintered without a sintering aid.

2. High-density ceramics can be produced instantaneously.

3. With high energy efficiency due to isotropic pressure application, materials with complex shapes can be produced.

4. By placing an ignition agent around a material to be sintered, a high-melting point material and a metal can be simultaneously sintered, i.e., a functionally gradient material can be produced by combining wide-ranging materials.

No. 5

Characteristics Required for Thermal Stress-Alleviating Functionally Gradient Materials (FGMs)

High-Temperature Side Material	FGM	Low-Temperature Side Material
(1) Heat-shielding capability (2) Heat stability (3) Oxidation resistance	(1) Thermal stress alleviating function (2) Thermodynamic stability	(1) Thermal conductivity (2) Strength (3) Toughness

No. 6

Prospective High-Temperature Side Materials for Thermal Stress-Alleviating FGMs

Material	Auto-exothermic reaction: Reaction	Auto-exothermic reaction: Heats of reaction ΔH^0, KJ/mol	Density, g/cm^3	Melting point, °C	Heat stability: highest use temperature, °C	Thermal expansion coefficient, x 10-6/K [illegible exponential]	Thermal conductivity, W/m·K	Specific heat, J/g·K (R.T. to 1100°C)	Strength: σ_B: tensile; σ_{Be}: bending	Young's modulus, GPa	Fracture toughness, KPa·R1/2	Remarks	
TiB$_2$	○	331	4.5	3225	1200	4.6~5.2	84 (R.T.) 79 (1027°C)	0.6~1.3	σ_{Be}·340 274 (1100°C)	529	5~10	・FGMの基礎材料研究用 ・1300°C付近で急速に酸化 ・大気中最高使用温度900°C	(3)
SiC	○	74	3.2	2540 2200°C から昇華開始 (1)	1650	5.0	42 (R.T.) 13 (1250°C	0.7~1.3	σ_B·172 σ_{Be}·398	386	3~6	酸化雰囲気中1650°C迄使用可 ・熱衝撃温度差： ΔT·300~500°C	(4)
Si$_3$N$_4$	△**	751	3.2	1900 (昇華) (2)	1800~1400	3.4	28 (R.T.)	0.8~1.3	σ_B· 294 (1200°C) σ_{Be}· 69~490 79~480 (1200°C)	55~313	5~6	***同系 _ 成膜困難 熱衝撃温度差： ΔT·500~600°C	(5)
MoSi$_2$	○	109	6.2	2030	1650	8.1	49 (R.T.) 17 (1100°C	0.5	σ_B· 284 (1200°C) σ_{Be}·344 99 (1100°C)	421		・1650°C迄の酸化雰囲気で安定 ・1400°C以上で急速に軟化	(6)
Al$_2$O$_3$	△**	843	4.0	2050	1750~1900	7~9	39 (R.T.) 6 (1000°C	0.8 (0.1~1.1)	σ_B ·245~304 11 (1468°C) σ_{Be}·245~539	343~392	3~5	***SiC との混合合成 $3SiO_2+4Al+3C \rightarrow 2Al_2O_3+3SiC$ 熱衝撃温度差 ΔT·200°C	(7)
ZrO$_2$	△**		6.0	2850	2100	7~10	2 (R.T.) 2.3 (1000°C	0.5~0.7	σ_{Be}·176~784	147~196	1 8~15 MPa	***TiC との混合合成 $TiO_2+2C \rightarrow 2/3O_2+TiC$ 熱衝撃温度ΔT·300~400°C	(8)
TiC	○	233	4.9	3257		8.0	32 (R.T.) 40 (1100°C	0.5~0.9	σ_B ·368 255 (1200°C) σ_{Be}·389~850	451		溶融炉材質で予備実験	(9)

(10) ・データは、下記の文献、資料などから引用した
◎佐多、他門：高温学会誌 15 (1987) 2, 103
◎中村、門崎：耐火物及び特殊断熱材料 (1984, 総文堂)
◎安本：耐火物工学 (1982, 技報堂)
◎ドイツ：ドイツの高温と金属研究 (1977, 日ソ通信社)
◎山口、高橋：金属間化合物 (1984, 日刊工業新聞社)
◎安本：ファインセラミックス (1974, 技報堂)
◎安本、小倉：日経マテリアル (1986, 7月13日号) 79
◎安本：セラミックス 22 (1987) 6, 489
◎L. Pitsar et al.: 5th Int. Conf. Comm. Mater. 1985, p.515
◎A. Cotler et al.: Ceram. Eng. Sci. Proc. 6 (1985) 7/8, 715

1 cal/g·cm·°C	= 419	J/m·K
1 cal	= 4.2	Joul
1 kgf/mm^2	= 9.8	MPa
1 kgf/mm$^{2.5}$	= 9.31	MPa·m$^{0.5}$

Key:

1. Sublimation started at 2200°C
2. 1900 (Sublimation)
3. ·Material good for fundamental studies on FGMs
   ·Rapidly oxidizes at about 1300°C
   ·Highest use temperature in atmosphere is 900°C
4. Usable up to 1650°C in an oxidizing atmosphere
   ·Thermal shock temperature gap: ΔT = 300 to 500°C
5. (*1)Difficult to be simultaneously synthesized and sintered
   Thermal shock temperature gap: ΔT = 500 to 600°C
6. ·Stable up to 1650°C in an oxidizing atmosphere
   ·Rapidly softens above 1400°C
7. (*2)Composite formation with SiC:
   $3SiO_2 + 4Al + 3C \rightarrow 2Al_2O_3 + 3SiC$
   Thermal shock temperature gap: ΔT = 200°C

8. (*2)Composite formation with TiC:
   $TiO_2 + Zr + C \rightarrow ZrO_2 + TiC$
   Thermal shock temperature gap: ΔT = 300 to 400°C
9. Preliminary experiments were conducted with the electric [illegible character] ignition method
10. *Data were taken from sources listed below:

   (1) Sata and Ikeuchi: Journal of Japan Ceramics Industry Association, 95, 2, 243 (1987)
   (2) Mohri and Kawashima: "Fire-Proof Materials and Special Heat Resistant Materials," Seibundo (1964)
   (3) Yoshiki: "Fire-Proof Material Engineering," Gihodo (1982)
   (4) Samsonoff et al.: "Handbook on High Melting Point Compounds," Nisso Tsushinsha (1977)
   (5) Yamaguchi and Magoshi: "Intermetallic Compounds," Nikkan Kogyo Shimbunsha (1984)
   (6) Motoki: "Fine Ceramics," Gihodo (1976)
   (7) Miyamoto and Koizumi: Nikkei Material, 13 Jul 86, p 79
   (8) Miyamoto: Ceramics, 22, 6, 489 (1987)

No. 7

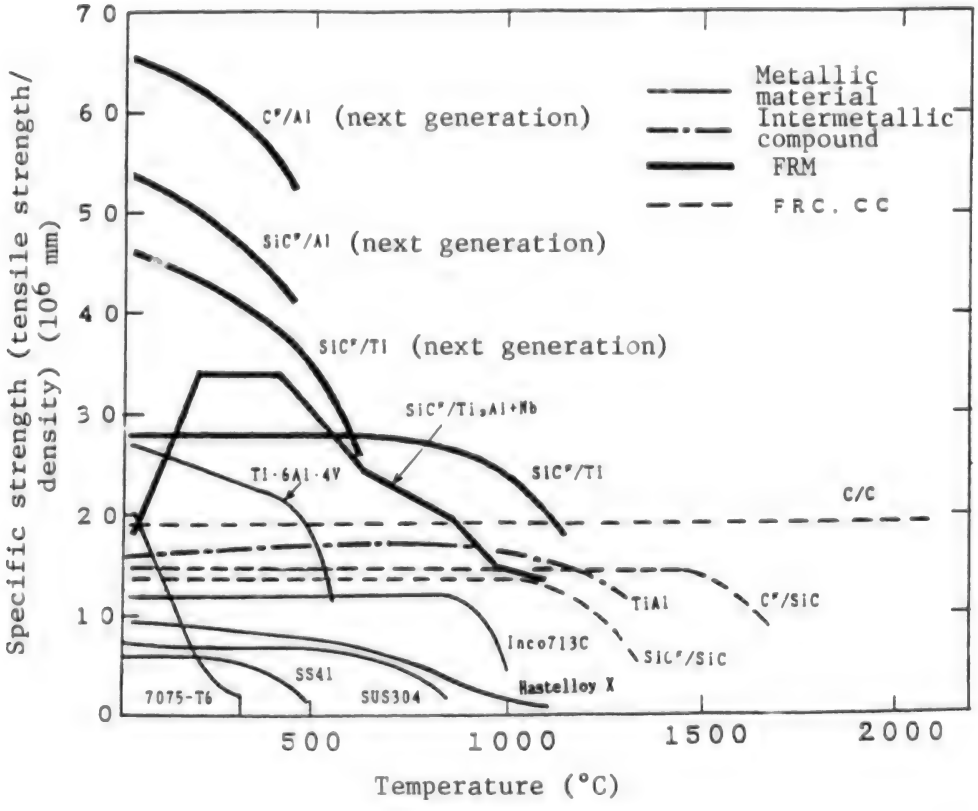

Relationship Between Specific Strength and Temperature of Prospective Low Temperature Side Materials of Thermal Stress Alleviating FGMs

No. 8

Production Method and Development Needs

	Production method	Development needs
1	Raw material powder lamination ·Powder: Mo, Si, $MoSi_2$, SiC, TiAl	(1) Optimal gradient distribution (2) Powder lamination technology ·Automatic powder lamination ·Doctor blade method
2	Molding and hardening ·CIP	(1) Selection of a binder (when the shape of a material is complex) (2) Binder removal technology
3	Encapsulation ·Glass capsule	(1) Vacuum encapsulation technology ·High-temperature encapsulation in a vacuum furnace
4	Gas pressure sintering ·HIP device	(1) Temperature control technology ·Ignition technology ·Heater-heating: temperature rise ·Dilute powder addition: temperature lowering (2) Low pressure sintering technology (3) Larger, more complex shape formation

No. 9

Distribution parameter : n = 1
Maximum specific stress: 5.1
Heat flux : 2.6 MW/m^{-2}

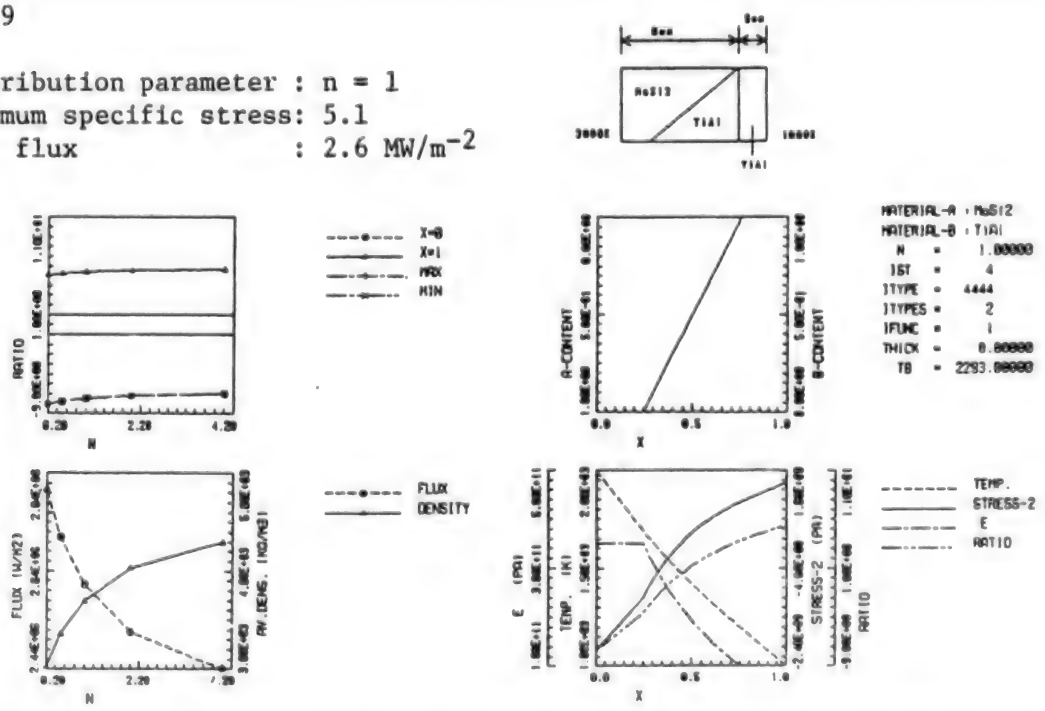

Design Results for ($MoSi_2$-SiC)/TiAl-Base FGM (0-Order Design Based on Literature Data)

No. 10

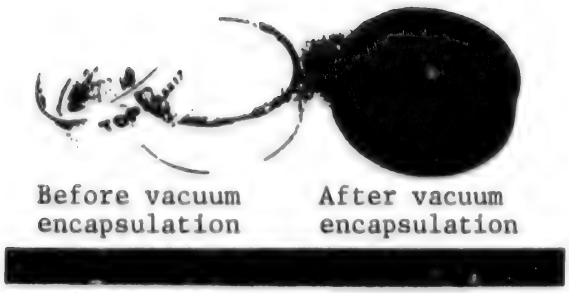

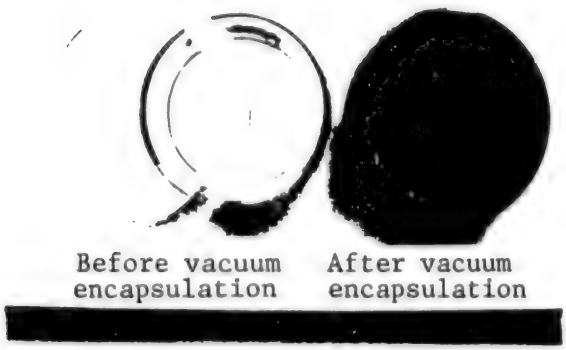

Encapsulation With Petri Dish

No. 11

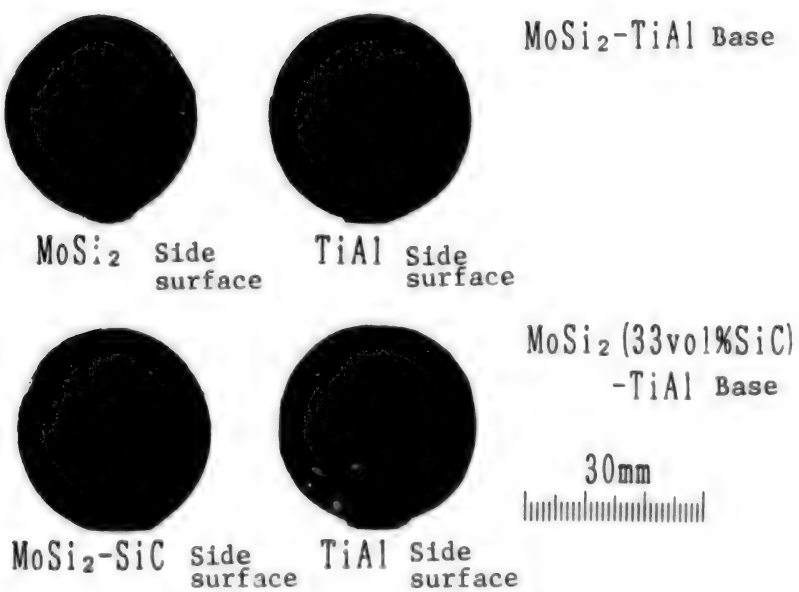

FGM 30 mm in Diameter (showing SiC-addition effect)

No. 12

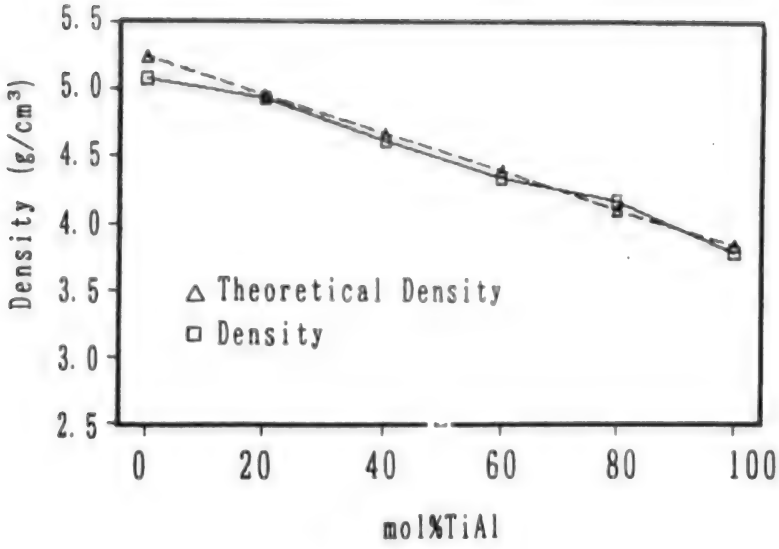

Density of ($MoSi_2$-SiC)-TiAl (0 to 100 weight percent) (NFGM)

No. 13

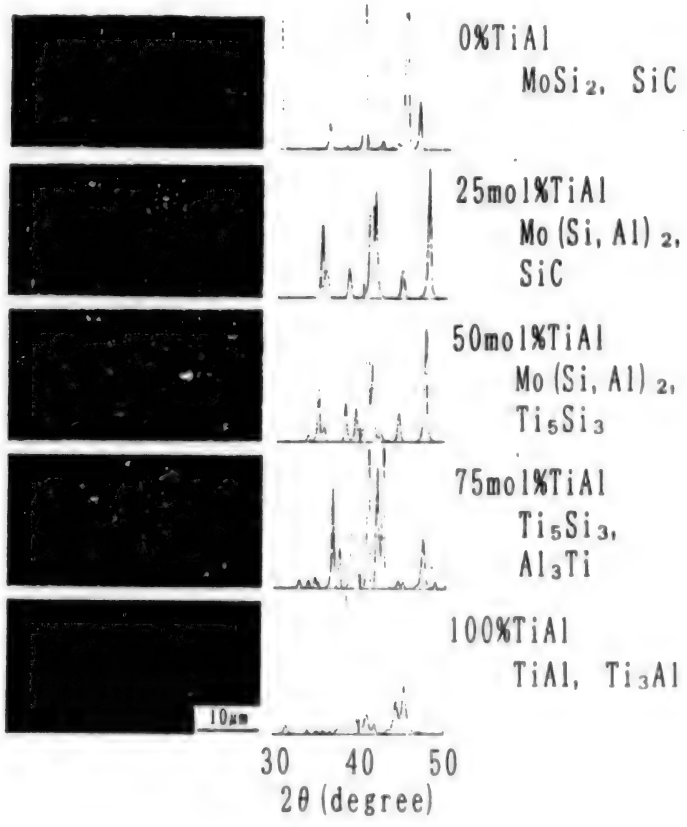

Microstructure and X-Ray Composition of NFGM

No. 14

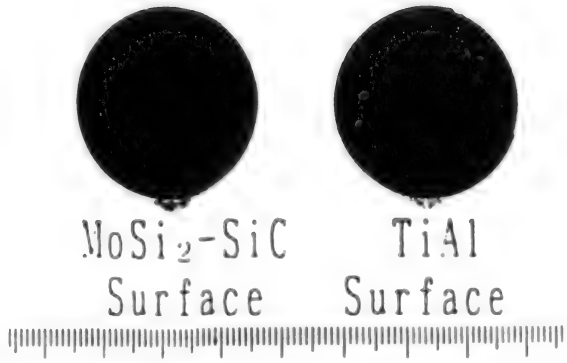

Compositional distribution parameter n = 2

Compositional distribution parameter n = 0.5

Compositional distribution function $f(x) = (x/t)^n$,

f(x): Mol percent of TiAl
x: Distance of FGM layer from surface
t: FGM layer thickness

FGM 30 mm in Diameter (showing the effect of compositional distribution function)

No. 15

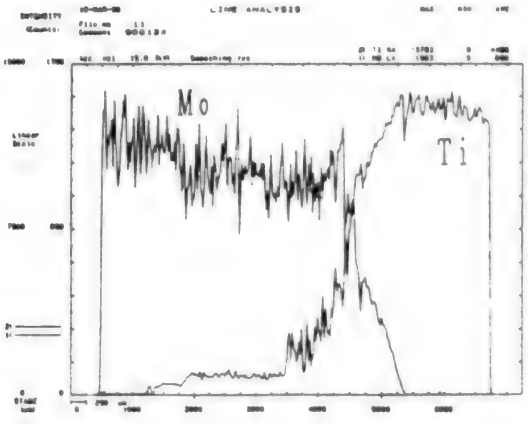

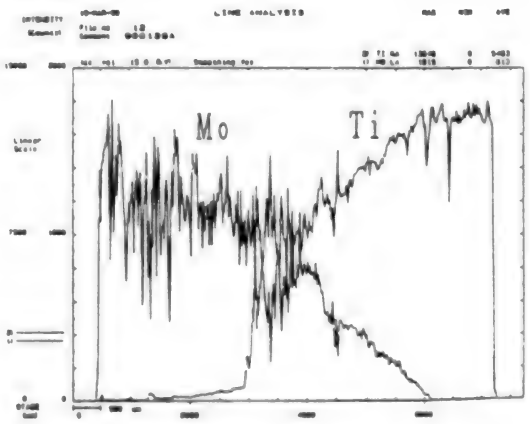

Element Concentration Distribution at Cross-Sectional Plane of FGM 30 mm in Diameter

(Left graph) Compositional distribution parameter n = 2
(Right graph) Compositional distribution parameter n = 0.5

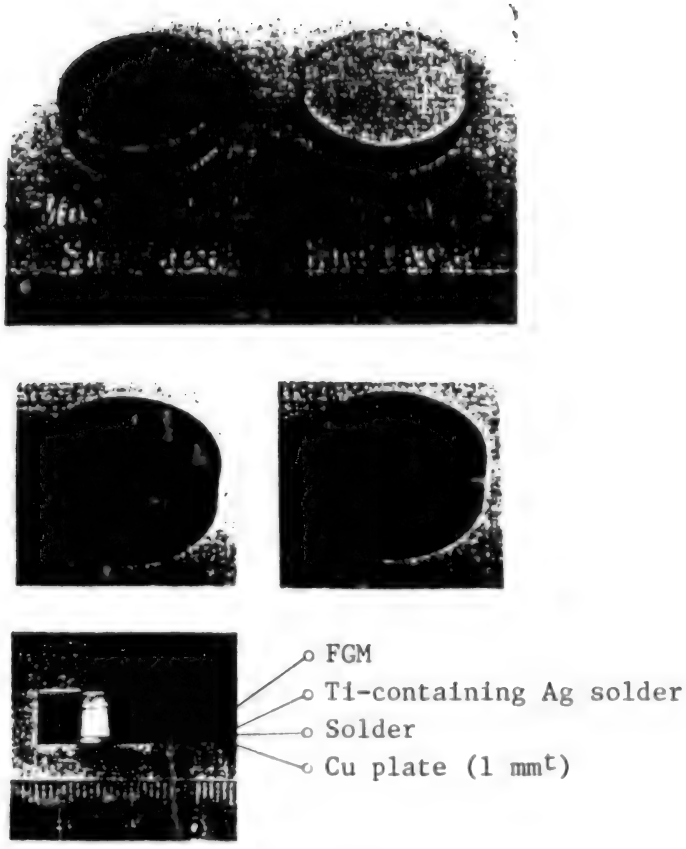

Samples for High-Temperature Gap Tests

No. 17

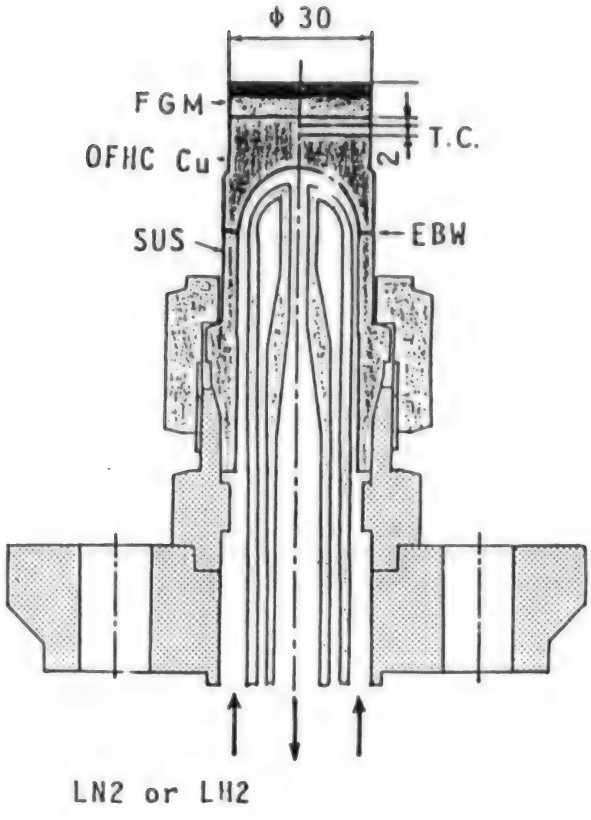

FGM Sample Mounted on High-Temperature Gap Test Apparatus
(Akinaga Kumagawa: Sixth Workshop Paper, FGM Research Association, 21 June 1989)

No. 18

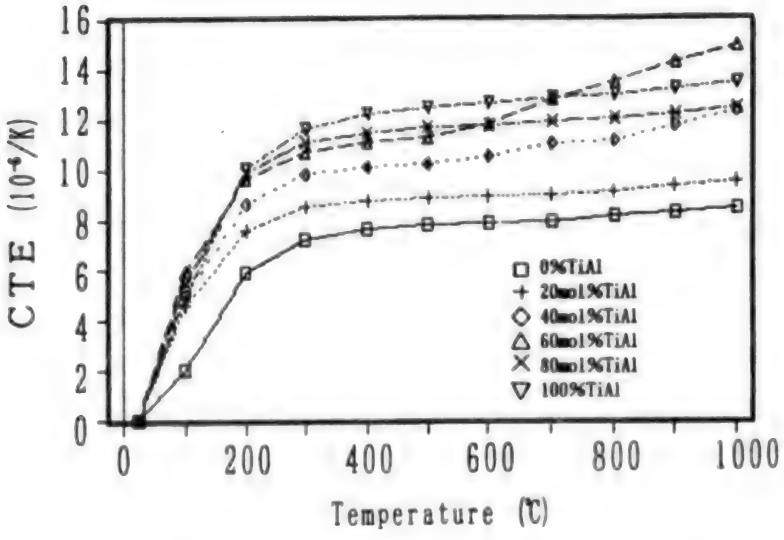

Average Thermal Expansion Coefficient of NFGMs

No. 19

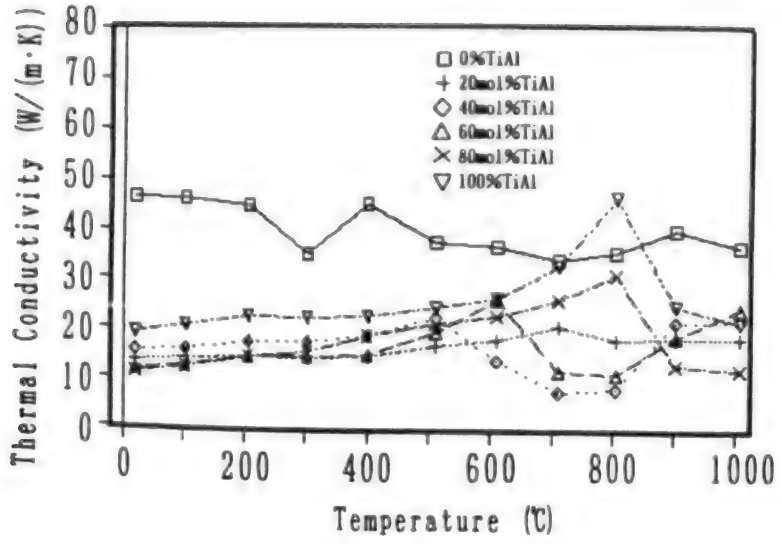

Thermal Conductivity of NFGMs ($MoSi_2$: 10W/(m·K) at 1600 to 1800K)

Fabrication Process, Evaluation of FGMs

90FE0317A Tokyo SHIN SOZAI 21 SEKI FORUM in Japanese 24 Apr 90
pp 29-34

[Article written by Ryuzo Watanabe, Material Processing Department, Faculty of Engineering, Tohoku University]

[Text] Introduction

Functions most suitable for a material to use environments may be distributed by creating gradients in the internal composition and microstructure of the material. If not, whatever material function one desires may be manifested through gradient formation of the material's composition and structure.

Functionally gradient materials (FGMs) were born as a product of these ideas. In other words, various different materials, including metals, ceramics and plastics, are combined, and gradients are formed in the mixtures' compositions and structures, in order to gradiently distribute material properties for functional manifestation. Industrial material fields that are expected to benefit from the application of FGMs are wide-ranging, as shown in Figure 1. In particular, applications of such functions as environmental stability, joint formation, electromagnetic, opto-acoustic, chemical and biocompatibility, are anticipated with great interest.

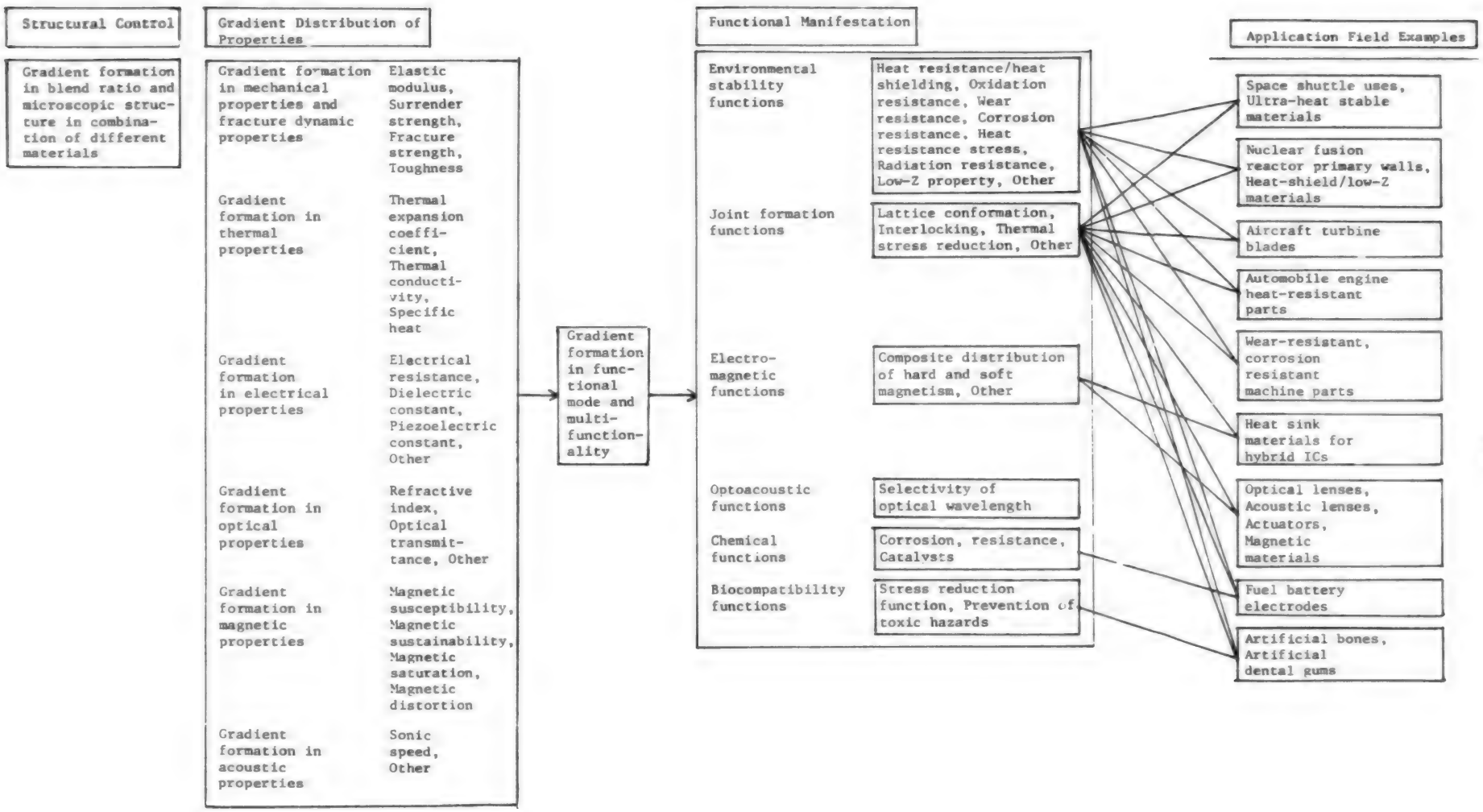
Structural Control
Gradient formation in blend ratio and microscopic structure in combination of different materials
Gradient Distribution of Properties
Gradient formation in mechanical properties and fracture dynamic properties
Elastic modulus, Surrender strength, Fracture strength, Toughness
Gradient formation in thermal properties
Thermal expansion coefficient, Thermal conductivity, Specific heat
Gradient formation in electrical properties
Electrical resistance, Dielectric constant, Piezoelectric constant, Other
Gradient formation in optical properties
Refractive index, Optical transmittance, Other
Gradient formation in magnetic properties
Magnetic susceptibility, Magnetic sustainability, Magnetic saturation, Magnetic distortion
Gradient formation in acoustic properties
Sonic speed, Other
Gradient formation in functional mode and multifunctionality
Functional Manifestation
Environmental stability functions
Heat resistance/heat shielding, Oxidation resistance, Wear resistance, Corrosion resistance, Heat resistance stress, Radiation resistance, Low-Z property, Other
Joint formation functions
Lattice conformation, Interlocking, Thermal stress reduction, Other
Electromagnetic functions
Composite distribution of hard and soft magnetism, Other
Optoacoustic functions
Selectivity of optical wavelength
Chemical functions
Corrosion, resistance, Catalysts
Biocompatibility functions
Stress reduction function, Prevention of toxic hazards
Application Field Examples
Space shuttle uses, Ultra-heat stable materials
Nuclear fusion reactor primary walls, Heat-shield/low-Z materials
Aircraft turbine blades
Automobile engine heat-resistant parts
Wear-resistant, corrosion resistant machine parts
Heat sink materials for hybrid ICs
Optical lenses, Acoustic lenses, Actuators, Magnetic materials
Fuel battery electrodes
Artificial bones, Artificial dental gums

Today, the development of FGMs targets primarily on ultra-heat-resistant materials of a thermal stress alleviation type, which can withstand high temperature gap environments, for ultimate applications for aerospace Today, the development of FGMs targets primarily on ultra-heat-resistant planes' fuselage and engine parts. In these applications, an extremely complex design is required of a material as follows. A heat-shielding property and heat resistance need to be imparted to the high-temperature side of a material, while high toughness and joint-formation function must be imparted to the low-temperature side, and in addition, the material as a whole needs to manifest a thermal-stress alleviation function to reduce thermal stresses caused by the temperature gap. There are many ways to blend different substances at a desired composition and to form a gradient of the composition in the composite. Methods range from the vapor deposition method, that deposits an atomic or molecular layer on top of another, to the method of laminating thin sheets. Methods currently under development include PVD, CVD, plasma sputtering method, electrodeposition method, auto-exothermic method, slurry lamination method and particle arrangement/sintering method[1]. Each of these method is characterized by the material size it can produce and by the microscopic structure it can form. Judging from today's level of technologies, we may be able to say that PVD and CVD are for thinner materials, the particle arrangement/sintering method is for thicker materials, and other methods are for intermediate materials. This paper will deal with the preparation and evaluation of thermal stress-alleviating type FGMs prepared by the powder process (particle arrangement/sintering method), which has the highest degree of freedom in composition control, structural control and shape formation.

Production Process

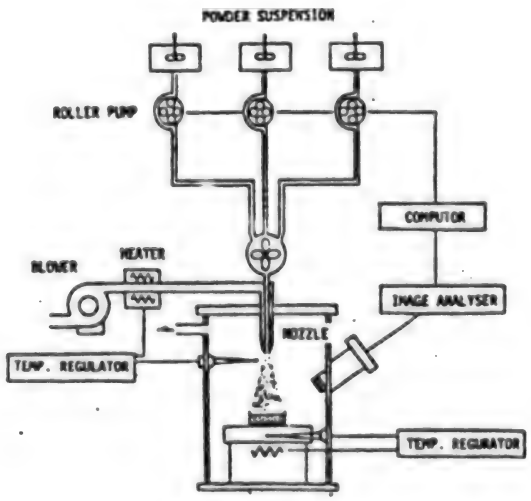

Figure 2. Particle Spouting Arrangement Device for Compositional Gradient Formation

First of all, raw material selection and material design must be carried out in order to achieve targeted functions (which may be heat-shielding, heat-withstanding, toughness and thermal stress alleviating functions). For raw materials, ceramic powders are used for the high-temperature side, while metal or plastic powders are used for the low-temperature side. In some instances, ceramics and metal whiskers are used to control various thermomechanical properties. Raw material powders will be arranged in either a step-wise lamination or a continuously changing distribution according to a blend ratio as designed in advance. Subsequently, the powders are molded in a metal mold under compression or molded with hydraulic pressure, and the green compact is sintered with or without pressure. The author's group developed a particle spouting arrangement device, as shown in Figure 2, to arrange particles under precision composition control. Because generally there are significant differences in sintering temperatures between ceramic and metallic powders, it is technically critical to ensure balanced sintering between different types of powders, as will be discussed in the next section[2]. Also being developed is a temperature gradient-added sintering device (Figure 3), which will give a sintering temperature appropriate for each component raw material, in order to expand the utility range of an available powder raw material, and therefore, to be able to manifest functions with a larger degree of freedom. In order to solve various technical problems concerning FGM preparation according to the above-described process, the author's group pursued fundamental studies primarily using combinations of zirconia ceramics and metals, including nickel, molybdenum and stainless steel[3,4,5,6].

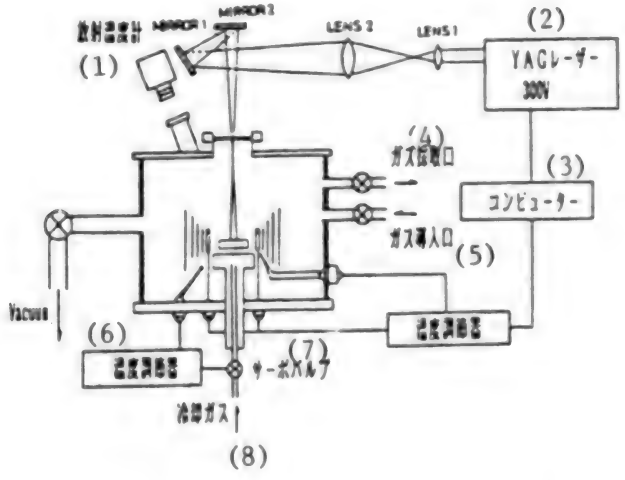

Figure 3. Temperature Gradient-Added Sintering Device

Key:

1. Radiation thermometer
2. YAG laser
3. Computer
4. Gas collection port
5. Gas inlet
6. Temperature adjusting device
7. Servovalve
8. Gas coolant

Sintering Characteristics Dependent On Composition

Sintering behaviors of a blend of ceramic and metallic powders are uniquely dependent on the blend ratio of the two powders. In general, when sintering shrinkage behaviors are not uniform due to a compositional difference, various flaws will be formed in a compositional gradient-arranged material. In Figure 4, typical flaws caused by sintering imbalance are schematically illustrated. Pressurized sintering methods, such as hot press and HIP methods, are extremely effective in reducing the influences of sintering balance, or lack of balance, due to composition.

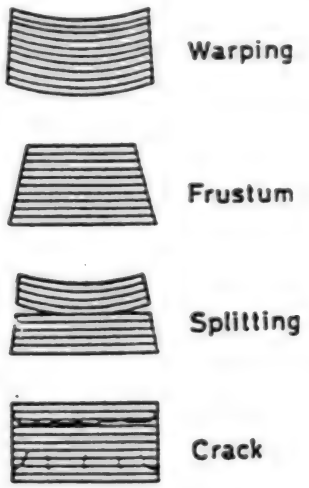

Figure 4. Flaws Created by Sintering Imbalance

Size of Composition Control Region

Today, the thickness of a layer of one composition is limited to approximately 100 microns in the case of the step-wise lamination arrangement packing. Therefore, through arrangement of 10 layers, approximately 1-mm-thick gradient layer will be formed. On the other hand, if a particle spouting arrangement device, as shown in Figure 2, is used, one can freely create compositional distribution ranging from ceramics to metals within a thickness of 100 to 200 microns. Shown in Figure 5 is a photograph of the structure of a zirconia/stainless steel-base thermal stress alleviating-type FGM which was prepared by the particle spouting arrangement method.

Material Design to Create Thermal Stress Alleviation Function

There are two key points to material design to create the thermal stress alleviation function. One is to predetermine the compositional distribution of a material so as to keep the thermal stress, which is generated during rapid cooling from a high temperature to room temperature, sufficiently smaller than the material's strength[7]. This point is unique to any high-temperature preparation process starting from powder raw

materials. The other is the design of a functional gradient for alleviating thermal stress due to the temperature gap in the real environment[5]. In order to design such a material, one needs data concerning relationships between composition and various physical properties (thermal expansion coefficient, thermal conductivity, elastic constant and fracture strength). Using these data and assigning a sample shape and size as well as temperature conditions, a compositional distribution that minimizes thermal stress will be obtained by the finite element method. It has been found from previous studies that an optimal design for alleviating thermal stress during a preparation process is also effective in alleviating thermal stress due to a temperature gap[5]. In addition, a study is underway concerning optimal designs that simultaneously consider thermal stresses at the preparation and at the actual use.

Structural Change Accompanying Compositional Change

An FGM made by sintering has unique structural transition, as shown in Figure 6. The structures at both extreme compositions are dispersions in which a matrix and a dispersed phase are reversed. The intermediate structure is a network structure in which the structure continually changes with the composition. The compositional phase changes continually and rapidly at a rate of 0.2 to 0.8 ceramic volume fraction[8].

Relationships Between Composition and Properties

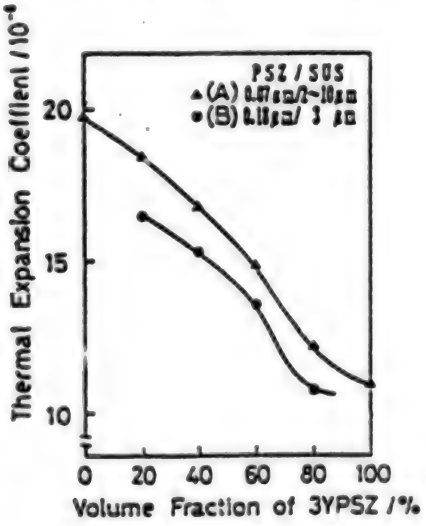

Figure 7. Relationship Between Thermal Expansion Coefficient and Composition for Zirconia/Stainless Steel-Base Sintered Mixture

The relationships between composition and properties, such as thermal expansion coefficient, thermal conductivity and electrical conductivity, are shown by reverse-S curves in Figures 7, 8 and 9 [TN: Captions for Figs. 8 and 9 are reversed], in correspondence with structural transition. These curves are considered to represent transitional forms of the

Maxwell formula, which concerns the two types of dispersed structure formed at the two extreme compositions, for the intermediate compositions[9]. On the other hand, properties, such as Young's modulus and bending strength, appear to behave in a complex manner depending on structural characteristics or the degree of bonding/debonding between ceramic and metallic phases[3,10].

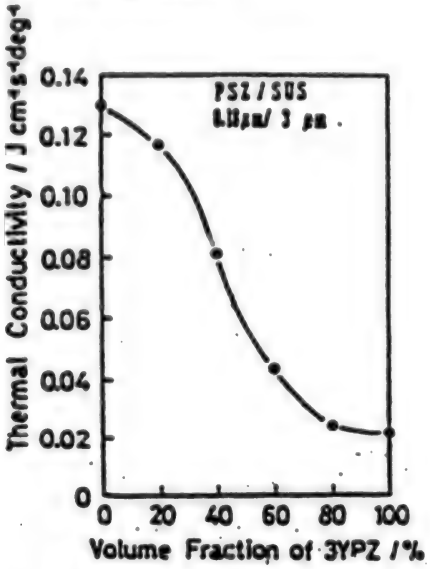

Figure 8. Relationship Between Thermal Conductivity and Composition for Zirconia/Stainless Steel-Base Sintered Mixture

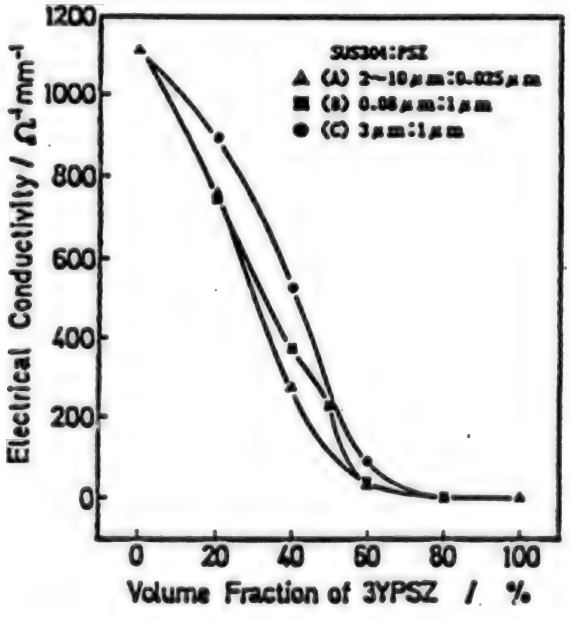

Figure 9. Relationship Between Electrical Conductivity and Composition for Zirconia/Stainless Steel-Base Sintered Mixture

Pliability and Brittleness Transition and SP Test

As the composition changes continually from a metal to a ceramic material, the material's pliability and brittleness will also change. These changes can be found through SP (small punch) tests [10,11]. An SP test device is schematically presented in Figure 10. The area (SP energy) bounded by a load-displacement curve obtained by this test will be a measure for a sample's pliability. Shown in Figure 11 is the relationship between SP energy and composition. The curve shows that the property changes from pliable nature to complete brittleness as the ceramics' volume fraction changes from 20 to 80 percent. It is keenly important to widen the pliable region in this pliability-brittleness transition for improving fracture toughness of an FGM and increasing the degree of freedom for designing it. Efforts are being made to widen the region through structural micronization and blending of metallic and ceramic whiskers.

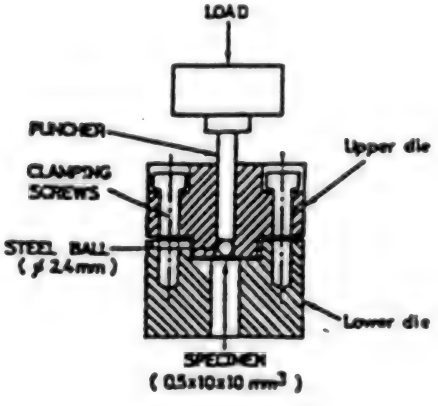

Figure 10. Schematic Diagram of Small Punch Tester for FGM Development

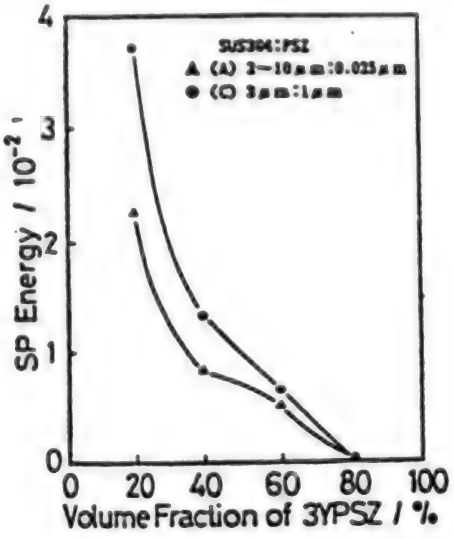

Figure 11. Transition from Pliability to Brittleness With Compositional Change in Zirconia/Stainless Steel-Base Sintered Mixture

Thermal Shock Test

A laser thermal shock test device, which was developed for testing FGMs for thermal shock resistance, is schematically illustrated in Figure 12[12]. The device uses an AE sensor to clearly describe a material's fracture behavior. By using this device, it was discovered that the zirconia/stainless steel-base FGM, prepared by the particle spouting method, was approximately three times more resistant to thermal shocks than pure zirconia (3YPSZ).

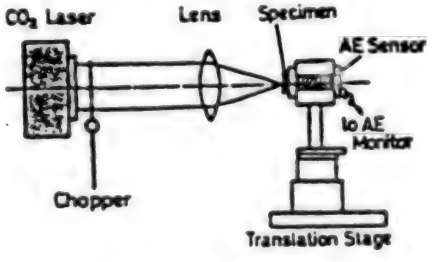

Figure 12. Schematic Presentation of Laser Thermal Shock Test for Thermal Shock Resistance Evaluation of FGMs

High Temperature Gap Subjection Test

A temperature gap tester, which applies a temperature gap between the front and the back of an FGM sample, has been developed to evaluate its heat shielding property and thermal stress alleviation function[13]. The device is capable of giving a constant thermal load of up to 5 MW/m^2 to a sample while cooling the sample's back with liquid nitrogen. In addition, the author's group devised a burner-heating test method which can evaluate more readily an FGM's performance against temperature gaps.

Thus far, a surface temperature of 1,400K and a temperature gap of 900K have been obtained with a 4-mm-thick, disc-shaped zirconia/stainless steel-base sintered FGM.

Epilogue

Three years have passed since the start of the FGM research project (sponsored by the Science and Technology Promotion Coordination Fund). It has been found that the first term's target, a 30-mm-diameter, 1 to 10-mm-thick FGM, can be prepared through several routes. FGMs are much more diverse than conventional, homogeneous materials in all aspects ranging from material preparation to application. The currently prevailing cooperation system between design and evaluation experts is likely to become increasingly important in the future.

References

1. Third FGM Symposium Lecture Collection, FGM Research Association (1989).

2. Watanabe: Kino Zairyo 8, 932 (1989).

3. Watanabe, Kawasaki and Murahashi: Sozai Busseigaku Zasshi 1, 36 (1988).

4. Kawasaki and Watanabe: Powders and Powder Metallurgy 37, 73 (1990).

5. Watanabe: Ceramics 24, 932 (1989).

6. R. Watanabe, A. Kawasaki and H. Takahasi: To be published in Proc. MECAMAT Intern. Confe. Saint-Etienne, France, Nov. (1989).

7. Kawasaki and Watanabe: Journal of Japan Metal Science Society 51, 525 (1987).

8. Uchiyama, Kawasaki and Watanabe: Third FGM Symposium Lecture Collection, p. 161.

9. Kawasaki and Watanabe: ibid. p. 35.

10. Kawasaki, Watanabe, Cheng and Takahashi: Powders and Powder Metallurgy 36, 143 (1989).

11. Saito, Cheng, Takahashi, Kawasaki and Watanabe: ibid. 37, 350 (1990).

12. Hashida, Takahashi and Miyawaki: ibid. 37, 307 (1990).

13. Kumakawa, Sasaki, Maeda and Adachi: ibid. 37, 313 (1990).

Thermally Resistant FGMs by CVD Method

90FE0317B Tokyo SHIN SOZAI 21 SEKI FORUM in Japanese 24 Apr 90
pp 35-40

[Article written by Chihiro Kawai et al., Sumitomo Electric Industries, Ltd.]

[Text] 1. Introduction

Recently, plans to develop ultrahigh speed airframes, including space shuttles, have been proposed in several countries. Super-heat resistant materials that have excellent strength and oxidation resistance at high temperatures are demanded for fuselage thermal insulators and burners of these airframes.

Carbon fiber-reinforced carbon composites (C/C composites) are one of the most promising materials for that purpose because of their excellent specific strength and specific rigidity at temperatures higher than 1,000°C. However, C/C composites have serious deficiencies in oxidation resistance and the difficulty of ceramic coating for imparting antioxidation stability. In other words, because C/C composites have an extremely small thermal expansion coefficient, a coating layer (SiC) will show thermal cracks in a post-coating heating cycle, significantly lowering oxidation resistance.

The objective of this research is to prepare a coated carbon fiber-reinforced composite with excellent antioxidation stability through the compositional gradient formation in the coating layer by the CVD method and the replacement of carbon, the matrix in the C/C composite, with a ceramic material, to reduce thermal stress between the matrix and the coating layer.

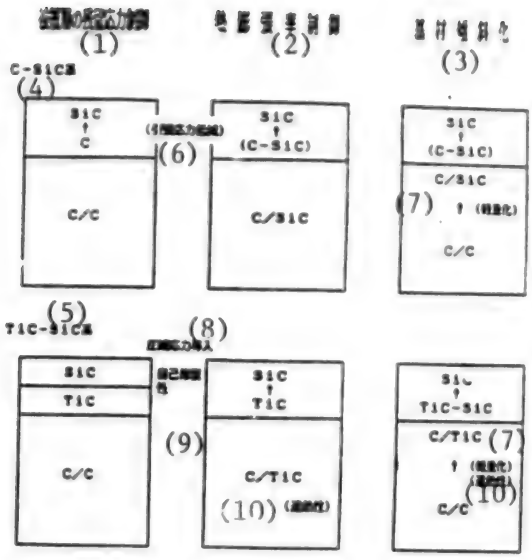

Figure 1. Conceptual Diagrams for Compositional Gradient Coating and Functional Gradient Matrix Formation To Produce Super Heat Resistant Structural Material

Key:

1. Control of Residual Stress in Coating Layer
2. Control of Thermal Expansion Rate
3. Formation of Gradient in Matrix
4. C-SiC-Base
5. TiC-SiC-Base
6. (Tensile Stress Reduction)
7. (Weight Reduction)
8. Compression Stress Introduction
9. Self-Restorativeness
10. (Thermal Insulation Capability)

The coating layer's thermal expansion coefficient was controlled by compositional gradient formation as follows. In order to reduce tensile stress generated in the surface layer of SiC, a C-SiC-base ceramic material, which contains carbon with a small thermal expansion coefficient and a small Young's modulus, is selected for the interface between the coating and a C/C composite, and compression stress was intentionally introduced to the surface layer of SiC to make it extremely strong. In order to control the occurrence of thermal cracks in the surface layer, a TiC-SiC-base ceramic material, which contains TiC with a thermal expansion coefficient larger than SiC's, was selected for the interface.

For controlling the substrate's thermal expansion coefficient, C/Ceramics composites, in which the matrix C of a C/C composite was replaced with SiC or TiC, were used to increase the substrate's thermal expansion coefficient.

Conceptual diagrams for the targeted, coated carbon fiber-reinforced composites are shown in Figure 1.

2. Preparation of FGMs by CVD Method

(1) C-SiC-base Compositional Gradient Coating[1,2]

The compositional gradient coating by the CVD method needs to be examined from the standpoints of composition control and precipitation rate.

The CVD-precipitation phase diagram with raw materials of $SiCl_4$, CH_4 and H_2, as shown in Figure 2, was prepared from thermodynamic data by computer simulation. The compositions of $SiCl_4$ and CH_4 were changed along the line A in Figure 2, and coating[4] was done with C-SiC-base materials of various compositions.

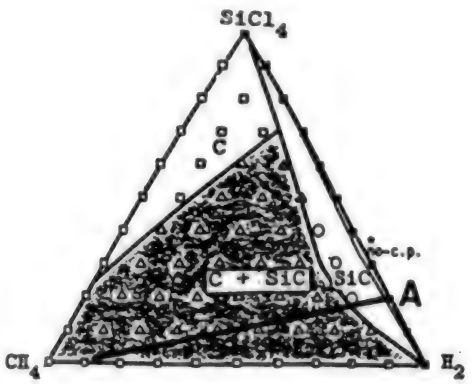

Figure 2. Equilibrium Precipitation Phase Diagram for $SiCl_4$-CH_4-H_2 System (at 1,400°C and 60 torr)

The relationship between the Si/C mol ratio in a raw material gas and the composition of a precipitated layer is shown in Figure 3. The experimental composition was richer in SiC than the thermodynamic equilibrium composition. The higher the C content in the precipitated layer, the total precipitation speed became slower.

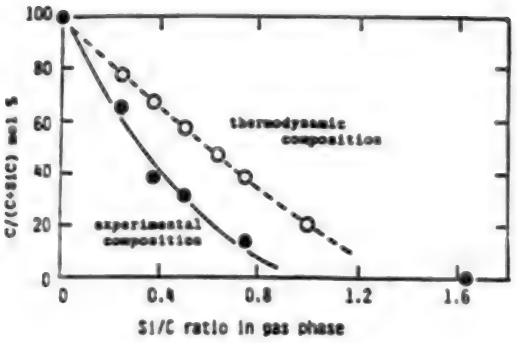

Figure 3. Relationship Between Raw Material Gas Composition and Precipitated Layer Composition

It is conjectured that the precipitation speed retardation is due to the slower precipitation speed of C than that of SiC. Structures of C-SiC-base composite layers of various compositions are shown in Figure 4. With increasing C content, the structure became more porous.

A cross sectional structure of a C-SiC-base compositional gradient layer, which has been coated over a C/C composite, is shown in Figure 5.

By using a C-SiC-base compositional gradient layer as the coating layer for a C/C composite, the occurrence of thermal cracks in the outermost layer of SiC was lessened but not completely eliminated.

This is presumably because (i) the thermal expansion coefficient of the coating layer is almost the same as that of SiC due to the lack of orientation by C in the C/SiC composite structure, and (ii) the composition distribution in the compositional gradient layer is not optimal due to the slow precipitation speed of C-rich composition regions.

From the above discussed data, it was clarified that the matrix would need a greater thermal expansion coefficient in order to thoroughly display the thermal stress alleviation function.

(2) TiC-SiC Double-Layer Coating[3,4,5]

The antioxidation stability of a C/C composite can be significantly improved by coating first a TiC layer over it and then an SiC layer over the TiC layer.

The antioxidation stability of a C/C composite after double-layer coating of TiC and SiC is shown in Figure 6 in terms of the weight lost due to oxidation against the thickness ratio of TiC/SiC in

the coating layer. Also, in Figure 7, the residual stress is plotted against the same thickness ratio.

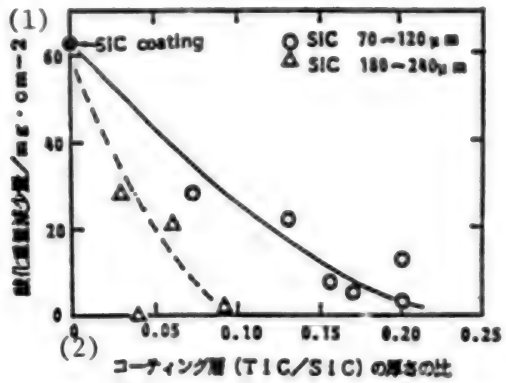

Figure 6. Antioxidation Stability of TiC/SiC-Double Layer Coated C/C Composite

Key:
1. Oxidation weight loss, mg/cm^2
2. Thickness ratio in coating layers (TiC/SiC)

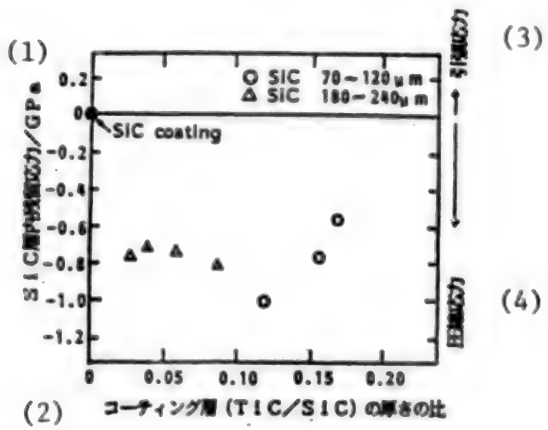

Figure 7. Residual Stress vs. TiC/SiC Thickness Ratio in Double Layer Coating

Key:
1. Residual stress in SiC layer, GPa
2. Thickness ratio in coating layers (TiC/SiC)
3. Tensile stress
4. Compression stress

The antioxidation stability increases presumably because (i) thermal crack formation in the SiC surface layer is controlled through the introduction of compression residual stress in the surface layer, and (ii) the composite can restore itself by having TiO_2, produced by oxidation reaction of TiC in the internal layers, fill in thermal cracks, as shown in Figure 8.

However, as long as some thermal cracks remain on the SiC surface layer, oxidation will slowly advance after each heating cycle. In order to effectively solve this problem, it is conjectured necessary to make the matrix's thermal expansion coefficient as close as possible to that of TiC and to completely prevent thermal crack formation by creating a TiC-SiC-base compositional gradient layer for the coating layer.

(3) TiC-SiC-base Compositional Gradient Coating[2]

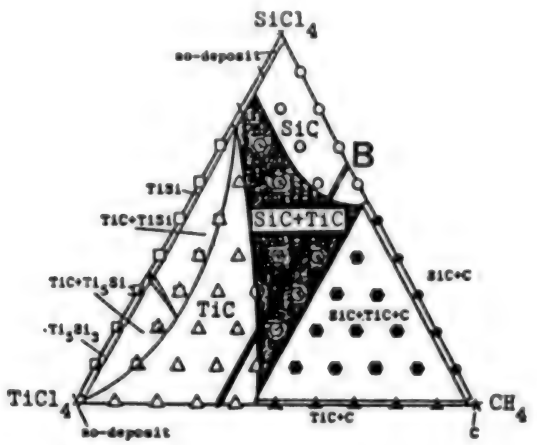

Figure 9. Equilibrium Precipitation Phase Diagram for $SiCl_4$-$TiCl_4$- CH_4-H_2 System (at 1,350°C and 60 torr)

The CVD-precipitation phase diagram with $SiCl_4$, $TiCl_4$, CH_2 and H as raw materials, as shown in Figure 9, was prepared from thermodynamic data by computer simulation. The compositions of $SiCl_4$ and $TiCl_4$ in a raw material gas mixture were changed along the line B in Figure 9 to vary the composition of TiC-SiC-base coating. After each coating, the composition, density and hardness of the precipitated layer were examined.

Shown in Figure 10 is the relationship between the Si/Ti mol ratio in a raw material gas mixture and the composition of a precipitated layer.

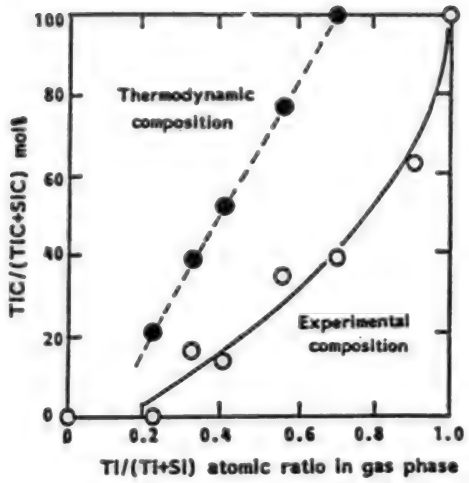

Figure 10. Relationship Between Raw Material Gas Composition and Precipitated Layer Composition

Shown in Figure 11 is the relationship between the composition of a precipitated layer and the precipitation speed. Unlike the C-SiC system, the precipitation speed was found not dependent on the composition but remaining roughly constant. Thus, the composition distribution of the compositional gradient layer could be controlled easily.

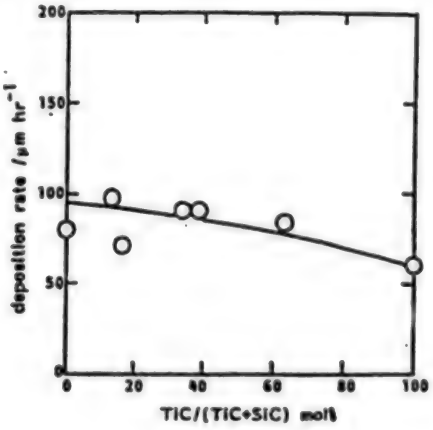

Figure 11. Relationship Between Precipitated Layer Composition and Precipitation Speed

The structures of TiC-SiC composite layers of different compositions are shown in Figure 12, and the relationship between the composition and the microscopic hardness is shown in Figure 13. In contrast with the C-SiC system with a porous structure, this composite has a dense and high-hardness structure, composed of oriented, prismatic crystals, over a wide range of composition.

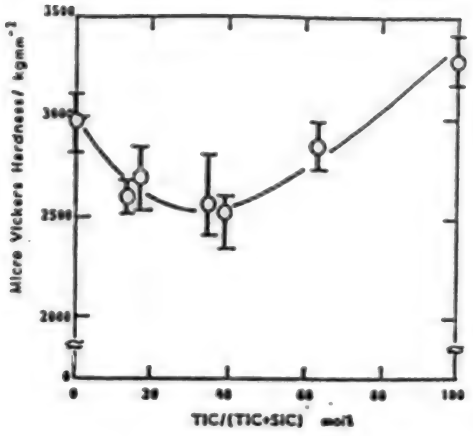

Figure 13. Relationship Between Precipitated Layer Composition and Hardness

Based on the above-described composition-control technologies, various carbon fiber-reinforced composites, including C/C composite, were coated with a TiC-SiC compositional gradient layer, and the coated materials were examined for their antioxidation stability.

The cross sectional structure of a TiC-SiC compositional gradient layer is shown in Figure 14.

The antioxidation stability of these coated composites is shown in Figure 15.

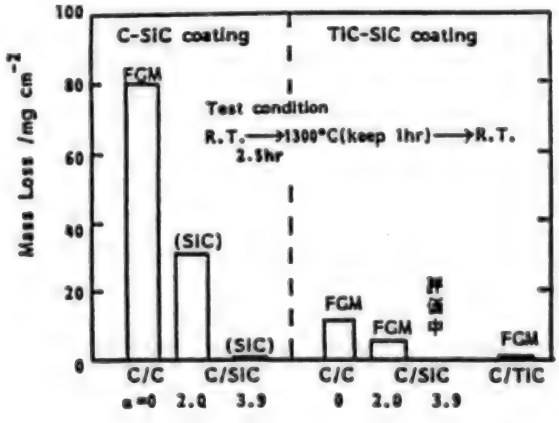

Figure 15. Antioxidation Stability of Various Coated Carbon Fiber-Reinforced Composites

By the same reason as that given for the TiC-SiC double layer coating, the coating of the compositional gradient layer significantly improved the antioxidation stability of the matrix. [TN: This sentence is incomplete in the text.]

3. Functional Gradient Formation in C/C Composite[8]

(1) Preparation of C/SiC and C/TiC Composites

It is effective to create a compositional gradient on the surface of a matrix, when a compositional gradient layer having the thermal stress alleviation function is to be formed by CVD-coating.

As a basic study of the technology to form a functional gradient in a C/C composite matrix, we used the powder sintering method to prepare various carbon fiber-reinforced composites in which the C-matrix was replaced with SiC; coated the composites with SiC and examined the effectiveness of the coating by antioxidation stability tests.

The surface structures of the coated layers are shown in Figure 16.

By controlling the thermal expansion coefficient of the matrix, we were able to coat the SiC layer without forming thermal cracks.

Added to previously mentioned Figure 15 is the antioxidation stability of a C-SiC coated carbon fiber-reinforced composite. It was found that the composite's antioxidation stability would significantly improve by controlling the matrix's thermal expansion coefficient through the replacement of its C-matrix with SiC.

We have also prepared a C/TiC composite, in which its C-matrix was replaced with TiC, and are now investigating its combination with a TiC-SiC compositional gradient layer. Our goal is to further increase the matrix's expansion coefficient and improve its heat shielding capability.

(2) Preparation of Compositional Gradient C/C-SiC Composite

We are also currently studying a C/C-SiC compositional gradient composite in which the matrix component of a C/C composite varies from total carbon at the internal layer to SiC at the outer layer. Our objective here is to prepare a carbon fiber-reinforced composite that can maintain excellent heat resistance and strength at high temperatures as in a C/C composite and can be coated with an antioxidation layer without forming thermal cracks.

Using electrophoresis, two kinds of prepreg sheet were prepared by depositing self-sintering coke powder, for one, and SiC powder, for another, onto pieces of woven carbon fiber cloth. These two sheets were laminated with various lamination patterns, followed by molding, compression and baking to produce compositionally gradient carbon fiber-reinforced composites.

One example of the composites is shown in Figure 17. By using this method, it is comparatively simple to prepare carbon fiber-reinforced ceramic composites having the matrix of different types of ceramics, in addition to C and SiC.

4. Future Studies

Our research has for the present established FGM synthesis technology, and is now at the stage of completing elementary evaluation of FGMs, including that of antioxidation stability. In order to further develop research concerning FGMs, it is extremely important to pursue not only synthetic technology, but also material design based on the evaluation of basic properties of non-functionally gradient materials (NFGMs).

At the same time, we are also pursuing research concerning the thermal stability of compositional gradients under a temperature gradient as well as a concentration gradient in a high temperature region, because FGMs are the so-called non-homogeneous materials[7,8].

References

1. Chihiro Kawai and Yasushi Igarashi: Third FGM Symposium Lecture Collection (1989) p 79.

2. Chihiro Kawai and Yasushi Igarashi: Lecture Abstracts, Japan Metal Science Society Fall Meeting (1989) p 721.

3. Chihiro Kawai, Yasushi Igarashi and Koichi Iwata: Lecture Abstracts, Japan Metal Science Society Spring Meeting (1989).

4. Chihiro Kawai and Yasushi Igarashi: Lecture Draft Collection, Annual Meeting, Japan Ceramics Association (1989) p 395.

5. Chihiro Kawai and Yasushi Igarashi: Lecture Draft Collection, Second Fall Symposium, Japan Ceramics Association (1989) p 222.

6. Tomoyuki Wakamatsu, Masanori Sakagami, Makoto Kawase, Chihiro Kawai and Yasushi Igarashi: Lecture Abstracts, 1989 Fall Meeting, Powder and Powder Metallurgical Association (1989) p 123.

7. Tomoyasu Aihara, Mikio Kaji and Yasushi Igarashi: Third FGM Symposium Lecture Collection (1989) p 111.

8. Tomoyasu Aihara, Mikio Kaji and Yasushi Igarashi: Lecture Abstracts, Fall Meeting, Japan Metal Science Society (1989) p 729.

Developing Independent Manned Space Technologies

91FE0125A Tokyo REPORT OF MANNED SPACE ACTIVITIES KEY TECHNOLOGIES RESEARCH WORKING GROUP in Japanese Mar 90 pp 1-12

Table of Contents

Introduction

The International Space Station Program (ISS), in which Japan has been participating, is expected to start in 1997. Worldwide construction of lunar bases and the manned exploration of Mars have also been seriously considered. In this environment, it is necessary for Japanese space development and utilization activities, which have so far been confined to the unmanned space technology, to be swept rapidly into the larger current involving manned space activities. Even in the General Guidelines for Space Development Policy, which were revised last year, it is stipulated that key technologies shall be established to develop independent manned space activities unique to Japan. It is expected that large scale research and developmental activities in this area will take place soon.

Under this condition, it is the natural responsibility of the National Aerospace Laboratory, the sole national laboratory for aerospace technology in Japan, to assume the leading and central role for the formulation of key technologies in the nation's manned space program. Nevertheless, manned space technology represents a field in which the Japanese have little experience, and its technological content is so vastly wide that it is not easy to grasp its total picture. This is the reason why the Laboratory has been conducting internal discussions as to what types of activities are expected of it, and as to what types of activities are made possible by it. The Research Council of the Laboratory has established the "Manned Space Activities Key Technology Research Working Group" consisting of the researchers from the relevant fields in the Laboratory. The charge of this working group is to develop detailed plans for key technologies in the manned space activities by taking into account previous research accomplishments as well as the current technological capability in the Laboratory, and to propose a new research agenda. This report summarizes the Working Group's findings.

As shown in the text of the report, throughout the long years of its research activities, this Laboratory has inadvertently been building up a considerable amount of accomplishments and capabilities necessary for manned space technologies. The conclusion of the Working Group is that "The Manned Space Activity Key Technology Research" is a very essential research theme of the Laboratory. In order to develop the detailed research and developmental program consistent with Japan's space development scenario (for example, the " Manned Space Platform Unique to Japanese Design" and others), the facilities and equipment plans, and the budget scale, it is necessary to continue more discussion. Although it is extremely important, the manned space transport system, which may be considered the infrastructure of the manned space activities, has not been addressed in this report simply because its technical content is too large.

2. Current Status of Japanese Technology and the Role of the National Aerospace Laboratory

Japanese aerospace development has been conducted in the past for unmanned technologies, mainly due to the constraints imposed from the political and economical standpoints. This is the reason that the only significant accomplishments for manned space activities have been the selection and the training of the scientist crew to conduct the First Material Testing Project (FMPT), and the development of part of the environmental control system for JEM, which constitutes the Japanese contribution to the International Space Station Project. There have been practically no key technologies developed in Japan for the manned space activities.

Expectations for the Japanese manned space activities have gradually, yet steadily, been increased under this situation, the process of which is described in the two successive reports published since 1987, such as the report for Long Term Policy Discussions and for the Special Committee for the Space Station, as well as in the General Guidelines for Space Development Policy. Especially in the General Guideline for Space Development Policy revised last year, it is stated that Japan must develop key technologies if the country wants to maintain its independence and freedom in research. At the same time Japan will be responsible for one of the central tasks in the world space station development activities which include international cooperation. The Guidelines point out that one important element in the key technologies is the manned space activity technology. Because of the current technological status in Japan, the Guidelines refrain from mentioning the development of specific and independent Japanese manned space activities addressing only the formulation of key technologies needed for long term development (See Appendix 2).

In order to implement this developmental project, it is necessary to accumulate actual manned space activity experiences in the space station, as well as to establish the key technologies for manned space activities and to maintain strong participation in the advanced research activities. As detailed in the next section, although it is fragmented, this Laboratory has already been conducting several essential segments of the manned space activity key technologies, such as the man-machine system technology in the Fan-Jet STOL project, research on effluent material processing systems, and for space sickness, under the Science and Technology Promotion Adjustment Fund Project, expert systems for support of space experiments in the Special Research Project under the Space Environment Utilization Experimentation Technology project, and others. In addition, research on the Closed Environment for Living Systems in Space (CELSS) project under the new Science and Technology Promotion Adjustment Fund project, and the research on Manned Flight Technology under the Special Research Program for the Aerospace Transport Element Technology Program are starting. It is very possible that this Laboratory can exert leadership as well as play the central

role for the establishment of Japanese-based key technologies by assembling and promoting, in a consolidated fashion, these past accomplishments and future research capabilities mentioned above in the "Manned Space Activity Key Technology Research." In this manner, this Laboratory will be able to meet its responsibility as the sole national laboratory for aerospace technology in Japan.

3. Accomplishments for Related Technologies at the National Aerospace Laboratory

Although there have been no large scale research projects directed toward the manned space activities at the National Aerospace Laboratory, several related technologies have been investigated as summarized below:

(1) Research Activities in the Special Project for Fan Jet STOL Plane

During the research and developmental efforts for the STOL prototype plane, the Laboratory identified man-machine interface problems between its pilot and the plane, and conducted research on the development and evaluation of various display systems, as well as the control motion analysis of the pilots.

(2) Research Activities for Special Research Project for Innovative Aerospace Transport Element Technologies

As a part of research on innovative aerospace transport element technologies, the Laboratory is expected to conduct research on manned flight technology to study the safety assurance problem (emergency exit) and heat rejection system for the manned transport system. The research on the intelligent cockpit has already been started.

(3) Programs under the Science and Technology Promotion Adjustment Fund Project

Under this program, research on the treatment of human effluent, and the integration of human sensation for rotational motions (space sickness) have been conducted. This research has lead to a three-year program starting in 1989 for the basic study of the material flow cycle between plants and atmosphere in the closed environment (research on CELSS) in the International Basic Study Project for Material Flow.

(4) Research for Special Project for Space Environment Utilization Experiments

In order to make effective use of precious orbital resources in space, research on recycling of water and gas, and the expert systems for supporting space experiments have been conducted to assist the space crew.

(5) Research for the First Generation Material Experiments (FMPT):

The research project to address the relationship between man's sensory perception and his body motion in the weightless environment has been conducted under the Standard Budget Program. The experimental research is expected to start in June 1991 as a FMPT mission.

(6) Standard Budget Program

From the human factor point of view, research on the cockpit display systems and the operation motion analysis were conducted as a part of the R&D for the STOL prototype. In the research for manned support technology, CELSS and flight clothes for the super high speed flying have been studied. In addition, the Laboratory initiated research on space robotics with a view toward developing the manned space activity maintenance system.

4. Manned Space Activity Key Technology System and The Area in Which the National Aerospace Laboratory Should Be Working Immediately

Depicted below is the Manned Space Activity Key Technology System. The transport technology system and the bus system technology, which are shown under the dotted line in the figure, are not addressed in detail by the Working Group. The Working Group, however, fully recognizes that the transport technology is a very important key technology for manned space activities, but its technological content is too wide and it is closely related to other technology research.

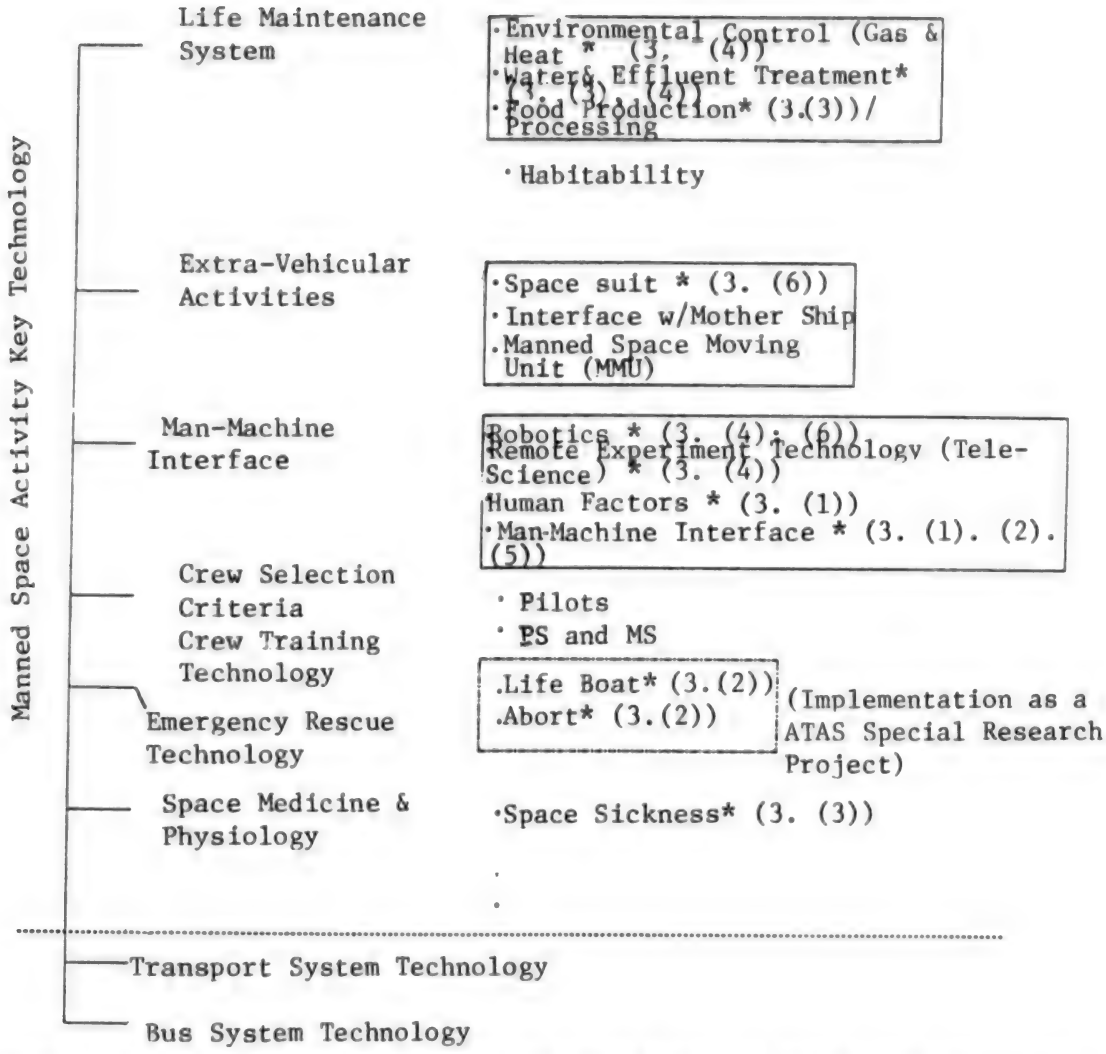

Note: Items with * are the research which have already been started.
( ) is the activities mentioned in section 3

Items in [ ] are technologies which are to be prioritized in the future

(More detailed technology breakdown is given in the Appendix 4)

5. Detailed Research Plans

This laboratory considers it necessary to make strong advances in research areas as detailed in Section 5.1 through 5.3 by taking into account of the Manned Space Activity Key Technology System and our previous accomplishments. Section 5.4 indicates detailed implementation plans for these research areas as an Integrated Key Technology Research Program.

5.1 Life Maintenance System Technology Research

The life maintenance system technology can be grossly divided into the room environment control technology, the treatment technology for waste water and effluent, and the production and processing of food (the details are given in the Appendix 4.1). Research on the component technology for room environmental control and waste water treatment has been carried out under the Special Research Program, while that for the effluent treatment technology has been carried out under the Science and Technology Promotion Adjustment Fund Project. It is considered appropriate that the future research is to integrate the results of this existing research under a Life Maintenance System. Moreover, the laboratory has been currently conducting research on an algae culture system and others for the food production and processing technology research. This activity should be increased to include the effective culturing system for higher level plants. Based on these considerations, research on the following items should take the priority:

(1) The Gas Regenerative Cycle Technology (removal and regeneration of CO_2 and O_2, and fixation and recovery of N_2)

(2) Detection and Removal Technology of Minute Quantity of Toxic Gases

(3) Treatment and Recycling of Waste water

(4) Collection and Recycling of Effluent

(5) Integration Technology for a System Including Food Production And Oxygen-Carbon Dioxide Exchange

5.2 Extravehicular Activity Technology

As the manned space activity program develops further in line with the Space Station Project and others, it is anticipated that the requirements for extravehicular activities will also drastically increase. The traditional Apollo/Shuttle space suit required an adaptation process of a few hours before and after the extravehicular activities because that the suit's inner pressure is as low as 1/3 of the atmospheric pressure. It is obvious that this adjustment requirement precludes its use for the extended extravehicular space activities. Also the heat rejection design of the Apollo/Shuttle suit is a sublimation

type, or the non-recirculation type, which is not suitable for an extended extravehicular stay. There are several more technical problems requiring further research and improvement on space suits for extended extravehicular stay in the areas of protection against radiation/cosmic dusts, its usability, maintainability/repairability, maneuverability, and others.

In the technology research at the Laboratory, it is necessary that these technical problems must be prioritized while the fundamentals of the key technologies involved in extravehicular activity are studied and established. As shown in Section 4, extravehicular activities can largely be classified into space suit technology, extravehicular activity support technology (interface with the mother ship), and the space movement technology (MMU technology) (the details are given in the Appendix 4.2). Our Laboratory has been conducting research on space suit technology for the past three years by a team of researchers, engineers and medical doctors in- and outside of the Laboratory as part of the "Super High Altitude Flying Suit Study Committee." We believe that future research should be conducted based on the findings of this committee's work as shown below.

(1) Study and Investigation of the Current Status of Space Activity Environment and Its Effect on Humans and Its Relevant Technologies

(2) Basic Research on Life Maintenance System for Extravehicular Activities (Oxygen Supply, Carbon Dioxide Removal, Toxic Gas Removal, Pressure Controls, and Temperature/Humidity Controls)

(3) Study of the Space Suit Systems to Identify Technical Research Agenda

o Studies of Subsystems for Exterior Envelope/Mechanism System, Thermal Control System, Gas Recirculation Control System, System Control System, and Others

o Understanding of Input/Output Relationships Among Various Subsystems

o Identification of Necessary Basic Design Data

(4) Examination and Testing of Basic Data Acquisition Method/ Prototyping of the Parts

(5) Total System Simulation (Development into the Prototyping of the BBM Model)

o System Simulation by Software Based On the Results of (3) and (4)

o System Simulation by Hardware Based on a Barrack Set Model

5.3 Man-Machine System Technology

The man-machine system can be largely divided into human factors, robotics, remote experiment technology (tele-science), and man-machine interface technology. The items listed below should be investigated on a priority basis.

5.3.1 Human Factors

Technology items for human factors are divided into endurance, quality maintenance, and motion characteristics of human beings in the space environment. In the past, research has been conducted for the deterioration of intellectual and motion capabilities under weightless conditions (FMPT Project), and the research on integration of rotational sensations (the Science and Technology Promotion Adjustment Funds Project). It is considered that the items listed below are priority research subjects:

(1) Implementation of Low Gravity Flight Tests (by Active Use of the Experimental Plane Dornie Do228)

(2) Research on Hand Control Under the Low Gravity Field

(3) Research on the Coriolis Force Effect Under the Low Gravity Field

5.3.2 Robotics and Tele-Science

The robotics technology to support the manned space activities consists of sensing and recognition technologies mainly by transducers, the manipulation technology by robot mechanisms and others, the autonomous operation technology based mainly on supervisory controls, and movement technology such as the space motion (see the Appendix 4, and section 3.2). The tele-science related technology consists mainly of remote experiment planning technology based mainly on experiment controls, remote experiment operational technology based mainly of the scientific crew support and tele-robotics, and data analysis capabilities (see the Appendix 4, section 3.3).

For research related to robotics and tele-science, it is necessary that a good interaction be maintained with the research activities of domestic research organizations in the related areas. Among the research topics mentioned above, the Group considers that the following tasks are to be advanced as an extension of previous research under the Special Research Fund Project and the Standard Budget Program at the National Aerospace Laboratory.

(1) Feasibility Study for Robot Operations For Operations To Be Automated And Robotized.

(2) Research on Robot Mechanisms For Delicate Operations, Flexible Operations And Operation Dynamics Under μG Environment.

(3) Layered Type Autonomous And Remotely Controlled Operation Technology by Supervisory Controls And Others

(4) Controls and Transmission of Scientific Knowledge, Such As Experimental Knowledge (Expert System)

(5) Identification and Evaluation of Experimental Operation Work Load

(6) Predictive Control Technology by the Orbital Motion Prediction Simulation and Others

(7) The Remote Operation Technology of Communication Delay Compensation Type

5.3.3 Man-Machine Interface

The man-machine interface technology is positioned as the integrating technology for human factors, robotics and tele-science technology. This technology can be divided into the design of the work station on the manned space platform and cockpits for space vehicles and others, and the task distribution technology for manned space work.

In the past, research on the cockpit display systems, and vehicle drive motion analysis have been conducted for the man-machine interface for piloted aircraft. Based on this previous research, the following priority tasks have been considered appropriate (see Appendix 4, section 3.4):

(1) AI type Operational System Research for Cockpit Design of the Space Vehicles (Round Trip Planes, and Orbit Change Planes)

(2) Study on the Inter-Man and Machine Work Sharing based on Task Analysis and Workload Analysis of Manned Space Work

5.4 Method for Implementing the Program as the Integrated Key Technology Research Program

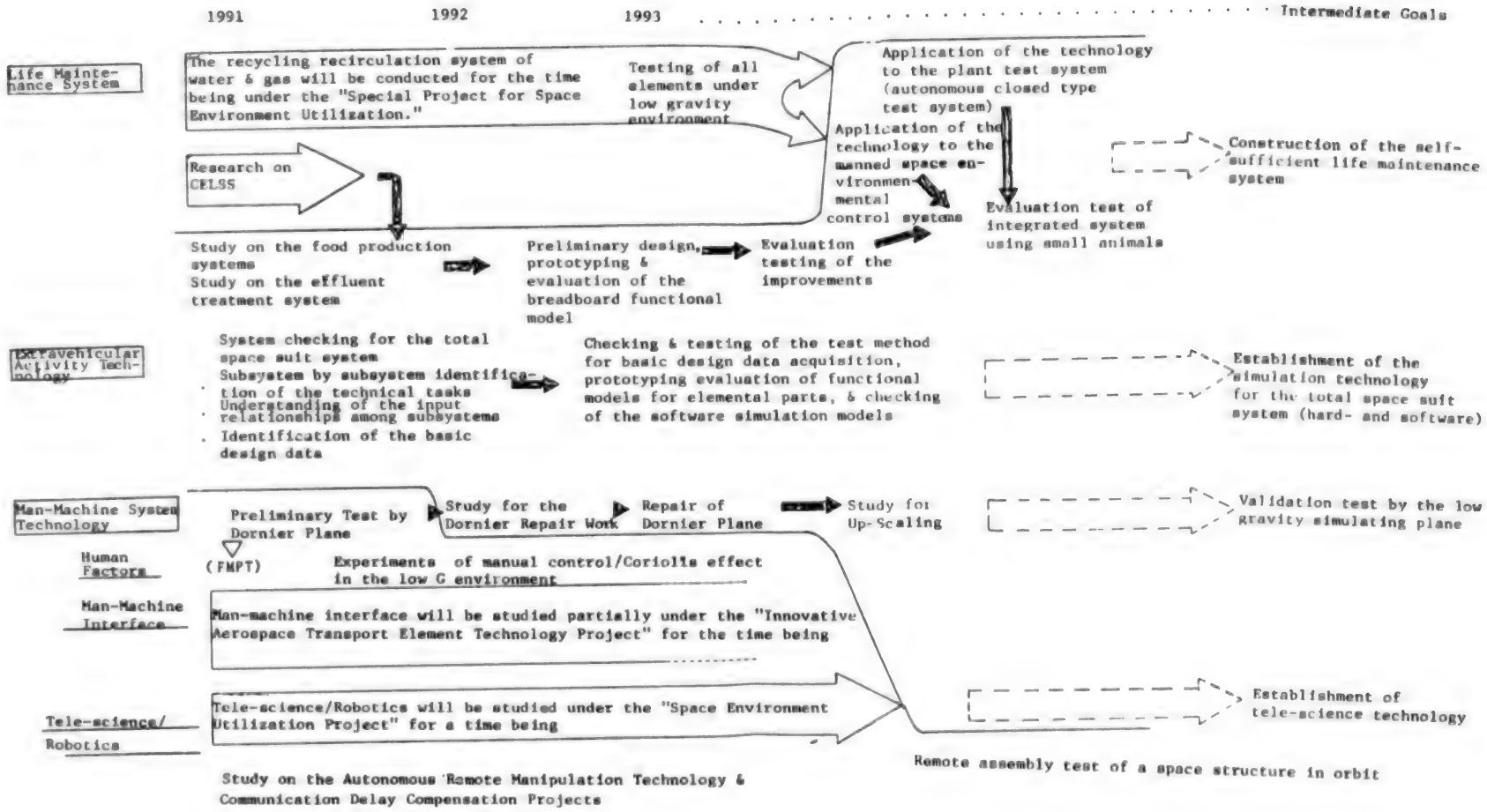
1991
1992
1993
Intermediate Goals
Life Maintenance System
The recycling recirculation system of water & gas will be conducted for the time being under the "Special Project for Space Environment Utilization."
Testing of all elements under low gravity environment
Application of the technology to the plant test system (autonomous closed type test system)
Application of the technology to the manned space environmental control systems
Construction of the self-sufficient life maintenance system
Research on CELSS
Evaluation test of integrated system using small animals
Study on the food production systems
Study on the effluent treatment system
Preliminary design, prototyping & evaluation of the breadboard functional model
Evaluation testing of the improvements
Extravehicular Activity Technology
System checking for the total space suit system
Subsystem by subsystem identification of the technical tasks
Understanding of the input relationships among subsystems
Identification of the basic design data
Checking & testing of the test method for basic design data acquisition, prototyping evaluation of functional models for elemental parts, & checking of the software simulation models
Establishment of the simulation technology for the total space suit system (hard- and software)
Man-Machine System Technology
Preliminary Test by Dornier Plane
Study for the Dornier Repair Work
Repair of Dornier Plane
Study for Up-Scaling
Validation test by the low gravity simulating plane
Human Factors
(FMPT)
Experiments of manual control/Coriolis effect in the low G environment
Man-Machine Interface
Man-machine interface will be studied partially under the "Innovative Aerospace Transport Element Technology Project" for the time being
Tele-science/ Robotics
Tele-science/Robotics will be studied under the "Space Environment Utilization Project" for a time being
Establishment of tele-science technology
Remote assembly test of a space structure in orbit
Study on the Autonomous Remote Manipulation Technology & Communication Delay Compensation Projects

Research Council for FY 1990

List of the Working Group for Manned Space Activity Key Technology Research

(In the order of the Japanese alphabet)

Chairman
Hisao Higashi
Research Council Member
Committee Members:
Yoshiaki Ookami
Leader, the 8th Research Group of the Space Research Group
Koji Otsubo
Leader, the 9th Research Group of the Space Research Group
Mitsuo Oguchi
Member, the Space Research Group
Shiro Kibuse
Principal Investigator, Structural Dynamics Section
Takao Suzuki
Chief, Human Factor Laboratory, Control Section
Hiroyuki Terui
Specialist, Flight Section, Space Research Group
Atsushi Nakajima
Leader, the 12th Research Group, Space Research Group
Yoshihiro Nakamura
Leader, the First Research Group, Space Research Group
Keiji Nitta
Leader, the 4th Research Group, Space Research Group
Masataka Maita
Principal Investigator, Thermo-Fluid Dynamics Section
Kotaro Matsumoto
Principal Investigator, Numerical Analysis Section
Nobuyuki Hachiyagi
Member of the Research Council

(Dates of the Meetings)

First Meeting/Dec. 5, 1989 (Tuesday)
Second Meeting/Dec. 15, 1989 (Friday)
Third Meeting/Jan. 12, 1990 (Friday)
Fourth Meeting/Jan. 31, 1990 (Wednesday)
Fifth Meeting/Feb. 16, 1990 (Friday)
Sixth Meeting/March 8, 1990 (Thursday)

RISC Processor Array for Artificial Neural Networks

90FE0178A Tsukuba HEIRETSU SHORI SHIMPOJIUMU JSPP '90 in Japanese May 1990 pp 385-392

[Article by Atsunobu Hiraiwa, Shigeru Kurose, Shigeru Arisawa and Kaoru Inoue, Sony Corporate Research Laboratories]

[Text] Abstracts

Artificial Neural Network (ANN) requires an excessive processing time because of its large network size to solve difficult problems and because it needs a large volume of learning patterns to be useful as a general purpose machine. In order to solve this problem, the Net-Data Division Method, which permits the efficient mapping of ANN algorithms in the mesh connected processor array, has been developed. Reported herein is this Net-Data Division Method and its simulation.

1. Introduction:

ANN has been used in many areas in recent years. A variety of models have been developed as it has become evident that the ANN application is very effective in areas such as image processing, voice recognition, controls, etc. In order to expand the effective application of ANN so as to make it more practical, it is necessary that the number of neurons must be increased and that the network size must be expanded. This, however, necessitates the rapid increase of the calculation volume, especially for the learning phase in which the data must be supplied iteratively to modify the network weights. In normal workstations, the simulation of ANN usually requires the computation time ranging from a few hours to a few days as long as the learning is included. This has been the bottleneck in conducting large scale ANN research and applications.

In order to improve this situation, it has been proposed that a special purpose hardware be prepared to increase the computation speed by parallel processing to take advantage of the parallelism intrinsic to ANN. One way to do the parallel computation is to assign one neuron to each individual calculation element, or to connect the processors assigned to multiple neurons. The former method requires such a large hardware that it is impractical to develop a large scale network at least with the present day technology.

Most systems proposed at present are based on the latter principle, and they consist of those using the DSP processor, those using the general purpose microprocessor, and those based on special purpose chips, etc. In any case, all of these methods are based on multiple processors performing parallel processing by communicating with each other. For the system using DSP, there is Sandy (Fujitsu) based on TM320C30, which is a 32 bit floating decimal DSP. This system has the processing speed of 500 M connections/sec (CPS) with 256 processors.[6][7]

We have been developing an ANN simulator called the GCN (Giga CoNnection) adopting the systoric array in its archtecture with the latest 64 bit microprocessor, 80860(40MHz) developed by Intel. Currently we are developing a system with 16 parallel processors.

We have also evaluated the mesh connected 128 processors in which the parallel processing is done by mapping the Back-Propagation model and the Kokonen Feature Maps by the net data division method, and have verified that this system can achieve the processing speed of 1.39 Giga CPS/1.88 Giga CPS.

In addition, a plan to develop a super-chip that integrates this architecture will be discussed in this paper.

2. Basic Array for GCN

The Neutral Network simulation is comprised mainly of the add/multiple operations to determine the sum of the weighted values of inputs to the neurons. Since the computation for each neuron is done independently of each other, the simulation speed can be increased if the processors to perform the high speed add/multiply operations are interconnected and work in parallel.

This type of system, however, has several shortcomings such as: it requires many large hardware for intercommunication among different processors; a processor overhead is required for processing communication; and its controls become very complicated. These are the reasons that we employed a systoric array as our GCN architecture in which the same processing elements (PE) are systematically arranged so that the communication will be limited to those between the adjacent PE's. Hence the communication hardware can be made small and the control becomes simpler. Moreover, the communication can be done asynchronously, and the processor overhead can be controlled to a small amount. The structure connecting the same PE makes its expansion easy, and permits the improvement of its overall performance by simply increasing the number of PE's.

Figure 1 depicts the schematics of the GCN architecture. Each PE in this figure has a 80860 microprocessor, a 4M byte local memory, and two FIFO's (64bits x 256W). The local memory is used to store the connecting weights among the neurons as well as the neuron outputs.

Each PE in this figure is connected to the adjacent four PE's through FIFO's to perform the asynchronous communication. In this manner, the data sending PE's can send the data and begin the next step operation without waiting for the receiving PE's to assume a receivable state. The data transfer speed of the FIFO is 160 Mbytes/sec with the 40 MHz clock.

The host EWS (NWS-1850/3800) and each PE are connected through the VME BUS.

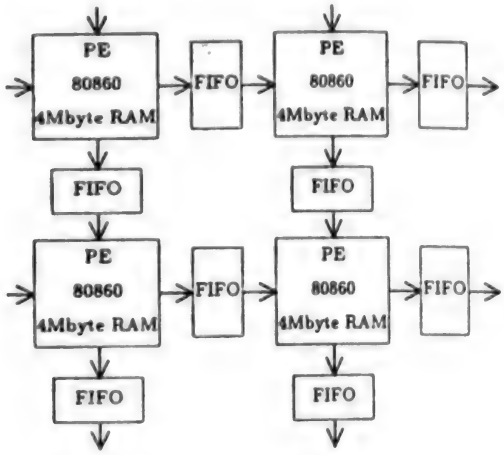

Figure 1. The Basic Architecture of GCN

Table 1. Properties of Intel 80860

Type	64 bit RISC Processor	
Arithmetic Unit	Integer/Control Core Unit	
	Floating Decimal	multiplier adder graphic unit
Pipeline	3 Stages	
Bus	External Internal	64 bits 128 bits
Cash	Instruction Data	4 Kbytes 8 Kbytes
Clock	33.3/40 MHz	
Peak Performance	Single Precision Floating Decimal 80 MFLOPS	
	Double Precision Floating Decimal 60 MFLOPS	
Process	CMOS 1.0 μ rule	

The 80860 is the 64 bit RISC type general purpose microprocessor developed by Intel, and careful attention has been given to achieve the high speed add-multiply operations. It has three independent units such as the core unit for the integer arithmetics and controls, the multiplier to do the floating point arithmetics, and the address unit. These three units can be operable in parallel. The multiplier and the adder have the three stage pipeline structure so that the continuous multiply/add can be done to obtain the results for clock by clock. The data loading/storing by the core unit, and the floating decimal add/multiply arithmetics can be done in parallel to communicate with the adjacent PE's without its process being interrupted. [Table 1]

The arithmetic operations in the GCN are performed in two levels by the pipelines/parallel processing. In the first level, it is done by the Fine-Grain Pipeline/parallel processing. The floating point arithmetic and floating point LOAD in the PE are pipelined by utilizing the pipeline function of the 80860. All arithmetic units can be parallel-processed.

The second level is the micro-pipeline processing.

The arithmetic operations of the entire system is made into a pipeline by the use of systoric algorithms. The arithmetic operations and data required in the ANN simulation are divided and separately assigned to PE's, and each PE transfers its processed result to the adjoining PE's. The process proceeds in this manner.

This architecture makes it possible to extract the processor array capability by the effective use of pipeline/parallel processing within the PE as well as between the PE's.

3. Mapping of BP Algorithms Over GCN

For the parallel processing of more than 100 PE's, a mesh type connection is used since the linear ring connection tends to increase the communication time.

This is the reason that we developed the net division method in which the BP algorithms can be mapped over the mesh connected GCN.

As shown in Figure 3, each PE in the horizontal ring is used in the data division method [2], and it has the same weight so that the time required for inputing the different data as well as the communication time can be shortened. (We call this the copy method.) Every time the entire data are seen, the derivatives of the connecting weights and revised connecting weights will go around along this ring.

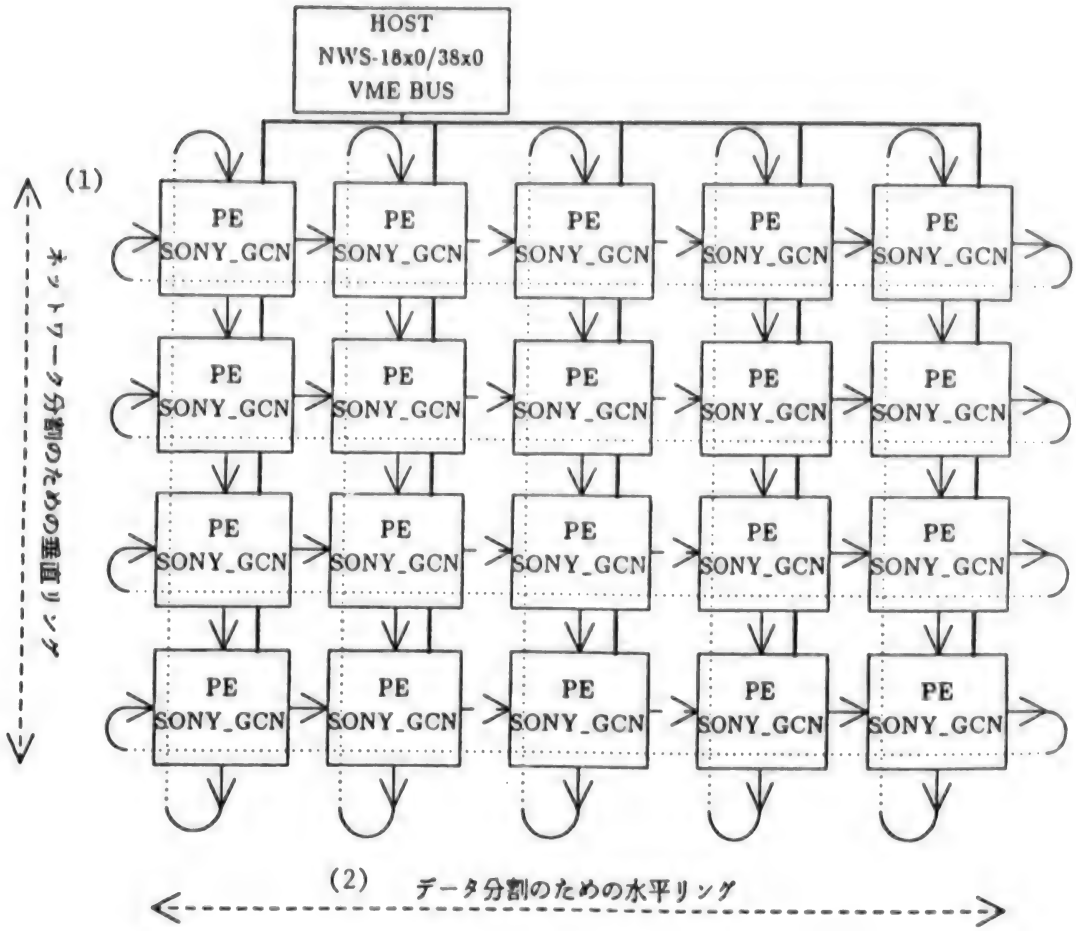

Figure 3. Net Data Division Method Over Mesh Connected GCN

Key:

1. Vertical ring for the network division
2. Horizontal ring for the data division

Moreover, the number of net divisions, (N) and the number of data divisions, (D) as well as the total number of data (AD) will be explained for the three layered net data division BP algorithms. Table 2 depicts the memory volume of each PE.

(1) When the input data 1 is given, the input to the hidden unit j is determined by

$$net_j = \sum_i W_{ji}\, 1_i$$

where W_{ji}: connecting weight

(2) The output of the hidden unit j will be determined by

$$Hj = \frac{1}{1 + e^{-netj+\theta j}}$$

Where θ_j = threshold value

(3) The Input to the output unit can be obtained by transferring the intermediate result similar to (1) onto the vertical ring.

(4) The output of the output unit can be determined in the same way as (2)

(5) The output layer error can then be determined by

$$\delta_{oj} = (T_j - O_j)O_j(1-O_j)$$

where T_j : Trainer Signal

O_j : Output of the Output unit

(6) The error of the hidden layer can be determined by the following equation as the errors are transferred onto the vertical ring

$$\delta_{hj} = H_j(1-H_j)\sum_{k=1}^{q}\delta_{ok}W_{kj}$$

where q: Number of the output unit

(7) The change of the connecting weight for the mth input data can be determined for each layer by

$$\Delta W_{ij}(m) = \delta_i O_j + \Delta W_{ij}(m-1)$$

where (m = 1, - -, AD/D)

Oj= Input -hidden layer ... output of the input unit
Hidden -output layer ... output of the hidden layer

(8) Steps (1) through (7) will be repeated for all divided data for (AD/D) times.

(9) The total summation will be obtained for the changes of the divided connecting weights by using the horizontal ring.

(10) The connecting weights will then be modified by the following equation

$$\Delta W_{ij}(t) = \eta \sum_{pe=0}^{D-1} \delta W_{ij}(AD/D) + \alpha \Delta W_{ij}(t-1)$$

$$W_{ij}(t) = \Delta W_{ij}(t) + W_{ij}(t-1)$$

where η : learning constant

α : stabilization constant

t : number of learnings

(11) With the use of horizontal ring, the revised connecting weights will be transferred to the other data divided PE's.

(12) Steps (1) through (11) will be repeated until the data reach the target values.

If the memory volume is to be reduced, the input data will be divided into N groups and dispersed over the vertical ring PE's. In this case, step (1) will be determined by transferring the intermediate results of the similar add/multiply operations to the vertical ring, and step (7) will be transferring the hidden layer errors on to the other PE's on the vertical ring.

Table 2. The Memory of Each PE in the Net Division BP Algorithms (Number of Net Division (N), Data Division (D))

Area	Memory Volume
Errors, Trainers, Hiddeness, Number of Output Units Connecting Weights, Changes of Connecting weights	1/N times
Number of Input Data	1/D times
Change of Connecting Weight in the Preceding Step (N divisions)	1/(ND) times

4. Mapping of Kohonen Feature Maps (KFM) onto GCN

The KFM is the two layer learning algorithms without trainers [9]. Hence, it requires an excessive amount of computations to perform the large amount of iteration for self-organizing the network with respect to the input data. In a similar manner to BP, each PE in the vertical ring will be used by the network division method and will possess the different and divided weight.

The intermediate results, the maximum values, and the revised neurons go around along this ring to perform the inner product, the maximum value search, and the search of the revised neurons.

Each PE on the horizontal ring is used by the data division method, and has the same weight so that the time required for handling different weights and communication can be reduced. Every time the total data is seen, the derivatives of the connection weights and revised weights will go around along this ring.[10]

Next we would like to describe the net data division KFM algorithm by denoting the number of net divisions by (N), the number of data divisions by (D), and the number of the total data as (AD).

(1) As depicted in Figure 4, the input vector 1 and the weight Wij will be divided into N groups. The inner products of these quantities will be obtained by transposing the intermediate results on the vertical ring.

(2) The local maximum of the inner product is determined for each PE, and the global maximum of the inner product will be obtained by going around the vertical ring once.

(3) The global maximum will be informed to each PE for every circulation of the vertical ring.

(4) Whether the neurons assigned to each PE need to be modified or not will be determined, and this information will be given to each PE by going around the vertical ring once.

(5) The change of the connecting weight for each PE will be determined by

$$\Delta Wij(m) = 1j - Wij + \Delta Wij(m-1)$$

where (m = 1, --, AD/D)

(6) Steps (1) through (5) will be repeated for all divided data for (AD/D) times.

(7) The changes for the connecting weights divided for each data will then be summed up with the use of the horizontal ring.

(8) The connecting weights are then revised by the following formula:

$$\Delta W_{ij}(t) = \eta \sum_{pe=0}^{D-1} \Delta W_{ij}(AD/D)$$

$$W_{ij}(t) = \Delta W_{ij}(t) + W_{ij}(t-1)$$

where η : Learning Constant

t : Number of learnings

(9) The revised connecting weights will then be transferred to other data divided PE's.

(10) Steps (1) through (9) will be repeated for K times.

$$O = W \cdot I$$

$$\begin{bmatrix} PE0 \\ PE1 \\ PE2 \\ PE3 \end{bmatrix} = \left[\begin{array}{c|c|c|c} T3 & T0 & T1 & T2 \\ T2 & T3 & T0 & T1 \\ T1 & T2 & T3 & T0 \\ T0 & T1 & T2 & T3 \end{array}\right] \begin{bmatrix} PE0 \\ PE1 \\ PE2 \\ PE3 \end{bmatrix}$$

PE0 | PE1 | PE2 | PE3

Figure 4. Network Division (4 divisions)
(The connecting weights to be used at time Tx)

(1) 入力ベクトル I

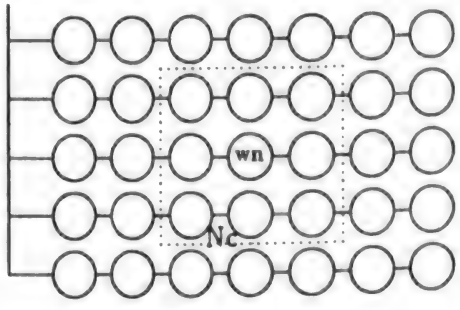

Figure 5. Kokonen Feature Maps
wn: winning neuron
Nc: neighborhood

Key:

1. Input vector 1

5. The Simulation Results:

The capability of our GCN can be evaluated by performing the algorithms on the Sim860, which is the software simulator for the 80860.

The three layer network evaluated by this simulation consists of 1600 input layers, 64 hidden layer and 32 output layers. The total input data is of 5100 patterns, and the PE's are performed by the 32 bit floating decimal arithmetics. The network is divided into four groups, the input data are dispersed into 32 PE groups mapped on the 128 mesh connected PE's.

The net-divided BP algorithms developed under these conditions are converted into a program consisting of 900 line assembler language statements and 600 line C-language statements. The simulation based on this program resulted in the 4.6 machine cycles per connection for each PE.

This result includes the forward and backward calculations, modification of the connecting weights and inter-ring communication time.

If each PE was operated on 50MHz (20 ns), the performance of 1.39 Giga CPS (Connection Per Second) could be obtained.

For the KFM, we mapped the 1600 input layers, 64 output layers, and total input of 5120 patterns in a similar manner for the simulation. The simulated result showed that each PE required 3.4 machine cycle per connection. If it was operated on the 50 MHz, it would have been possible to obtain the performance of 1.88 Giga CPS.

6. Concluding Remarks:

In the large scale neural network simulation, we have verified with the use of software simulator that the mesh connected RISC processor array based on the net data division method can attain the high performance.

In the future, we plan to evaluate the mapping of neural network algorithms onto the GCN. This architecture can be integrated, with the use of multichip module technology, into developing superchips similar to the 80860 having CPU core, two FIFO and 4 Mbyte memory. If this is done, it is possible to realize a parallel neuro-accelerator having the performance of 1 Giga CPS on a (printed circuit) board. It is also expected by the year 2000 the realization of a Tera CPS which would allow the parallel processing of a few thousands to a few ten thousand units.[11],[12],[13]

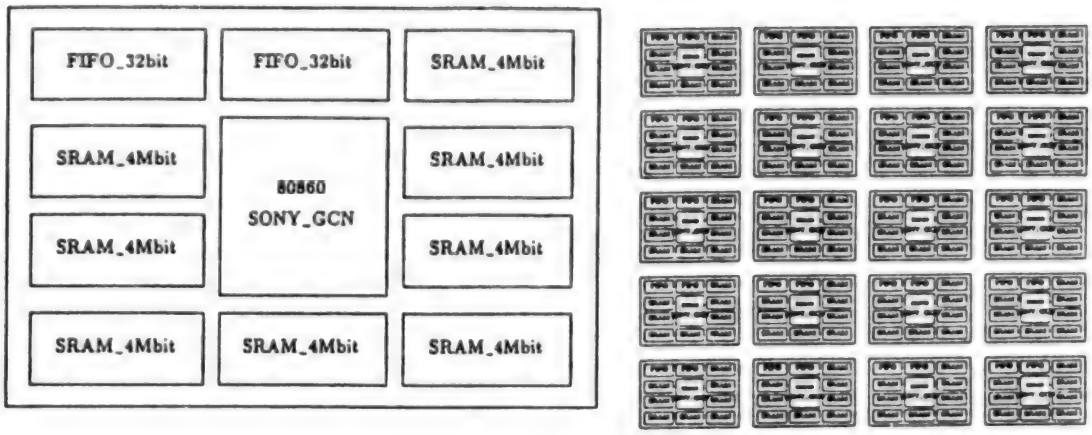

Super-chip for GCN

Acknowledgement:

We would like to express our appreciations to Directors Miyaoka and Matsuda, and Section chief Iga who gave us the opportunity to present this paper during this conference.

Table 3. Comparison Between GCN and Warp

Systems	Warp	GCN
Pipeline	7 stages	3 stages
Local Memory	16 kbytes Activation Learning Data	4 Mbytes Activation Learning Data Connecting Weights
Communication Between PE's	80Mbytes/sec	160Mbytes/sec
PE's Computation Speed	10MFLOPS	80MFLOPS
Number of PE's	10	128
PE Connection	Ring Type	Mesh type
Performance	17MCPS	1.1GCPS

References

(1) D.E. Rumehart, G.E. Hinton and R.J. Williams: Learning Internal Representations by Error Propagation in Parallel Distributed Processing, Vol. 1, pp 318-363, 1986.

(2) D.A. Pomerlean, G.L. Gusciora, D.S. Touretoky and H.T. King: Neural Network Simulation at Warp Speed: How we get 17 Million Connections Per Second. ICNN88, Vol 2, pp 143-150, 1988.

(3) S.Y. King, J.H. Hwang: Parallel Architectures for Artificial Neural Nets, ICNN88, Vol 2, pp 165-172, 1988.

(4) S.Y. Kung: VLSI Array Processors., Prentice Hall Inc., 1988.

(5) A. Iwata, Y. Yoshida, S. Matsuda, Y. Sato and N. Nakamura: An Artificial Neural Network Accelerator Using General Purpose 24 bit Floating Point Digital Signal Processors., IJCNN89, Vol 2, pp 171-175, 1989.

(6) H. Kato, H. Yoshizawa, H. Iciki and K. Asakawa: A Parallel Neurocomputer Architecture Topward Billion Connection Updata Per Second, IJCNN90-Wash. DC, Vol 2, pp 47-50, Jan 1990.

(7) A. Hiraiwa, S. Kurosu, S. Arisawa, and M. Inoue: A Two Level Pipelined RISC Processor Array for ANN, IJCNN90-Wash. DC, Vol 2, pp 137-140, 1990.

(8) N. Fukuda, Y. Fujimoto and T. Akabane: A Transputer Implementation of Toroidal Lattice Architecture for Parallel Neurocomputing, IJCNN90-Wash. DC, Vol 2, pp 43-46, 1990.

(9) T. Kohonen: Self-Organization and Associative Memory. (Second Edition), Springer-Verlag, 1988.

(10) R. Mann and S. Haykin: A Parallel Implementation of Kohonen Feature Maps on the Warp Systoric Computer, IJCNN90, Wash. DC, Vol 2, pp 47-50, Jan. 1990.

(11) R. Johnson: Multichip Modules: Next Generation Package, IEEE Spectrum, Vol 27, No 3, 1990.

(12) "Special Edition; Multichip Module" Nikkei Microdevice, No 54, 1989.

(13) P. Geslinger, P. Gargini, G. Parker and A. Yu: Microprocessors Circa 2000, IEEE Spectrum, Vol 26, No 10, 1989.

(14) Mitsuo Kawato: Neural Network, Spectrum, Vol 13, No 4, 1990.

(15) Intel Corp., i860 ™ 64 bit Microprocessor Programmer's Reference Manual, 1989.

Information Processing and Equipment Arrangement in the Pressure Hull of 'Shinkai 6500'

916C0003A Tokyo KAIYO KAGAKU GIJUTSU SENTA SHIKEN KENKYU HOKOKU in Japanese Mar 90 pp 303-314

[Article by Shuichiro Hamaguchi, Itsuro Maeda, and Kazuhiko Baba, Deep Sea Technology Department, Mitsubishi Heavy Industries, Ltd., Kobe Shipyard, Submarine Department]

[Text] [Abstract]

The 6,500 m deep research submersible Shinkai 6500 is operated by a crew of three seated in the pressure hull which is a 2 m diameter sphere of titanium alloy.

Much equipment for maneuvering, navigation, communication and observation, etc. is installed in the pressure hull.

In order to operate the submersible safely and smoothly, it is very important to arrange the equipment effectively in the narrow space so that the crew can easily operate and monitor it, and also offer necessary information instantaneously in an easily understandable form.

This report explains the outline of the design procedure and the results of the actual equipment layout in the pressure hull. The Integrated Information Display System (IIDS) uses a CRT to display various information. Information processing and display modes etc. of the IIDS, and data reproduction after recovery on the support vessel "Yokosuka" are also discussed.

Key words: Shinkai 6500, Pressure Hull, Arrangement, Information Processing, Integrated Information Display System, CRT Display.

1. Introduction

The 6,500-meter-deep research submersible Shinkai 6500 was completed at the end of November 1969, and delivered to the Japan Marine Science and Technology Center. The submersible, operated by a three-man crew, has the following features: 1) To ensure that its navigation--steering and survey and observation activity--will be conducted safely and efficiently,

ingenuity from a human engineering viewpoint is employed in the arrangement of the observation portholes and equipment inside the pressure hull. 2) Various information and data necessary for the submersible's navigation are centrally processed and displayed on an integrated information display system using a CRT on board, and are simultaneously recorded in a magnetic bubble cassette. 3) The recorded information and data may be reproduced in the integrated information display system's data reproduction division aboard the support ship Yokosuka, and processed into forms which can be easily utilized.

This report describes the arrangement of the observation portholes and the equipment inside the pressure hull, and gives outlines of the integrated information display system and the information processing and display methods being adopted in the equipment.

2. The Layout of the Observation Portholes and the Equipment Inside the Pressure Hull

2.1 Positions of Crewmen Inside the Pressure Hull and Observation Portholes

Inside the pressure hull the three crewmen are positioned with the pilot seated in the center facing front, the co-pilot seated on his right and the observer on his left. The pilot can see the outside through the observation porthole at all times while steering the submersible. This layout was adopted based on experience obtained from actually operating Shinkai 2000. In the Shinkai 2000, the pilot is designed to steer the submersible while observing the instruments on the console and a monitor TV, and he is to look into the observation porthole to see the outside world only when needed. It has been discovered, however, that in actual navigation the pilot finds it much easier to steer his vessel if he can see the outside world at all times through the porthole. As a result, in Shinkai 6500 the console system was abandoned, and in its place a new layout was adopted. The pilot is seated at the center to the submersible's front and an observation porthole for monitoring the submersible's direction of advance was also installed at its front. In order to improve the side views, the observation portholes for the co-pilot and observer on Shinkai 6500 are installed farther to the outside direction (sideways direction) than their counterparts on Shinkai 2000, affording a vision of field close on the beam (plus or minus 90 degrees).

Figure 1 gives a comparison of the inside of the pressure hull of Shinkai 2000 and that of Shinkai 6500, Figure 2 is a comparison of the locations of the view ports for the two submersibles, and Figure 3 shows a comparison of the fields of view on the sea floor.

In Figure 3, Shinkai 2000 appears to have a better field of view than Shinkai 6500 in the area directly to the front of the pressure hull, but in Shinkai 6500 the shortfall is compensated for by upgrading the capabilities of the TV cameras (two cameras are provided, and one of them can make a 360-degree turn or can have its camera angle raised or lowered).

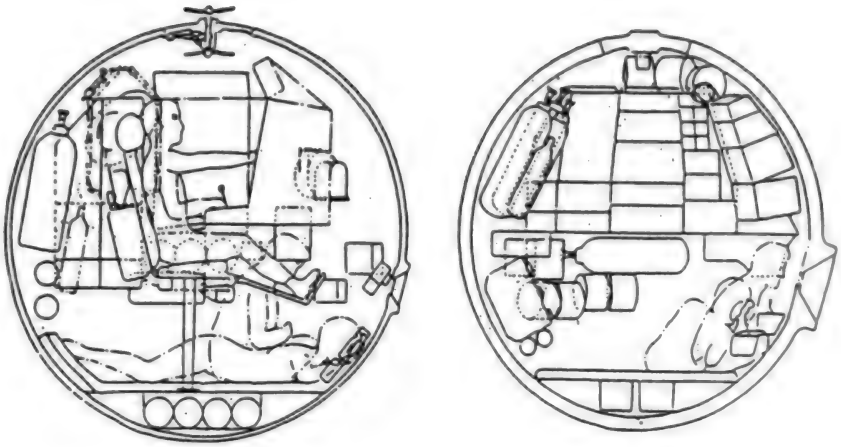

Figure 1. Inside of the Pressure Hull of Shinkai 2000 (left) and Shinkai 6500 (right)

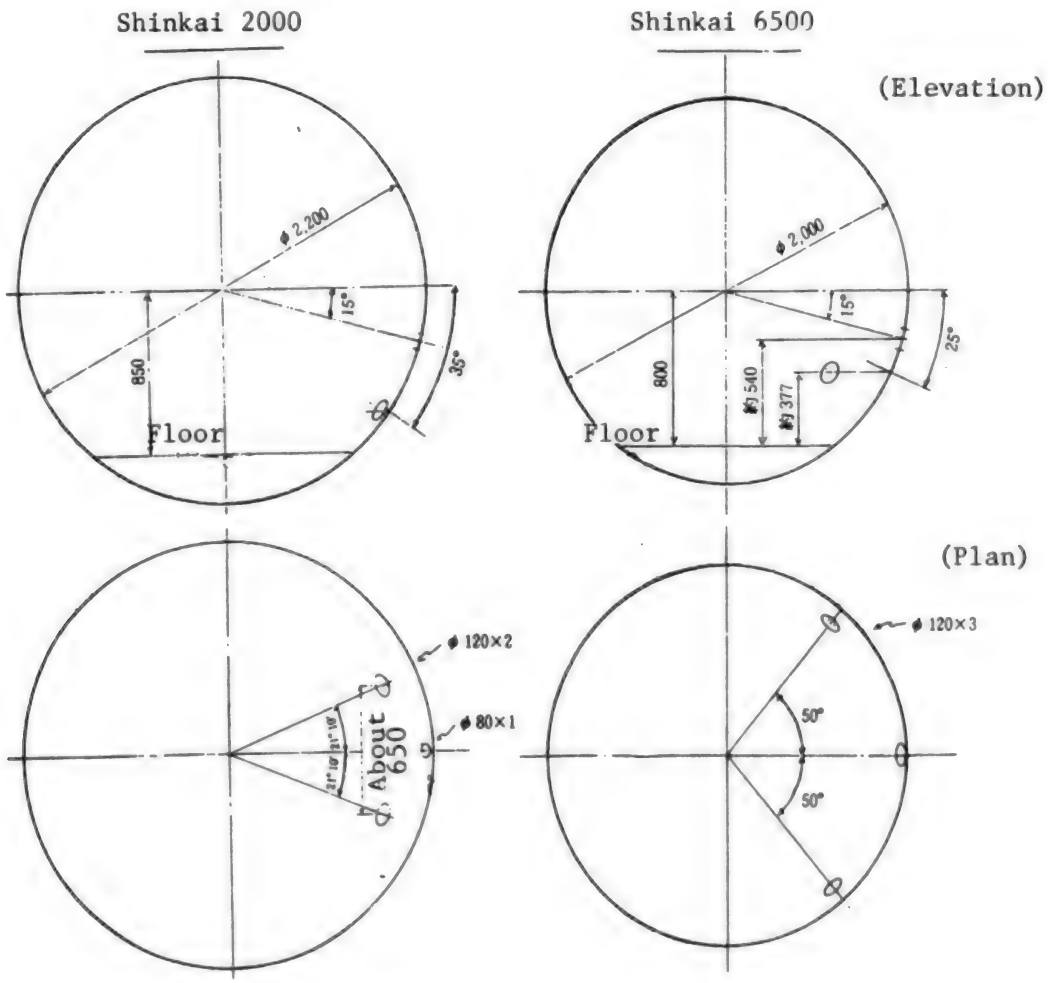

Figure 2. Comparison of the View Port Location

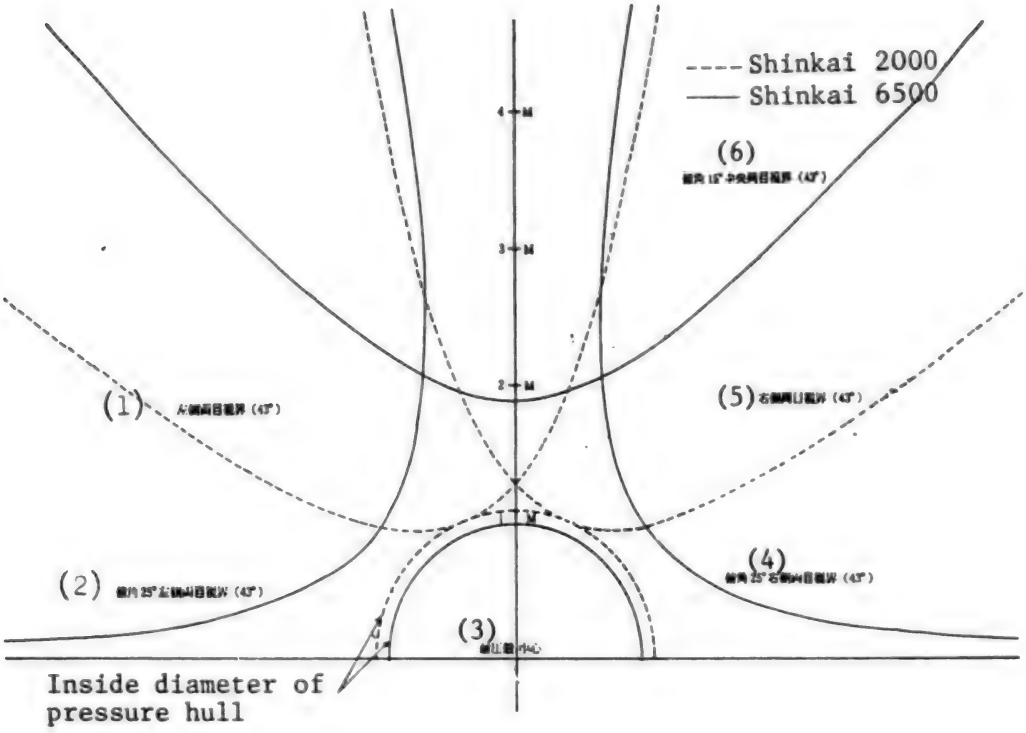

Figure 3. Comparison of the Field of View on the Sea Floor

Key:

1. Field of view to the left of both eyes (43 degrees)
2. Field of view to the left of both eyes when the angle of depression is 25 degrees (43 degrees)
3. Center of pressure hull
4. Field of view to the right of both eyes when the angle of depression is 25 degrees (43 degrees)
5. Field of view to the right of both eyes
6. Field of view to the front of both eyes when the angle of depression is 15 degrees (43 degrees)

2.2 The Layout of Equipment Inside the Pressure Hull

As explained earlier, in Shinkai 6500 the console system has been abandoned and various instruments are arrayed as if they are pasted onto the wall (the boxes containing instruments are embedded in a skeleton called a "bird cage"). Photograph 1 gives the layout of various instruments inside the pressure hull.

As described before the decision as to where to install what equipment has been made with due consideration to the positions of the crew so that each will be able to operate or monitor the instruments with ease. For example, the integrated information display system and navigation instruments such as an advanced sonar, and an acoustic position finder are positioned closer to the direct front of the pilot and co-pilot, while systems that need to be handled while steering the submersible, such as the weight trim operation panel, are placed immediately to the front of the pilot. The control box

for the main propulsion system, the manipulator master arm and the joy stick for the grabber, among others, are built portable so that the pilot will be able to shift his position inside the pressure hull while observing the outside world through the view port.

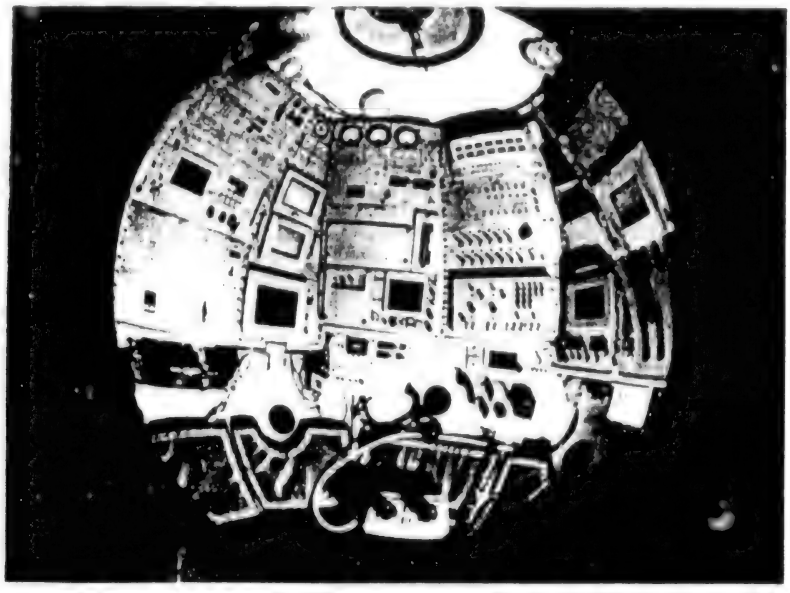

Photo 1. Inside of the Pressure Hull

The manipulators for the underwater still camera and the payload instruments which are used mainly by the observer, however, are concentrated on the left side. The monitor for an underwater TV is installed near the view port for the observer on the left side of the pressure hull. He, himself can manipulate it into making a rotation or raising its camera angle upward or downward (using a portable controller) so that he will be able to have a broad field of view.

Equipment and instruments which are not used ordinarily, such as the emergency breathing equipment and the distribution panel for communications, are concentrated in the aft section of the pressure hull.

Figure 4 gives the layout of major equipment inside the pressure hull.

In order to determine the shapes and dimensions of the equipment and instruments, and best utilize the small space inside the pressure hull, each instrument was actually placed in position in a mockup of the pressure hull manufactured in advance.

3. The Integrated Information Display System

Due to the advance in electronics technology, the technique of CRT display of information, centered on data loggers for surface ships, was employed as early at 1975. The adoption of the CRT technology for the information

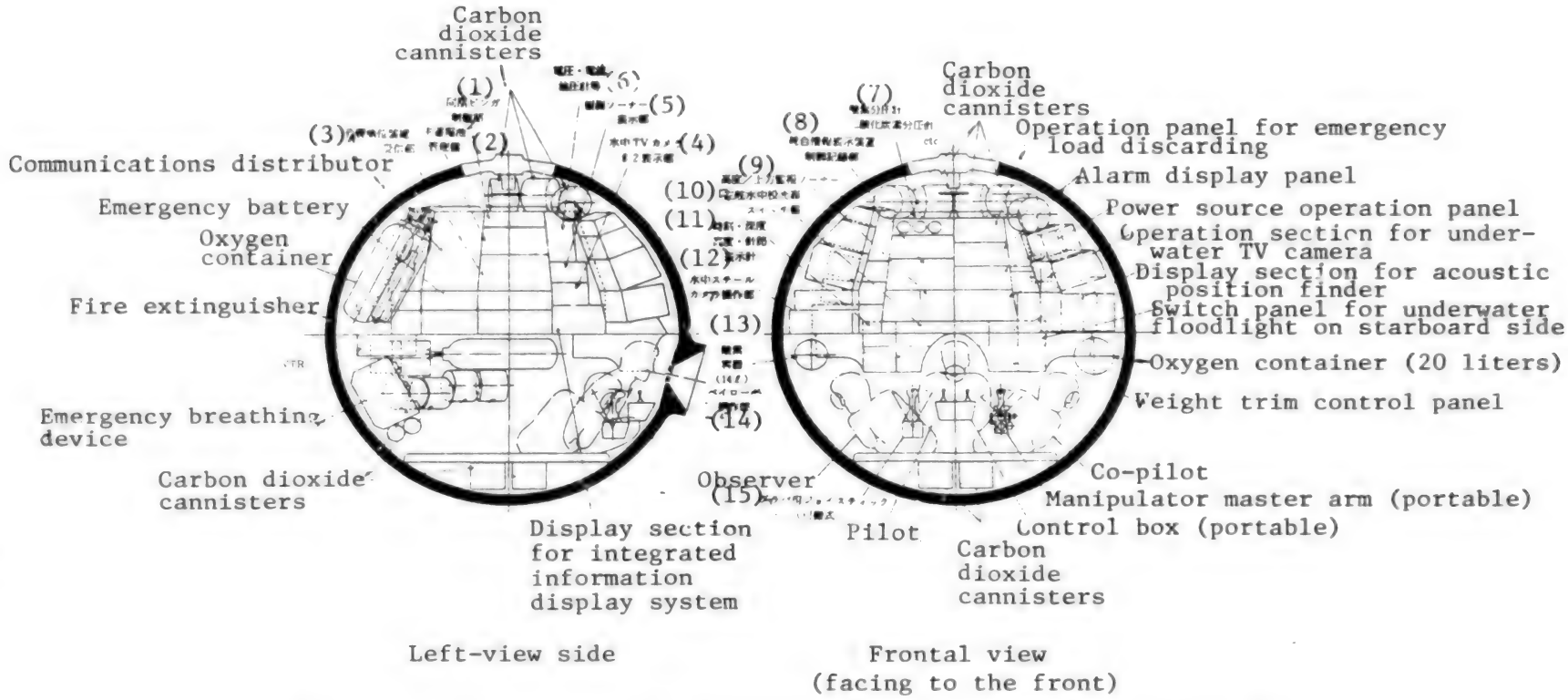

Figure 4. Arrangement of the Principal Equipment in the Pressure Hull

Key:

1. Synchronizing pinger control section
2. Main battery management panel
3. Receiving section for acoustic position finder
4. No. 2 display for underwater TV camera
5. Display section for observation sonar
6. Voltage, current and oil pressure meters
7. Oxygen potentiometer, carbon dioxide potentiometer, etc.
8. Control and record section for integrated information display system
9. Sonar for monitoring altitude/upper side
10. Switch panel for underwater floodlight on the port side
11. Time, depth, altitude and course indicators
12. Underwater still camera operation section
13. Oxygen container (14 liters)
14. Payload operation section
15. Joy stick for grabber (portable)

system for Shinkai 6500 was determined from the initial stage of the submersible's construction program, and the effort was realized in the form of the integrated information display system on board. Data from the various systems and instruments carried by Shinkai 6500 (both those located inside and outside the pressure hull) are input in the integrated information display system and comprehensively exhibited on a CRT display. The system simultaneously records the necessary data in a magnetic bubble cassette. This enables the crew to see the submersible itself and its surroundings at a glance (unlike the Shinkai 2000). It eliminates the need for the crew to check the gauges on the consoles and equipment, thereby contributing greatly to the ease of steering.

The gauges/displays for the equipment are built in duplicate, which raises their reliability. An outline of the integrated information display system is described below.

3.1 Configuration of Hardware and Performance

The integrated information display system has the following hardware configuration and performance.

--Control and record section

CPU (16 bits, 8 MHz)
Two bubble cassette slots (512 kilobytes x 2) (recording time of 10 hours)
Eight serial input channels
Two serial output channels (each having a 10 mA current loop)
Parallel input x 32 bits
24 analog input channels (voltage--±10 V, or current--4 to 20 mA)

--Input/output section

AC 100 V, 60 Hz, 1 ϕ
(Power source) A built-in speaker for voice alarms

--Display section

A 9-inch color CRT display with a touch sensor panel

3.2 Input Signal

The majority of signals input (automatic input) into the integrated information display system come from the submersible's various equipment, but some of the signals are manually input by the operator via the touch sensor panel.

Table 1 gives a list of input signals.

Table 1. List of Input Signals

Signal name	Input mode	
	Automatic	Manual
Electric power system		
Bus voltage	0	
No. 1 main battery current	0	
No. 2 main battery current	0	
Amount of discharge from No. 1 main battery	0	
Amount of discharge from No. 2 main battery	0	
Insulation resistance bus	0	
Insulation resistance AC 100 V	0	
Insulation resistance DC 28 V	0	
Communications system AC 100 V voltage	0	
Communications system AC 100 V current	0	
Communications system DC 28 V voltage	0	
Communications system DC 28 V current	0	
Propulsion and steering system		
Main propeller rotation number	0	
Main propeller angle of oscillation	0	
Rotation number and direction of vertical thruster	0	
Rotation number and direction of horizontal thruster	0	
Hydraulic system		
Oil pressure	0	
Weight trim and adjustment system		
Quantity of liquid in trim tank	0	
Quantity of liquid in auxiliary trim tank	0	
Internal pressure of auxiliary trim tank	0	
Retention/release of ballasts for diving	0	
Retention/release of ballasts for surfacing	0	
Pressure of air storage device(air pipe)	0	
Navigation and communications system		
Depth	0	
Altitude	0	
Direction of bow	0	
Vertical angle of inclination	0	
Horizontal angle of inclination	0	
Diving/surfacing speed (descent/ascent speed)	0	
Position of submersible	0	
Second, minute, hour, day, month, year	0	
Air pressure inside ship		0
Temperature inside ship	0	
Humidity inside ship	0	
Flow direction	0	
Flow velocity	0	
Environmental control system		
No. 1 oxygen partial pressure		0
No. 2 oxygen partial pressure		0
Carbon dioxide partial pressure		0
Oxygen flow		0
Pressure in oxygen container		0

[Continued on following page]

Signal name	Input mode	
	Automatic	Manual
Survey and observation system		
Salt content (electrical conductivity)	0	
Water temperature	0	
Depth (pressure in the depth)		
Sound speed		
Emergency and safety		
Various alarms	0	

3.3 Software

The software for the integrated information display system consists of four kinds of operation programs which correspond to the operation flow of Shinkai 6500 and a kind of test program, for a total of five kinds of programs. Each is recorded in an individual bubble cassette.

Figure 5 gives the operation flow and corresponding software, while Figure 6 gives the configuration of software.

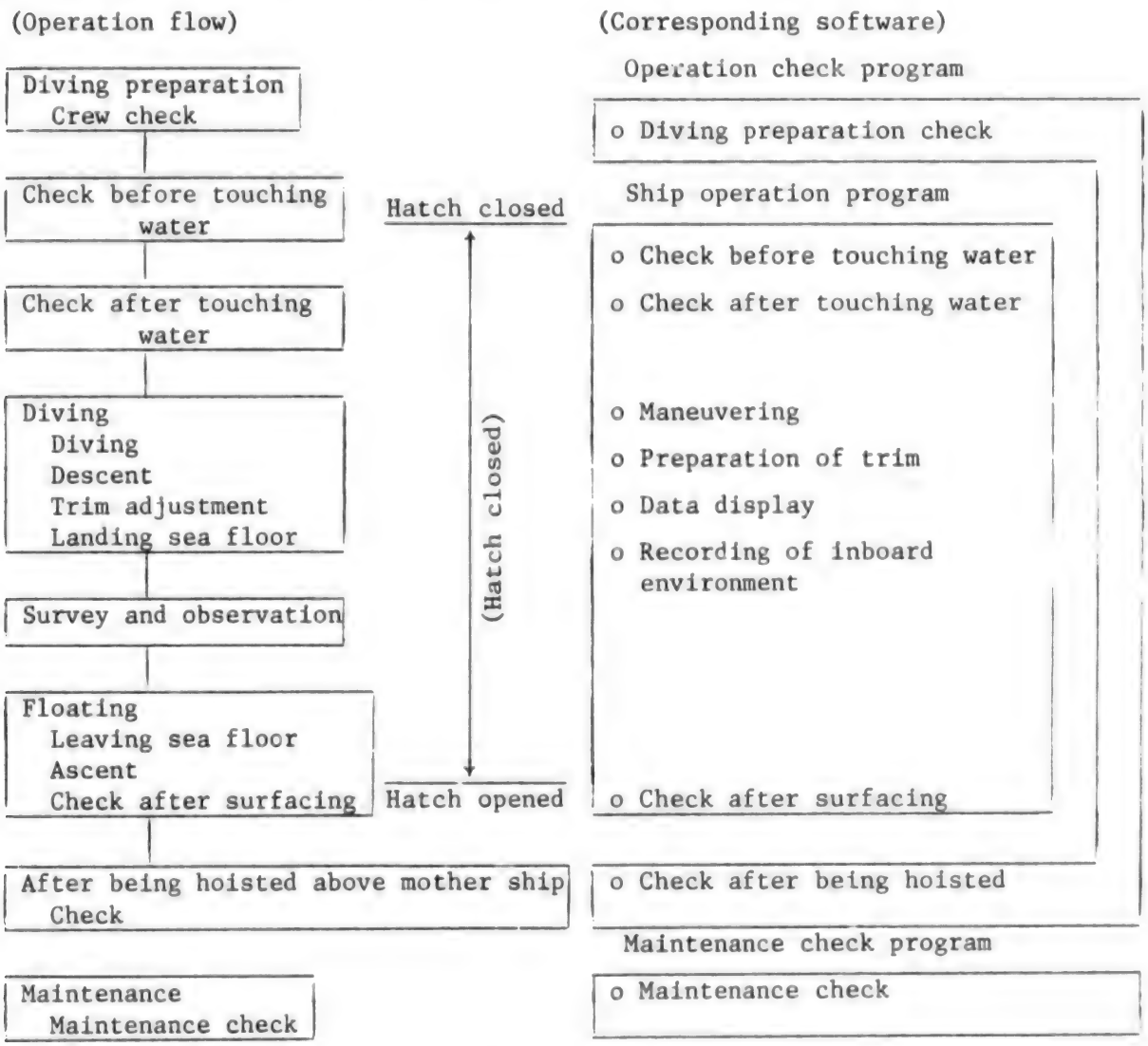

Figure 5. Operation Flow and Corresponding Software

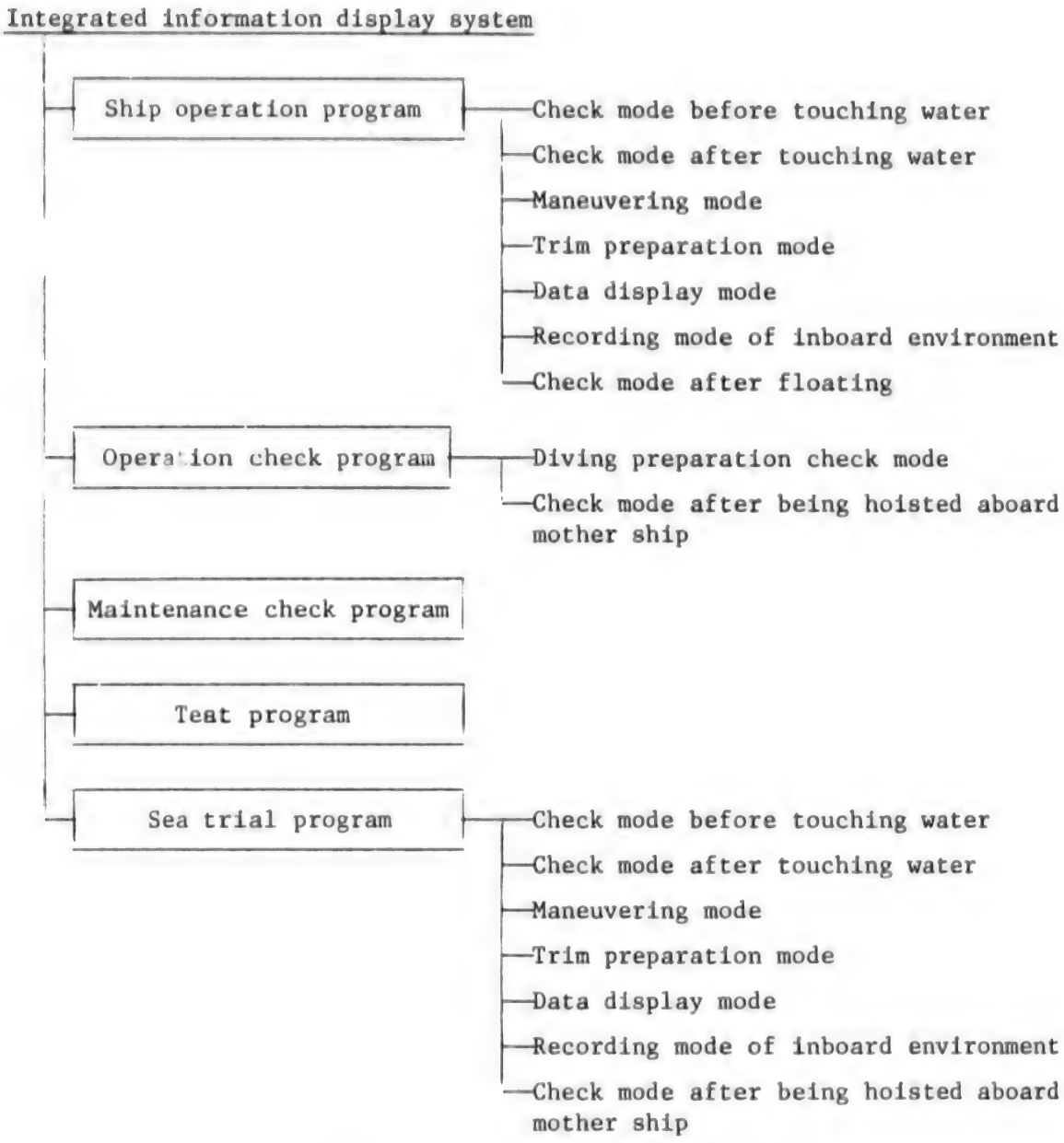

Figure 6. Configuration of Software

3.4 Information Display Method

As a represenative example of the information display method employed in the integrated information display system, brief explanations are given on the maneuvering mode and the data display mode of the operation program when alarms have been sounded.

3.4.1 Maneuvering Modes

The maneuvering mode is displayed at almost all times while Shinkai 6500 is submerged (the mode selection is effected by selecting the appropriate mode in the "Menu" at the start of the operation program via the touch sensor panel). Data are displayed in graphics so that the operator will be able to see the submersible and its surroundings at a glance.

Photograph 2 gives the display pattern of maneuvering mode, and Figure 7 and Table 2 give explanations of the display pattern.

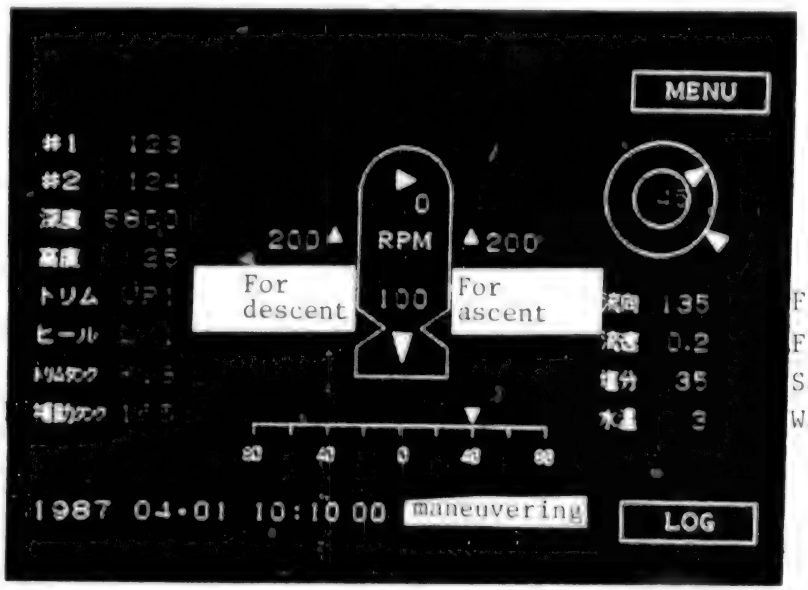

Photo 2. Display Pattern of Maneuvering Mode

3.4.2 Data Display Mode

The data display mode displays data on the power source, oil pressure, etc. as bar graphs, and consists of a three-page screen. For scrolling to the next page, you need to touch the area marked "NEXT" on the screen.

Each page contains the data listed below.

--1/3 page--source voltage (bus bar, ac system, dc system)
insulation resistance (same as above)

--3/2 page--amount of discharge from main battery (Nos. 1 and 2)
current (main battery, ac system, dc system)

--3/3 page--hydraulic system pressure
air storage tank pressure (air pressure)
amount of liquid in the auxiliary tank and pressure
amount of liquid in trim tank

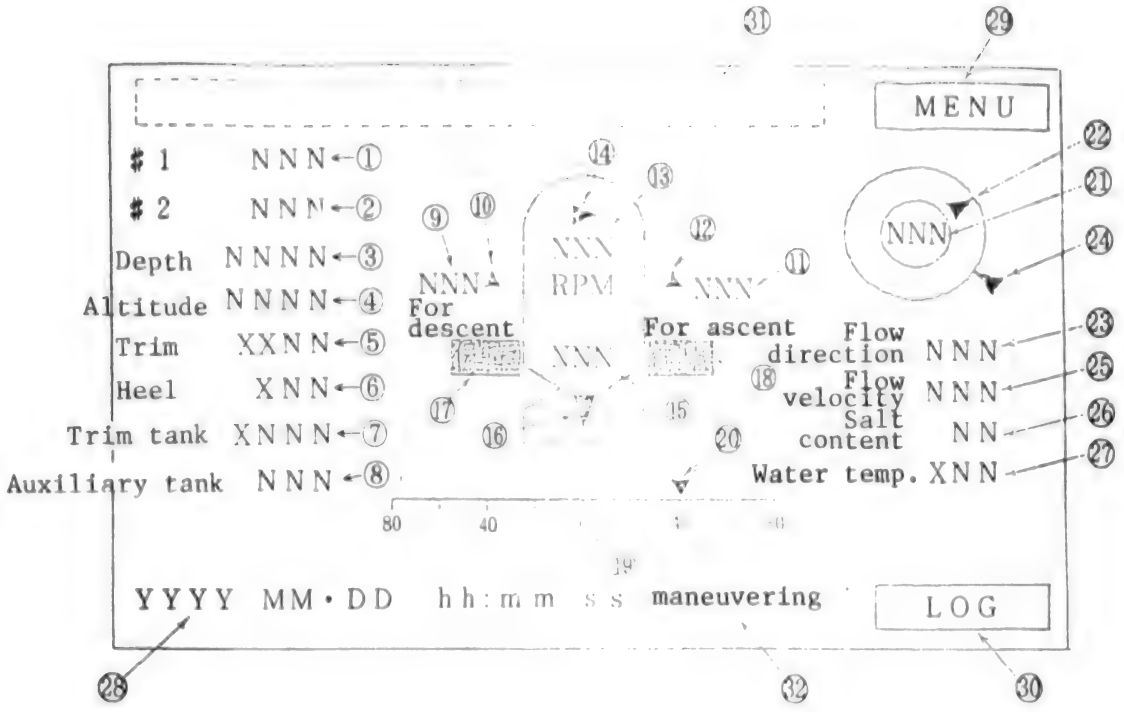

Figure 7. Display Pattern of Maneuvering Mode

Photograph 3 gives the display pattern of the data display mode (of 1/3 page), while Figure 8 and Table 3 give explanations of the display pattern.

3.4.3 Displays When an Alarm Is Sounded

When an alarm has been sounded, the ongoing display is interrupted and a voice alarm is heard while the contents of the alarm are flashed on the upper left side of the screen (see Photo 2). Simultaneously, the time when the alarm was sounded and its contents are recorded in the bubble cassette.

Alarm signals themselves are input from the alarm display panel which has built-in display lamps and an alarm buzzer.

Since the flashing alarm display area and the information display area are two different areas, even when an alarm is being flashed, other data are displayed on the screen.

Table 4 gives a list of alarms.

3.5 Recording and Reproduction of Data

When the operation program is activated, time and date, the position and height and the direction of the bow of the submersible, the direction and velocity of (current) flow, as well as CTDV data are automatically recorded at intervals of two seconds in the bubble cassette, while the majority of other data are recorded when the "LOG" area on the screen is depressed (LOG recording).

Table 2. Maneuvering Mode

No.	Contents of display	Explanation of display	Display color
1	No. 1 main battery quantity of discharge	Unit Ah	Yellow
2	No. 2 main battery quantity of discharge	" "	"
3	Depth	" m	"
4	Altitude	" "	"
5	Trim (vertical angle of inclination)	" degrees (UP for bow up)	"
6	Heel (horizontal angle of inclination	" " (R for starboard up)	"
7	Trim tank level	" kfg (forward trim tank)	"
8	Auxiliary tank level	" "	"
9	Vertical thruster (left) rotation number	" rpm	"
10	" directional indication	▲ ascent, ▼ descent	"
11	Vertical thruster (right) rotation number	Unit rpm	"
12	" directional indica.	▲ ascent, ▼ descent	"
13	Horizontal thruster rotation number	Unit rpm	"
14	" directional indication	▶ right turning, ◀ left turning	"
15	Main propeller rotation number	Unit rpm	"
16	" directional indication	▲ forward, ▼ astern	"
17	Ballast for descent	"Ridatsu" (abandon) in red, "Hoji" (hold) in green	Black background
18	Ballast for ascent	"	"
19	Main propeller oscillating angle scale	Unit degrees	White
20	" oscillating angle indication	The position on the scale indicated by an arrow is the oscillating angle	Yellow
21	Direction of the bow	Unit degrees	Green
22	" indication	The direction of the arrow is the direction of the bow	Yellow
23	Flow direction	Unit degrees	"
24	" indication	The direction of the arrow is the direction of the oncoming current (true bearing)	Blue
25	Flow velocity	Unit cm/s (relative flow velocity)	Yellow
26	Salt content	(Practical salt content)	"
27	Water temperature	Unit degrees	"
28	Second, minute, hour, day, month, year		White

[Continued on following page]

No.	Contents of display	Explanation of display	Display color
29	Menu key area	Depressing the area allows you to select the menu mode	White
30	LOG recording area	Depressing the area allows you to start LOG recording	"
31	Alarm display area	Flashing alarms appear in the area	Red
32	Mode display	Shows the screen is in the maneuvering mode	White

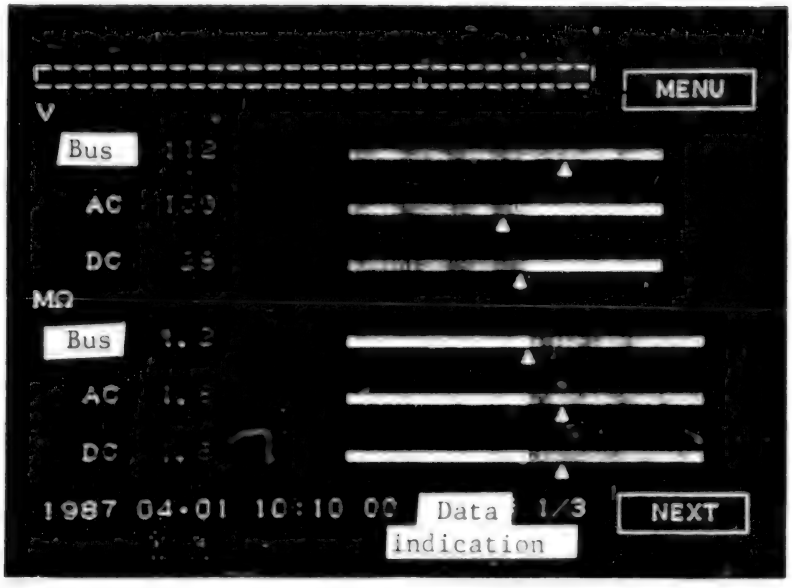

Photo 3. Display Pattern of Data Display Mode (1/3)

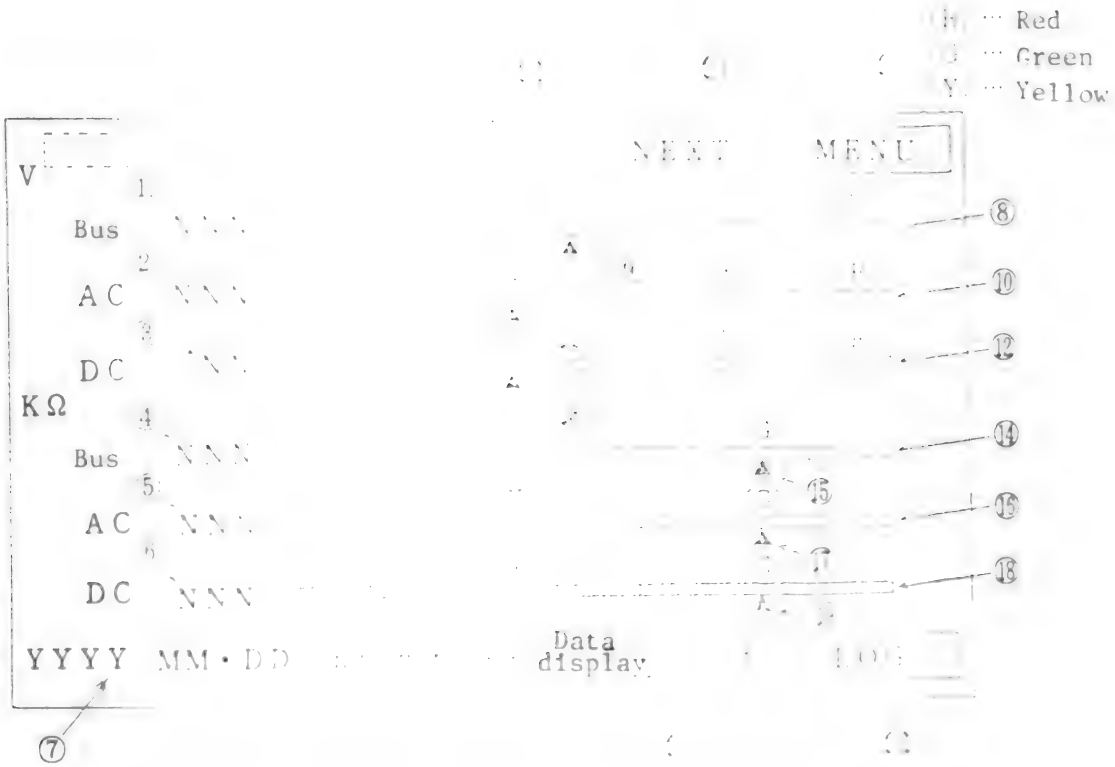

Figure 8. Display Pattern of Data Display Mode (1/3)

Table 3. Data Display Mode

No.	Contents of display	Explanation of display	Colors
1	Bus voltage	Unit V	Yellow
2	Communications system AC 100 V	" "	"
3	" DC 28 V	" "	"
4	Bus insulation resistance	" kΩ	"
5	Communications system AC 100 V insulation resistance	" "	"
6	" DC 28 V "	" "	"
7	Second, minute, hour, day, month, year		White
8	Bus voltage scale	Full scale 150 V	Green, red
9	" indication		Yellow
10	Communications system AC 100 V voltage scale	Full scale 150 V	Green, yellow, red
11	" indication		Yellow
12	Communications system DC 28 V voltage scale	Full scale 50 V	Green, yellow, red
13	" indication		Yellow
14	Bus insulation resistance scale	Full scale 1 MΩ	Green, yellow, red
15	" indication		Yellow
16	Communications system AC 100 V insulation resistance scale	Full scale 1 MΩ	Green, yellow, red
17	" indication		Yellow
18	Communications system DC 28 V insulation resistance scale	Full scale 1 MΩ	Green, yellow, red
19	" indication		Yellow
20	Next area	Depressing the area gives you data display 2/3 mode	White
21	Menu area	Depressing the area gives you menu mode	"
22	LOG recording area	Depressing the area gives LOG recording	"
23	Alarm display area	Flashing alarms are displayed	Red
24	Mode display	Shows the screen is in data 1/3 mode	White

Table 4. List of Alarms

No.	Item	Display contents	Voice output	Condition	Wiring
1	No. 1 main battery current warning	No. 1 BATT current ooo	No. 1 main battery current warning	Judged from input signal	0
2	No. 2 main battery current warning	No. 2 BATT current ooo	No. 2 main battery current warning	"	0
3	Main battery discharge quantity warning	Main battery discharge quantity	Main battery discharge quantity warning	Contact input from warning display panel	0
4	Insulation resistance meter bus trouble	Bus insulation drop	Bus insulation drop warning	"	0
5	Insulation resistance AC100V warning	Warning insulation drop AC100V 25 kΩ	AC100V insulation drop warning	"	0
6	Insulation resistance DC 28V warning	Warning insulation drop DC 28V 25 kΩ	DC 28V insulation drop warning	"	0
7	No. 1 main battery trouble	No. 1 main battery	No. 1 main battery warning	"	0
8	No. 2 main battery trouble	No. 2 main battery	No. 2 main battery warning	"	0
9	Main propulsion inverter trouble	Main propulsion inverter	Main propulsion inverter warning	"	0
10	Main propulsion inverter warning	Warning main propulsion inverter overcharge	Main propulsion inverter warning	"	0
11	Vertical thruster inverter trouble	Vertical thruster inverter	Vertical thruster inverter warning	"	0
12	Vertical thruster inverter warning	Warning vertical thruster inverter overcharge	Vertical thruster inverter warning	"	0
13	Horizontal thruster inverter trouble	Horizontal thruster inverter	Horizontal thruster inverter warning	"	0
14	Horizontal thruster inverter warning	Warning horizontal thruster inverter overcharge	Horizontal thruster inverter warning	"	0
15	Seawater pump inverter trouble	Seawater pump inverter	Seawater pump inverter warning	"	0

[Continued on following page]

No.	Item	Display contents	Voice output	Condition	Wiring
16	Seawater pump inverter warning	Warning seawater pump inverter overcharge	Seawater pump inverter warning	Contact input from warning display panel	0
17	Hydraulic pump inverter trouble	Hydraulic pump inverter	Hydraulic pump inverter warning	"	0
18	Hydraulic pump inverter warning	Warning hydraulic pump inverter overcharge	Hydraulic pump inverter warning	"	0
19	Communications inverter trouble	Warning communications inverter overcharge	Communications inverter warning	"	0
20	Trim tank liquid quantity warning	Trim tank	Trim tank liquid quantity warning	"	0
21	Auxiliary tank trouble	Auxiliary tank	Auxiliary tank warning	"	0
22	Air storage device (air pipe) pressure warning	Air system	Air system warning	"	0
23	Oxygen partial pressure trouble	O2 partial pressure	Oxygen partial pressure warning	"	0
24	Carbon dioxide partial pressure warning	CO_2 partial pressure	Carbon dioxide partial pressure warning	"	0
25	Hydraulic pressure trouble	Hydraulic system	Hydraulic system warning	"	0

For reproducing these data, they must be fed into the integrated data display system's data reproduction section aboard the support ship Yokosuka, after the submersible is hoisted aboard the mother ship. The reproduced data are processed as needed, and the results are forwarded to the printer or plotter, while simultaneously being recorded on a floppy disk, to be output as a daily report or as graphics.

Of the recorded data, those concerning the submersible's position, CTDV, etc. are delivered to the acoustic navigation system (ANS) aboard the mother ship for sound speed corrections and are recorded as the corrected diving data. The conversion of the recording format (MSDOS ↔ IBM format), a process necessary for effecting an exchange of data with ANS, is also conducted in the integrated information display system's reproduction section.

4. Conclusion

The foregoing gives brief outlines of the layout of equipment inside the pressure hull of Shinkai 6500 and information displays by the integrated information display system aboard the submersible.

Much has been left out about the integrated information display system and the system's data reproduction section in this technical report, and we would like to give a more detailed report the next time around if it is possible.

References

1. Shinichi Takagawa, "Shinkai 6500 Challenges an Unknown World," Marine, Vol 21, No 10, pp 62-72, 1989.

Design and Construction of Spherical Pressure Hull of 'Shinkai 6500'

916C0003B Tokyo KAIYO KAGAKU GIJUTSU SENTA SHIKEN KENKYU HOKOKU in Japanese Mar 90 pp 329-343

[Article by Shinichi Takagawa, Daisuke Kiuchi, and Kenji Takahashi of the Deep Sea Technology Department and Yutaka Yamauchi and Kazuya Inoue of the Kobe Shipyard, all of Mitsubishi Heavy Industries Ltd., and Takashi Nishimura of Kobe Steel Co., Ltd.]

[Text] [Abstract]

The pressure hull of a research submersible is required to have enough reliability and strength to ensure the safety of the crew against the water pressure, and at the same time lightness in weight is also required for good performance of the submersible. It is therefore very important in the design and construction to select a reliable and high strength material, to apply an appropriate design method fit this material and to apply minute machining technologies for required qualities.

JAMSTEC has decided to use a spherical pressure hull made of titanium alloy (Ti-6Al-4V ELI) for the "Shinkai 6500" submersible after confirming the characteristics of the material by pressure test of scale models, considering production capability of the material and the development of design and machining technologies.

This paper describes the development of the pressure hull from the selection of material to the final test.

Key words: Spherical Pressure Hull, Titanium Alloy, Three-Dimensional Machining, Electron Beam Welding.

1. Introduction

In bodies like research submersibles that move around underwater on their own, it is very important to build the hull as small and as lightweight as possible. Since the amount of energy that a research submersible can carry is limited, it cannot travel on its own to the survey point. Consequently, it is transported, carried aboard the support ship, to the survey point where it is lowered to water and hoisted aboard another support ship.

The submersible must be small and lightweight if the job of lowering it to water or hoisting it aboard the mother ship is to be done when the sea is rough. Furthermore, if the surveying activity underwater or on the sea floor is to be conducted efficiently, the submersible will have to be able to move around nimbly. Such agility could not be expected of a large submersible. Therefore, the submersible will have to be built as small as possible. In downsizing a submersible if the design of any constituent element took on large dimensions, everything else would have to be built large; the related supportive elements would have to be built large, including the propeller, in order to obtain the required thrust. The battery, the energy source, must be built large and their supportive elements must be built large. Consequently, when seeking to downsize a submersible, we must strictly apply the principle of downsizing to the design of every one of the ship's components.

The largest and heaviest of all components of a manned research submersible is the pressure hull that houses the crew. A success or failure in downsizing it has a great impact on whether or not the whole research submersible can be built small and lightweight. Therefore, in the development of Shinkai 6500, a research submersible, the key was how to reduce the size and weight of its pressure hull.

The pressure hull of a large depth research submersible must be small and lightweight yet it must guarantee the safety of the crew. A spherical pressure hull is most desired, but there is a limit to how far it can be downsized because it also must accommodate the crew. As a result of a human engineering study conducted using a prototype, it was decided that the pressure hull of Shinkai 6500 should take a spherical form with 2 meters in inner diameter. With the size of the pressure hull determined, the next question was focused on how to make it lightweight.

To that end, the requirements were, 1) to selectively use high-reliability material of high relative strength (0.2 percent proof stress divided by specific gravity) and 2) to apply an appropriate design method and engineering technology that would reduce the superfluous flesh as much as possible.

In the course of selecting the material, factors which included the domestic technology of manufacturing such material, the record of development of the technology to manufacture a prototypical pressure hull, and the progress in the development of the design technology centering on the collapse strength, were taken into consideration. Repeated pressure and crush tests were conducted using scale models before finally deciding on the adoption of a titanium alloy (Ti-6Al-4V ELI) for the pressure hull.

The planned outline of the pressure hull, the procedure pertaining to the selection of the material used, the design, the manufacture and the results of tests are described below.

2. An Outline of the Pressure Hull

The pressure hull of Shinkai 6500 is a spherical of 2,000 mm in inner diameter. It has a 500-mm-diameter hatch at its top which is used as the entry and exit port for the crew and three observation portholes of 120 mm in inner diameter on its down side. Two central watertight cable glands that contain various wires and cables for power or electrical signal exchange between the pressure hull and the outside, are installed at the rear of its top.

The observation portholes and integrated wire and cable conduits were not ground out of the pressure hull material, but they were installed later on. That is, the separately manufactured window frames (viewport coamings) and casings for the integrated wire and cable conduits, were fixed in place and welded.

An outline of the pressure hull is given in Figure 1.

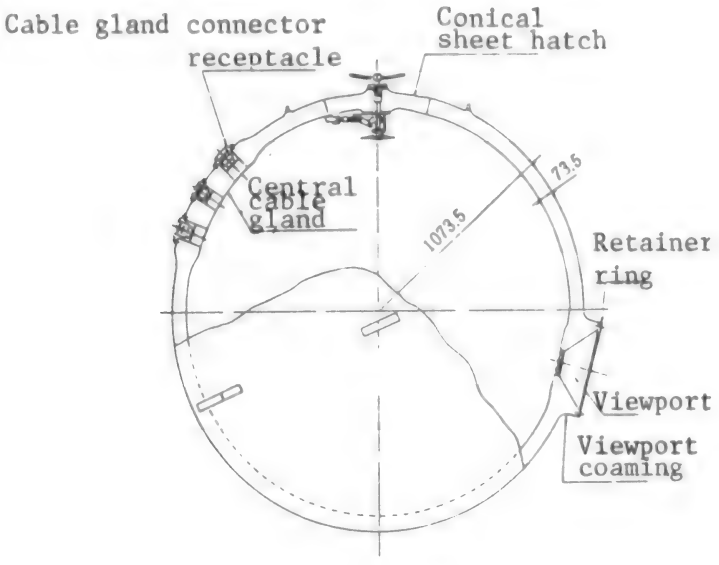

Figure 1. Structure of Pressure Hull

3. Material Used

A titanium alloy was used for the pressure hull. Compared with steel, titanium alloy has a smaller specific gravity and a larger relative strength (0.2 percent proof stress divided by specific gravity), so the material can greatly reduce the weight of the pressure hull. Thanks to titanium alloy's corrosion resistance to seawater, a feature that is not available with steel, a titanium alloy-based pressure hull does not need to be built an extra millimeter thicker as a precaution against corrosion. In the case of Shinkai 2000, the hull was of the plate thickness considered necessary for the safety design, plus an additional 1 mm as a measure to counter corrosion.

Table 1 gives a comparison of calculated weights of the pressure hulls, one made of titanium alloy Ti-6Al-4V ELI and the other of ultrahigh tensile strength steel 10Ni-8Co steel. From the table, one can learn that the titanium alloy-based pressure hull is lighter than the ultrahigh strength steel-based pressure hull by some 20 percent.

Table 1. Estimation of Pressure Hull Weight for Material Composition

Item / Material	0.2% proof stress $\sigma_{0.2}$ (kgf/mm^2)	Specific gravity γ (g/cm^2)	Specific strength $\sigma_{0.2}/\gamma$	Pressure hull: Plate thickness* (mm)	Pressure hull: Weight (ton)	Difference in weight (ton)
Ti-6Al-4 ELI titanium alloy	Above 81	4.42	18.3	73.5	4.39	1.07
10Ni-8Co steel	Above 120	7.85	15.3	52.5**	5.46	

* Inside diameter 2 m; safety factor 1.55; sphericity 1.00
** To include 1 mm as a margin for corrosion

4. Design of the Pressure Hull

4.1 Design Conditions

The design conditions for the pressure hull are given below.

(1) The pressure at the maximum diving depth was set at 680 kg/cm^2, a value equivalent to the pressure at a depth of about 6,500 meters.

(2) In accordance with the regulation on steel ships set by the Nippon Kaiji Kyokai (Japan Marine Association), the design crush pressure was set at a value above 1,058 kg/cm^2, a value equivalent to the pressure at a depth of about the submersible's maximum diving depth, times 1.5, plus 300 meters.

(3) The 0.2 percent proof stress of the titanium alloy used was set at 81 kg/cm^2 in accordance with the regulation of the governing standard AMS4907.

(4) The sphericity, which is the ratio between the standard radius R_o and the local radius of curvature R_{10}, was set at 1.004. One mm and 0.45 mm machining tolerances were given for the radius and the plate thickness, respectively. As described in paragraph 3, no special allowance was given for corrosion.

The strength of the pressure hull is given by formula (1) or formula (2), described later, and it is determined by the ratio between the plate thickness and the local radius of curvature. When manufacturing a pressure hull, the plate thickness cannot be changed according to the local radius of curvature, and it is a constant within the limits of a given machining

tolerance. Consequently, if a pressure hull, having a strength to withstand a given pressure is to be made under the condition that the local radius of curvature fluctuates greatly, the plate thicknesses all over the spherical hull will have to be in conformity with the largest local radius of curvature. The result is that in areas where the local radius of curvature is smaller than the largest local radius of curvature, the plate thicknesses are larger than the required values, that is, those areas are burdened with excess amounts of flesh.

For reducing the weight of a pressure hull, eliminating the extra amount of flesh is highly important. To that end, it is necessary to minimize the fluctuations in the local radius of curvature and the index for the change, which is the ratio between the standard radius and the local radius of curvature (i.e., sphericity) and must be brought to as close a value as possible to 1. The sphericity of the pressure hull for Shinkai 2000 was 1.07 but the corresponding value for Shinkai 6500 was set at a figure smaller by more than an order of magnitude, at 1.004.

4.2 Formulae for Calculating Collapse Strength

For calculating the collapse strength of the pressure hull, we used the collapse strength formula of spherical shells developed by M. Krenzke et al. at the David Taylor Research Center (DTRC) in the United States.

The formulae for calculating strength are given below.

Elastic collapse formula

$$P_3 = 1.4\, E/\sqrt{3(1-\nu^2)} \cdot (h_a/R_{10})^2 \cdots (1)$$

Elastic and plastic collapse formula

$$P_E = 1.4\sqrt{E_t,\ E_s/3(1-\nu^2)} \cdot (h_a/R_{10})^2 \quad \cdots\cdots (2)$$

where R_{10} = the local radius of curvature
h_a = the local thickness of plate
E = Young's modulus
ν = Poisson ratio
E_t = Tangent modulus to the average stress
E_s = Secant modulus to the average stress
Modulus

$$\sigma_{avg} = P_E R_{10}^2/2h_a(R_{10}-h_a/2)$$

$$P_k = k P_t$$

k = the correction factor for collapse strength by the machining method

Since the formulae for calculating collapse strength developed by Krenzke et al. are empirical ones, in order to confirm their reliability, the correction factor k was obtained in a series of tests which were undertaken

by considering the size of the initial-stage inaccuracy, the material used, the effect of openings, etc.

The design curve obtained from the results of these tests was used in the formula (3) by Krenzke et al. It is given in Figure 2. The design curve is the same as that used for the pressure hull of Shinkai 2000.

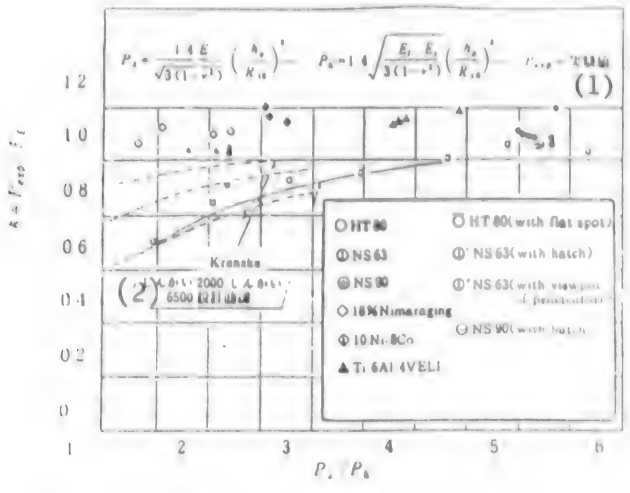

Figure 2. Compressive Strength for Spherical Pressure Hull

Key:
1. Experimental value
2. Design curves for Shinkai 2000 and Shinkai 6500

4.3 Local Strength and Allowable Stress

The formulae described above apply to the general area of the spherical shell. However, a pressure hull is not a simple spherical body. It has fixtures that differ from the general area of the spherical shell, such as openings like a hatch and observation windows, as well as central watertight cable glands. The aforementioned formulae cannot be applied to these fixtures. Therefore, these local strengths were designed whereby the allowable stresses met the following two conditions.

(1) The total of membrane stress and bending stress is below 75 percent of the 0.2 percent proof stress prescribed for the material used.

(2) The local stress is less than the 0.2 percent proof stress prescribed for the material used.

Along with the above, in the design of the openings and coamings the following considerations were given.

4.3.1 Observation Porthole Coamings

The observation porthole has the shape of a truncated cone having a 90-degree apex angle. The observation porthole coaming to which the observation porthole is fixed is of a shape that enables its rigidity to equal that of the pressure hull, and consideration is given to making the bending moment, where it joins the pressure hull, as small as possible.

The results of stress calculations by the finite element method of a spherical shell having an observation porthole coaming are given in Figures 3 and 4. Figure 3 is a stress contour along the longitudinal direction (the North-South Pole direction) while Figure 4 gives a stress contour along the latitudinal direction (the direction parallel to the Equator). The maximum value of the sum of membrane stress and bending stress, which was -60.4 kg/mm^2, occurred at the root of the observation porthole coaming, while the maximum value of the local stress, which was -77.4 kg/mm^2, was generated in the bore of the observation porthole coaming opening. All the stresses were within the limits of the allowable stresses.

Figure 3. Stress Contour Along Longitude Section (External pressure 680 kgf/cm^2)

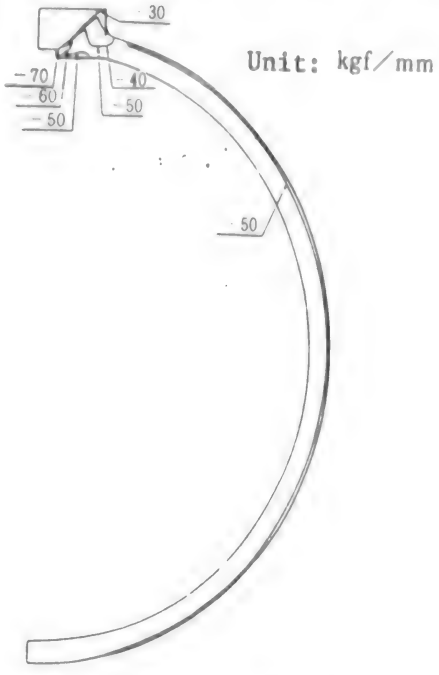

Figure 4. Stress Contour Along Latitude Section (External pressure 680 kgf/cm^2)

4.3.2 Central Watertight Cable Glands

The centralized watertight cable gland is of a multipore plate type in which a reinforcing insert plate contouring, along the spherical hull, is provided with openings. These are for the attachment of the receptacles for the connectors for the penetration pieces. The insert plate has a shape

that enables it to have a rigidity on a par with the general area of the spherical hull and consideration is paid to making its bending moment as small as possible.

The result of calculations by the finite element method, using a three-dimensional thick shell element of the stresses that a spherical shell, provided with a centralized cable gland, receives when subjected to an external pressure of 680 kg/cm^2, is given as a contour of the maximum main stress in Figure 5. The maximum value of the local stress was generated at the outer side of the opening on the external circumference of the shell, and the value at -69.1 kg/mm^2 satisfied the allowable stress.

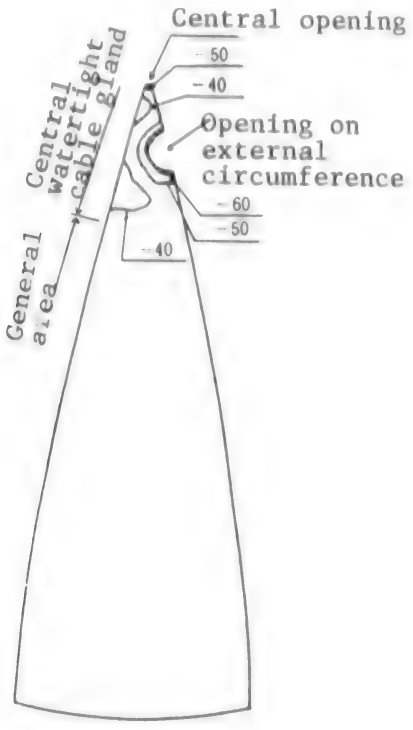

Figure 5. Contour of Maximum Main Stress (External pressure 680 kgf/cm^2)

4.3.3 Hatch

The hatch, which is a conical sheet hatch of a truncated cone shape, looks as if it was made by cutting out a part of the spherical hull. It has a structure which when subjected to external pressure, retains continuity with the pressure hull proper. The key to retaining the strength of a hatch is to make sure that it will not slide when subjected to an external pressure. The behavior of a hatch is affected by the chamfer angle (the angle created by the line extending from the external circumference of the globe to its center and the truncated cone generatrix), so, based on the results of friction and behavior tests of titanium alloy and the repeated pressure and collapse tests using spherical shell models having a conical sheet hatch (described in paragraph 4.3.4), the chamfer angle was set at 3 degrees.

The stress analysis by the finite element method was conducted for a spherical shell having a conical sheet hatch. In the analysis, the existence of a gap friction element was considered between the conical sheet hatch and the sheet surface of the pressure hull proper, but the hatch generated no slide when subjected to external pressures and the stresses were all within the limits of the allowable stress.

4.3.4 Tests Using Scale Models

In generating aforementioned designs and calculations, we conducted tests using scale models.

First we produced three titanium alloy models (a model with no opening, a model with an observation window, and a model with a hatch) for the testing. Our collapse tests and analyses confirmed the following:

(1) It is possible to estimate the collapse pressure of a titanium alloy spherical shell by the conventional design methods.

(2) The use of the conventional methods enables the effect of openings, such as an observation window or a hatch, on the collapse behavior to be ignored.

(3) A creep at ordinary temperature does not have any effect on the collapse behavior.

Then, we manufactured a 35-percent scale model, made of titanium alloy, of the actual pressure hull, using the same design and manufacturing method. We subjected the model to a repetition of compression tests numbering 1,500 compressive actions under conditions equivalent to the pressure at 6,500 meters below sealevel, and then subjected the model to a crush test. From the experiment, the following have been confirmed:

(1) There was not observed any deformation in the shape of the pressure hull nor a crack in it even after it had been subjected to a repetition of 1,500 compressions.

(2) The hatch and observation portholes were well sealed even after repeated compressions and decompressions.

(3) The repeated application of pressures numbering 1,500 times had no effect on the collapse behavior of the pressure hull.

(4) The crush pressure was 1,397 kg/cm^2.

The crush pressure in (4) is 1.32 times as high as the design collapse pressure, and a survey has revealed that the large crush pressure was mainly due to the fact that the proof stress of the material used was larger than the 81 kg/cm^2 described in paragraph 4.1.3. The proof stress of material, however, varies from manufacturing lot to manufacturing lot, and it is not practical to confirm the proof stress of the material to be used each time

and accordingly change the design, so we decided to adopt the guaranteed performance in the standards, 81 kg/mm^2, in the design of the real pressure hull.

5. Manufacture of the Pressure Hull

Manufacture of the pressure hull was undertaken in the order of these described procedures: manufacture of rolled plates; hot forming (heating the plate in a furnace and pressing it into shape while it is hot); heat treatment; preliminary machining of hemisphere; putting into place of the watertight cable gland and welding; three-dimensional machining and processing; equator line welding; machining and processing of the equatorial section; fixing into place of the observation porthole/watertight cable gland connector receptacle/conical sheet hatch; compressive strength and leakage tests; and coating. A schematic flow of these procedures is given in Figure 6, and explanations are given on some of the major steps of these procedures.

5.1 Manufacture of Raw Material

The raw material for the pressure hull's hemispheres was dissolved in vacuum (mixing the raw material porous titanium with the additives such as aluminum and vanadium and dissolving the mixture by an electric arc in vacuum to obtain titanium alloy); the obtained ingot was forged, beta-processed (the heat treatment involving high-temperature heating and rapid quenching in order to obtain finer grains of the titanium alloy) and rolled to obtain a rolled plate of the titanium alloy 125-mm thick. A disc of about 3 meters in diameter, cut from the rolled plate, was subjected to hot forming in a press to obtain the raw material for the hemisphere. Further, after the hot forming the raw material for the hemisphere received a solution treatment and over aging (STOA) (the heat treatment involving quench-and-temper to increase the strength and tenacity of titanium alloy). An external view of the hemisphere after hot forming is given in Photo 1 [not reproduced].

Test pieces were obtained from the extra portions of the hemisphere material after heat treating and they were subjected to tensile strength tests in order to confirm quality. The results of the analytical test of the rolled plate are given in Table 2, while the results of the tensile strength tests of the extra portions of the hemisphere material are given in Table 3. The test results were all satisfactory.

Forged material of titanium alloy, manufactured by forging, beta processing, and billet forging of the ingot obtained by means of vacuum melting, was used as the starting material for the observation porthole coamings, central watertight cable glands and the conical sheet hatch. The material for the central watertight cable glands was manufactured by forming and forging, hot shaping and heat treating the forged material, in this order. The material for the observation porthole coamings and the conical sheet hatch was manufactured by forming and forging and then heat treating the forged material. As with the material for the hemisphere, both materials were subjected to analytical tests and tensile strength tests to confirm their good quality.

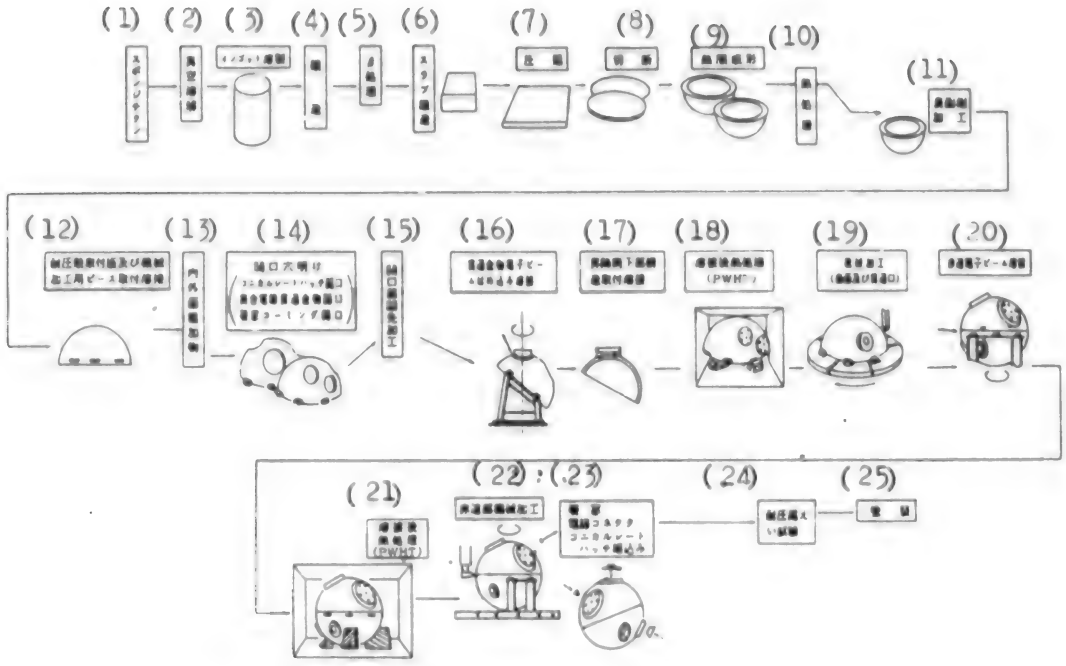

Figure 6. Production Procedure of Pressure Hull

Key:

1. Sponge titanium
2. Melting in vacuum
3. Ingot
4. Forging
5. Beta processing
6. Slab forging
7. Rolling
8. Cutting
9. Hot forming
10. Heat treatment
11. Preliminary machining of surface
12. Attachment of the mount for pressure hull and of the pieces for machining and their welding
13. After preliminary machining of inside and outside surfaces
14. Drilling of openings
    Conical sheet hatch opening
    Central watertight cable gland opening
    Viewport coaming opening
15. Edge preparation of openings
16. Fixing into place of penetration piece and its electron beam welding
17. Attachment of lower structure of hatchway and its welding
18. Post-welding heat treatment
19. Machining (surface and passages)
20. Electron beam welding in equator
21. Post-welding heat treatment
22. Machining of the equator
23. Fixing into place of viewports, cable connectors and conical sheet hatch
24. Compressive strength and leakage tests
25. Coating

Table 2. Composition Analysis for Titanium Alloy

Division			Al	V	Fe	O	C	N	H	Y	Other		Ti
											Individual	Total	
Titanium alloys for hemispheres	Rolled plate for southern sphere	Top	6.39	4.20	0.219	0.094	0.011	0.0038	0.0042	<0.0010	<0.10	<0.30	Remain
		Bottom	6.45	4.15	0.189	0.097	0.011	0.0035	0.0033	<0.0010	<0.10	<0.30	Remain
	Rolled plate for northern sphere	Top	6.44	4.25	0.215	0.094	0.013	0.0046	0.0023	<0.0010	<0.10	<0.30	Remain
		Bottom	6.42	4.12	0.213	0.092	0.012	0.0058	0.0029	<0.0010	<0.10	<0.30	Remain
Prescribed value			5.50~6.50	3.50~4.50	0.25 Below	0.13 Below	0.08 Below	0.05 Below	0.0125 Below	0.005 Below	0.10 Below	0.30 Below	Remain

Table 3. Tensile Strength of Titanium Alloy of Hemispheres

Division		Where sample was taken	What direction sample was taken	0.2% proof stress (kgf/mm^2)	Tensile strength (kgf/mm^2)	Elongation (%)	Contraction of area (%)
Titanium alloys for hemispheres	Alloy for northern hemisphere	1/2 t	L	85.7	91.7	11	26
				84.5	90.2	14	24
			T	85.5	91.5	12	26
				84.4	90.7	14	26
	Alloy for southern hemisphere	1/2 t	L	86.7	93.0	15	25
				85.7	90.7	15	19
			T	84.5	90.4	16	23
				84.7	90.7	16	12
Prescribed value				Above 81	Above 88	Above 10	Report only

5.2 Penetration Piece Fixed Into Place and Welded

The material for the hemisphere was cut in a preliminary machining so that the inside and outside surfaces retained a margin to machine later on; and then the openings for the observation hole coamings and the penetration piece for the central watertight cable glands were drilled, followed by the drilling of the opening for the conical sheet hatch. The penetration piece was also cut so that the inside and outside surfaces retained a margin to machine later on, and it, together with the openings on the hemisphere and the penetration piece, was machined for edge preparation.

Fixing into place of the penetration piece and its welding was conducted by electron beam welding by attaching a backing strip so that the beam would not pierce through. The welding work of the penetration piece is given in Photo 2 [not reproduced]. After the welding was over, the welded part was subjected to a post-welding heat treatment mainly aimed at removing the residual stress.

After the fitting and welding and the post-heat treatment were over, the welded part was subjected to color contrast penetration testing, ultrasonic testing and a radiographic inspection to confirm its soundness, and the results showed that both the surface and the interior were sound.

5.3 Three-Dimensional Machining

After the penetration piece was fixed into place and welded, the external and internal surfaces of the hemisphere were subjected to three-dimensional machining. In the work the position of the cutting edge of the cutting tool was precision-controlled three-dimensionally by computer and the bulging portions of the spherical shell, such as observation porthole coamings and the penetration piece, were cut and machined at levels of high precision to remove the superfluous flesh from the pressure hull as much as possible. The machining work is given in Photo 3 [not reproduced].

In the case of the manufacture of the pressure hull of Shinkai 2000, the hemisphere was first machined to the finish dimensions and then the penetration piece was fixed into place and welded by TIG welding, and the result was that the deformation resulting from the welding stayed put in the finished pressure hull. In the case of the pressure hull of Shinkai 6500, the penetration piece was fixed into place in the preliminary machined hemisphere with a margin for machining later on and welded by electron beam welding, and thereafter the inside and outside surfaces of the hemisphere, including the bulging portion of the penetration piece, was three-dimensionally machined and ground to the finish dimensions. This enabled the finished pressure hull to take the shape of a rough sphere.

In the machining of the hemisphere, the external surface near the equatorial joint was cut with a margin for machining later on, left intact, and it was machined to a finish after hemisphere welding in equator was over.

5.4 Hemisphere Welding in Equator and Machining of the Equator Section

After machining of the hemispheres was over, the north and south hemispheres were welded together in the equator. Electron beam welding, the technique used for the insertion and welding of the penetration piece, was also used for the equatorial welding. Photo 4 [not reproduced] gives a view of the equatorial welding.

After the welding was over, the whole sphere was subjected to a post-welding heat treatment to remove the residual stress. The work followed the same procedure as described in Paragraph 5.2. After the post-welding heat treatment was over, the sphere was subjected to nondestructive testing to confirm that both the surface and the inside of the weld were sound.

Later, the margin for machining on the external surface near the equatorial joint was cut and ground to the planned dimensions.

5.5 Testing Welding Work

It is impossible to directly test the mechanical properties of the welds of the actual pressure hull. We therefore used a testing method in which test pieces were welded by the welding techniques that were used in the real pressure hull and subjected to a post-welding heat treatment. These test pieces were then examined for their mechanical properties.

The results are given in Table 4, and all of the measurements satisfied the prescribed values.

Table 4. Welding Procedure Test Results for Pressure Hull

Division		Judgment standards	Equatorial joint of the pressure hull	Joint between pressure hull and penetration piece
Tensile strength of welded metal	0.2% proof stress (kgf/mm^2)	Above 81	93.5	87.2
	Tensile strength (kgf/mm^2)	Above 88	104.4	97.5
	Elongation (%)	Above 5	8.1	6.2
	Elongation (%)	Only need to be reported	21.6	14.8
Tensile test of welded joint		Tensile strength above the base material's standard value (88 kgf/mm^2)	Tensile strength 100.4 kgf/mm^2	Tensile strength 100.8 kgf/mm^2
Side bending test		Bending at an angle of 105 degrees when the bending inside radius R=12t does not give rise to any crack larger than 3 mm on the bent surface	O.K. (no crack	O.K. (no crack)

5.6 Shape Measuring

The plate thickness of the completed pressure hull and its shape were measured. An external view of the completely assembled pressure hull is given in Photo 5 [not reproduced].

The thickness of the plate in the general area of the sphere other than its equator ranged from 73.24 to 73.93 mm for the northern hemisphere and from 73.40 to 73.95 mm for the southern hemisphere, thereby satisfying the specifications of plus or minus 0.45 mm.

Figures 7 and 8 give the contour maps of the northern and southern hemispheres of the pressure hull, prepared based on the results of the measurements of their shapes, respectively. The sphericity (local radius of

of curvature divided by the standard radius) at 1.004 satisfied the specifications. Results of the measurements of the shape of the pressure hull are summed up in Table 5.

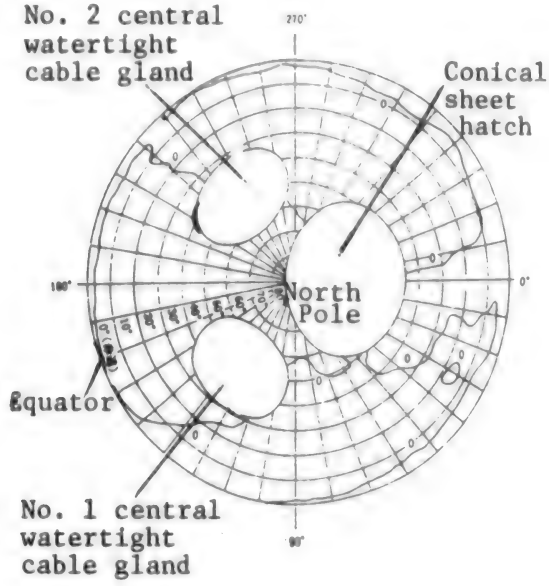

Figure 7. Sphericity Deviation (Radius) Distribution of N-Hemisphere

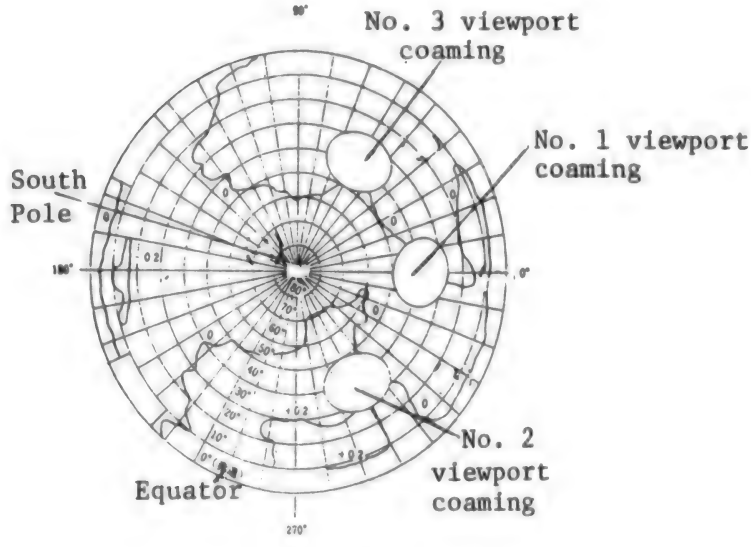

Figure 8. Sphericity Deviation (Radius) Distribution of S-Hemisphere

Table 5. Results of Sphericity Measurements

Item	Specifications	Results of measurements	
		Northern hemisphere	Southern hemisphere
Outside radius (mm)	1073.5 ± 1	Maximum 1074.03 Minimum 1073.51	Maximum 1074.06 Minimum 1073.49
General area plate thickness (mm)	73.5 ± 0.45	Maximum 73.93 Minimum 73.24	Maximum 73.95 Minimum 73.40
Sphericity	Below 1.004	1.004	

6. Compressive Strength and Leakage Tests

The "Submersible Special Standards" of Japan stipulate that pressure shells must be given compressive strength and leakage tests. The compressive strength test is conducted to confirm that the pressure shell is free from any abnormality when subjected to a pressure of 1.1 times the pressure equivalent to its maximum diving depth. The leakage proof test is a test that is conducted to confirm that no water has seeped into the pressure hull under the above pressure condition.

Japan, however, has no facility for testing as large a pressure shell as ours. So, after the pressure hull in question was completed, we sent it to the United States and tested it on facilities leased from the DTRC there.

6.1 Procedures of Compressive Strength and Leakage Tests

The conditions of the compressive strength and leakage tests regarding the composition, maximum pressure, and retention time are given in Table 6 and the procedures of compression and decompression are given in Figure 9.

Table 6. Condition of Compressive Strength and Leakage Test

Division		Maximum pressure (kgf/cm^2)	Retention time (minutes)
Compressive strength test	Preliminary pressurization test*	748	15
	Compressive strength test	748	15
Leakage test		748	15

* In the preliminary pressurization test, pure water was poured into the inside of the pressure hull (in accordance with the DTRC test procedures and standards).

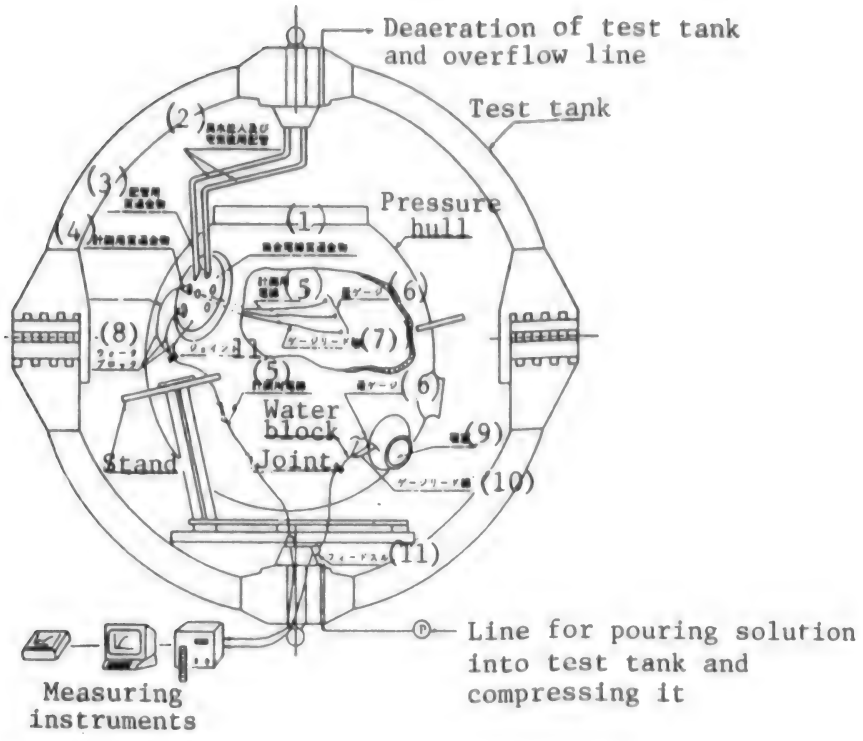

Figure 9. Arrangement of Pressure Test in DTRC

Key:

1. Central watertight cable gland
2. Pipes for pouring water in and deaeration
3. Penetration piece for piping
4. Penetration piece for measuring
5. Cable for measuring
6. Strain gauge
7. Lead wire for a gauge
8. Water block
9. Viewport
10. Lead wire for a gauge
11. Feedthrough

The maximum pressure was set at 1.1 times the pressure at the pressure hull's maximum diving depth (748 kg/cm^2) and the retention time at 15 minutes. The prevailing pressure at each of the steps shown in Figure 9 was retained and the strain of the pressure hull was measured.

Insulating oil was used as a medium of compression in the pressure test, and strains at various parts of the pressure hull were measured using a strain gauge. Pure water was used as the medium of compression in the leakage test to confirm the pressure hull's water tightness. In the leakage test, strains were measured at four points on the external surface of the general section of the pressure hull to confirm its behavior.

6.2 Facilities for Compressive Strength and Leakage Tests

The compressive strength and leakage tests were conducted using the 10-feet-diameter spherical test tank installed in the deep-sea simulation experiment building of the structure division of DTRC. The two-part test tank,

consisting of the upper and lower tiers, is a spherical tank of a laminated structure.

For the leakage test the pressure hull was placed inside the test tank and attached to the jigs inside the test tank. A schematic arrangement of the pressure test is given in Figure 10. The observation portholes and water-tight cable gland connector receptacle used in the test were identical to the actual products mounted in the pressure hull.

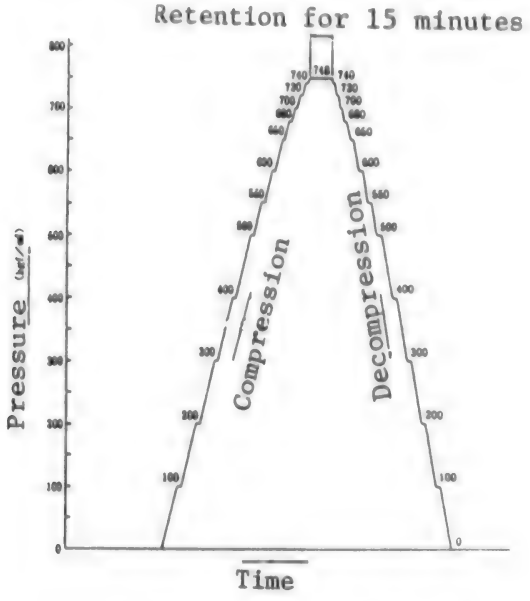

Figure 10. Procedure of Compression and Decompression

6.3 Results of the Compressive Strength and Leakage Tests

Shown in Photo 6 [not reproduced] is the pressure hull being subjected to compressive strength and leakage testing. The relationships between stresses and strains, as measured by a strain gauge in the compressive strength and leakage testing, are given in Figures 11 and 12. The stress-strain relationships followed a linear line, and there was no residual strain observed. The results were excellent.

Comparison is made of the actual values of the strains measured in the vicinity of the viewport coaming, and in the vicinity of the central water-tight cable gland with their calculated values, and the results are given in Figures 13 and 14. Although there was observed partial scattering in the measurements, the two types of values showed good agreement. The stresses detected by the strain gauge were all within the allowable limits. For reference, in the leakage test, measurements were taken of the stresses at the external surface of the general area of the pressure hull and the measurement results were roughly in agreement with the measurement results obtained in the pressure test, thereby revealing a good reproducibility.

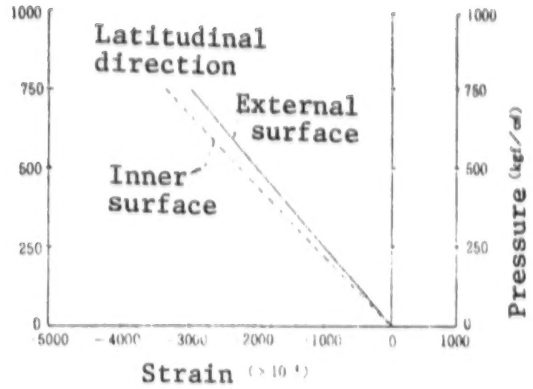

Figure 11. Stress-Strain Transition (General Part of Hull)

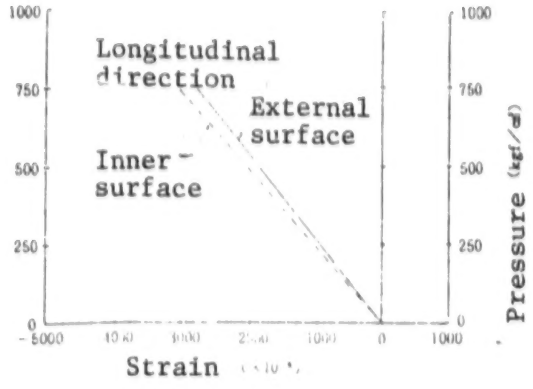

Figure 12. Stress-Strain Transition (Bottom of Viewport Coaming)

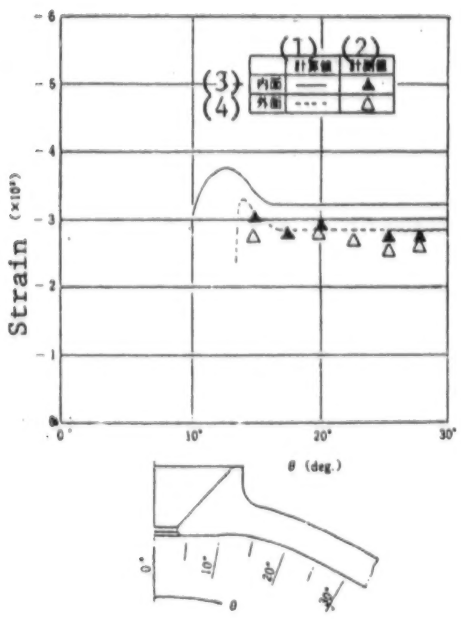

Figure 13. Longitudinal Strain Distribution Around Viewport Coaming (external pressure 680 kgf/cm^2)

Key:
1. Calculated value
2. Measured value
3. Inner surface
4. External surface

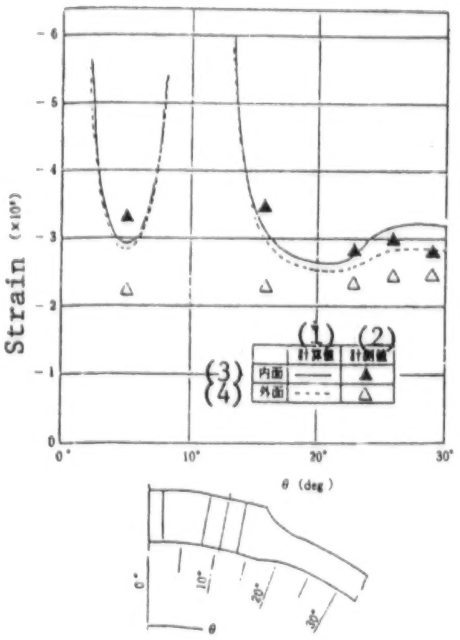

Figure 14. Latitudinal Strain Distribution Around Central Watertight Cable Gland (external pressure 680 kgf/cm^2)

Key:
1. Calculated value
2. Measured value
3. Inner surface
4. External surface

While the maximum pressure was retained during the compressive strength and leakage testing, no abnormal occurrences such as drops or fluctuations in pressure were observed. We examined the existence or nonexistence of leaks to the inside of the pressure hull, but to our satisfaction, no leakage was observed.

The results of the compressive strength and leakage tests gave us confidence that the pressure hull has ample enough compressive strength and water tightness. After the compressive strength and leakage tests were over, major weld joints were subjected to dye penetrant tests and the results revealed that the welds were sound.

7. Conclusion

This paper has described the design, manufacture and testing of the 6500-class survey submersible Shinkai 6500. A summary of its contents follows.

(1) The pressure hull of Shinkai 6500, the first large-scale thick plate structure manufactured in Japan by using titanium alloy (Ti-6Al-4V ELI), was excellent in terms of the material and shape accuracy.

(2) As for the properties of the base material titanium alloy, they were proved to satisfy--more than enough--the required performance capabilities in the structural and mechanical tests.

(3) As for welding, the electron beam welding employed enabled us to obtain sound welds inside and outside of the surface and the joints had strength that fully satisfied the demanded values.

(4) For geometrical accuracy, the adoption of the technique--first welding the reinforcements for the openings to the hemisphere by electron beam welding and then machining the entire hemisphere three-dimensionally--enabled the sphericity of the pressure hull to obtain 1.004, an accuracy close to a sphere.

(5) The compressive strength and leakage tests conducted under the condition of 1.1 times the maximum pressure of the maximum design pressure, confirmed that the pressure hull fully met the demanded performance capabilities in terms of compressive strength and water tightness.

References

1. Ryoichiro Sasahara, Tsutomu Toyohara, Katsuhito Fuchigami, and Genta Takano, "Basic Research on Electron Beam Welding of Thick Plate Ti-6Al-4V Alloy," MITSUBISHI JUKO GIHO (MITSUBISHI HEAVY INDUSTRIES TECHNICAL JOURNAL), Vol 20, No 2, 1983.

2. Norimasa Endo, Kimio Yokota, Ryoichiro Sasahara, Tsutomu Toyohara, Genta Takano, Takashi Nishimura, and Kenichi Yasui, "Research on Engineering Methods of Titanium Alloy Pressure Hulls for Deep Sea Research Submersibles (No 1)," JOURNAL OF THE SOCIETY OF NAVAL ARCHITECTS OF JAPAN, Vol 156, 1984.

3. Norimasa Endo, Kimio Yokota, Ryoichiro Sasahara, Tsutomu Toyohara, Genta Takano, Takashi Nishimura, and Kenichi Yasui, "Research on Engineering Methods of Titanium Alloy Pressure Hulls for Deep Sea Research Submersible (No 2)," JOURNAL OF THE SOCIETY OF NAVAL ARCHITECTS OF JAPAN, Vol 157, 1985.

4. Kimio Yokota, Hidemasa Morihana, Koichi Uragami, and Yutaka Yamauchi, "Research on Collapse Strength of Spherical Shell Models of Titanium Alloy," JOURNAL OF THE KANSAI SHIPBUILDING ASSOCIATION, Vol 198, 1985.

5. Tamotsu Shinohara, Shinichi Takagawa, Kimio Yokota, Hidemasa Morihana, Koichi Uragami, and Yutaka Yamauchi, "Research on Collapse Strength of Spherical Shell Models of Titanium Alloy (No 2)," JOURNAL OF THE KANSAI SHIPBUILDING ASSOCIATION, Vol 207, 1987.

6. Masanobu Sato, Takatoshi Yamauchi, Genta Takano, Hidemasa Morihana, Katsuhito Fuchigami, and Katsuji Miyamoto, "Properties of Titanium Alloy for Deepsea Research Submersibles and Their Evaluations," MITSUBISHI HEAVY INDUSTRIES TECHNICAL REPORT, Vol 15, No 6, 1978.

7. Norimasa Endo, Hidemasa Morihana, Katsuhito Fuchigami, Yutaka Yamauchi, Tsutomu Toyohara, and Toshihiko Hiraishi, "Pressure Vessels of Titanium Alloy for Deepsea Research Submersibles," MITSUBISHI HEAVY INDUSTRIES TECHNICAL REPORT, Vol 17, No 5, 1980.

8. M. A. Krenzke, "The Elastic Buckling Strength of Near-Perfect Deep Spherical Shells With Ideal Boundaries," DTMB Report 1713, 1963.

9. M. A. Krenzke and T. J. Kiernan, "Test of Stiffened and Unstiffened Machined Spherical Shells Under External Hydrostatic Pressure," DTMB Report 1741, 1963.

10. M. A. Krenzke and T. J. Kiernan, "The Effect of Initial Imperfections on the Collapse Strength of Deep Spherical Shells," DTMB Report 1757, 1965.

11. Japan Marine Machinery Development Association (JMDA, "R&D Report on 6,000-Meter Research Submersible," 1971.

12. JMDA, "R&D Paper on 6,000-Meter Research Submersible," 1972.

13. JMDA, "R&D Paper on 6,000-Meter Research Submersible," 1973.

14. JMDA, "R&D Paper on 6,000-Meter Research Submersible," 1974.

15. JMDA, "R&D Paper on 6,000-Meter Research Submersible," 1975.

16. Kazuhiko Kanai, Hidemasa Morihana, Toshiki Yamazaki, and Kunio Terada, "Experiment and Research on Collapse Strength of Spherical Shells," JOURNAL OF THE SOCIETY OF NAVAL ARCHITECTS OF JAPAN, Vol 132, 1972.

- END -

END OF FICHE

DATE FILMED

20 Feb. 1991